

**Layer like porous materials with hierarchical structure**

Journal:	<i>Chemical Society Reviews</i>
Manuscript ID	CS-REV-06-2015-000508.R1
Article Type:	Review Article
Date Submitted by the Author:	21-Sep-2015
Complete List of Authors:	Roth, Wieslaw; Jagiellonian University in Krakow, Faculty of Chemistry Gil, Barbara; Jagiellonian University in Krakow, Faculty of Chemistry Makowski, Wacław; Jagiellonian University in Krakow, Faculty of Chemistry Marszalek, Bartosz; Jagiellonian University in Krakow, Faculty of Chemistry Chlubná-Eliášová, Pavla; Academy of Sciences of the Czech Republic,

Layer like porous materials with hierarchical structure

Wieslaw J. Roth,^{*a} Barbara Gil,^a Waclaw Makowski,^a Bartosz Marszalek,^a Pavla Eliášová^b

^a Faculty of Chemistry, Jagiellonian University in Kraków, ul. Ingardena 3, 30-060 Kraków, Poland. E-mail: wieslaw.roth@uj.edu.pl

^b J. Heyrovský Institute of Physical Chemistry, Academy of Sciences of the Czech Republic, Dolejškova 2155/3, 182 23 Prague 8, Czech Republic

ABSTRACT

Many chemical compositions produce layered solids consisting of extended sheets with thickness not greater than a few nanometers. The layers are weakly bonded together in a crystal and can be modified into various nanoarchitectures including porous hierarchical structures. Several classes of 2-dimensional (2D) materials have been extensively studied and developed because of potential usefulness as catalysts and sorbents. They are discussed in this review with focus on clays, layered transition metals oxides, silicates, layered double hydroxides, metal(IV) phosphates and phosphonates, especially zirconium, and zeolites. Pillaring and delamination are the primary methods for structural modification and pore tailoring. The reported approaches are described and compared for the different classes of materials. The methods of characterization include identification by X-ray diffraction and microscopy, pore size analysis and activity assessment by IR spectroscopy and catalytic testing. The discovery of layered zeolites was a fundamental breakthrough that created unprecedented opportunities because of (i) inherent strong acid sites that make them very active catalytically, (ii) porosity through the layers and (iii) bridging of 2D and 3D structures. Approximately 16 different types of layered zeolite structures and modifications have been identified as distinct forms. It is also expected that many among the over 200 recognized zeolite frameworks can produce layered precursors. Additional advances enabled by 2D zeolites include synthesis of layered materials by design, hierarchical structures obtained by direct synthesis and top-down preparation of layered materials from 3D frameworks.

1. Introduction

Layered objects, defined as having one of the three principal dimensions significantly smaller than the other two, are ubiquitous at various length scales from macroscopic to nano-size level. Molecular layered materials, also called 2-dimensional (2D), consist of extended sheets with thickness of up to few nanometers corresponding to roughly one or a fraction of crystallographic unit cell. The atoms within the layers are connected by strong, mostly covalent, bonds while the interlayer interactions are much weaker and usually breakable.^{1,2} Layered solids are hierarchical by definition as materials “organized (hierarchically) by the combination of smaller (physically distinct, discontinuous) entities”³ (in parenthesis are additions by the present authors) thus fitting the general definition of structural hierarchy. The non-covalent weaker forces that keep the layers together, often in some state of organization up to being periodic in 3 dimensions (3D), can in most cases be broken allowing various modifications with preservation of the original internal structure of these layers. The increasing of interlayer space and creation of additional level of hierarchy are the most common goals of the layer materials modification.⁴⁻⁶ The intercalation between layers of molecules or ions, which are referred to as

guests, is the principal characteristics of 2D materials and is often a prerequisite step in transformation into other structural and chemical forms. From that perspective layered materials are recognized as host lattices with structural dimensionality equal to 2.⁵ There are of course materials with dimensionality of 3 – e.g. zeolites, 1 – chains and 0 – individual molecules.⁵ It has been suggested that single 2-dimensional layers can be also viewed as (macro)molecules because of contiguous covalent character. Except for the 3D fully connected frameworks,^{7,8} all of the other types of host lattices can be modified by intercalation but none have been studied and developed as extensively as the 2D layered ones. This may be simply because in practice they are more manageable and tractable, e.g. by structure characterization techniques, than the 1D and 0D have been so far. At the same time, the rigidity of the layers and their topotactic interactions and reactivity offer unique opportunities for organization and control allowing generation of novel materials with desirable characteristics, such as adjustable porosity.

The hierarchic nature exhibited by the layered/2D solids is distinct from the other types/materials^{9,10} because it is intrinsic at the molecular level. Consequently it does not need to be created, e.g. by degradation or fabrication, but rather it is instantly available for further manipulation and optimization by design according to the statement that “a central aspect of chemical engineer is to design or optimize certain property”.³ What is important to realize is that at the nanoscale the manipulation is most often achieved by chemical means or at least the chemical environment plays a decisive role if for example a mechanical process is applied. Layered structure formation is intrinsic to many chemical compositions and is generated spontaneously as the result of their preparation. These materials provide many practical benefits that have already been exploited in diverse applications including electronics, optics, fabrication of nanocomposites, catalysis, etc. The entire area of 2D materials together with their intercalation and modification processes can be viewed as pertinent to hierarchical structures. However, what is of particular interest from the hierarchy perspective is not so much what the 2D materials offer in their original form but the novel materials and hierarchy that can be created from them upon modifications: structural, topotactic and compositional. In accordance with the theme of this issue - recent progress in hierarchically-structured porous materials – this review will focus on porosity generated by modification of layered materials. In that sense it will not be limited to the commonly recognized two level hierarchical porosity exemplified by combinations of micro- and meso-porous structures, but will consider such combination of structure and pore hierarchy as one of the particularly desirable outcomes.¹¹

2. Overview of primary layered materials

Table 1 Major classes of layered materials^{1, 5, 6, 12}

Main classes	Subgroups
	<u>Insulator layered materials</u> -mainly oxides
Aluminosilicate based ('sheet silicates')	1:1 Neutral clays (kaolinite) 2:1 Anionic clays ¹³ Crystalline silicates, acids ¹⁴ Layered zeolites ^{15, 16}
Metal(IV) phosphates and phosphonates ¹³	α -M(IV) phosphates (and arsenates) $M(\text{HXO}_4) \cdot \text{H}_2\text{O}$; M=Ti,Zr,Ge,Sn,Pb, X=P,As γ -M(IV) phosphate $M(\text{PO}_4)(\text{H}_2\text{PO}_4) \cdot 2\text{H}_2\text{O}$, M=Ti,Zr α -M(IV) phosphites and phosphonates (arsenates) $M(\text{RXO}_3)$, R=H,alkyl,aryl, X=P,As Vanadyl phosphates Tin(IV) H-chloro-phosphate $\text{HSn}(\text{OH})\text{ClPO}_4 \cdot 2\text{H}_2\text{O}$ α -Zirconium aminophosphate $\text{Zr}(\text{NH}_3\text{C}_2\text{H}_4\text{PO}_3)_2 \cdot 2\text{Cl} \cdot 2\text{H}_2\text{O}$
,M(V) hydrogen phosphates $\text{HM}(\text{V})(\text{PO}_4)_2$	M(V) = Nb, Ta, As, Sb
Layered transition metal oxides $\text{A}_x\text{M}_y\text{O}_z$ ¹⁷	MO_6 octahedra sharing edges/corners
Layered double hydroxides, hydrotalcites ¹⁷	$[\text{M}^{2+}_{(1-x)}\text{M}^{3+}_x(\text{OH})_2]\text{X}^{n-}_{(x/n)} \cdot (\text{H}_2\text{O})_y$
Lanthanide (Ln) hydroxides ¹⁸	$[\text{Ln}(\text{OH})_{2.5}]\text{Cl}_{0.5} \cdot m\text{H}_2\text{O}$
<u>Redox</u> - larger variety of compositions than insulators; can undergo topotactic redox reactions	
Graphite, hexagonal-BN	-
Redox layered oxides	AMO_2 (A=Li,Na; M =Ti,V,Cr,Mn,Fe,Co,Ni,Nb,Mo,Ru) MoO_3 ; MO_3 Binary Ti, Nb and Mn oxides; V_2O_5 Perovskites and niobates Ternary oxovanadates
Oxyhalides	MOCl ; MO_xX_y
Oxycuprate superconductors	$\text{YBa}_2\text{Cu}_3\text{O}_7$; quasi-layered $\text{Bi}_2\text{Sr}_2\text{CaCu}_2\text{O}_x$
Redox chalcogenides	MX_2 , MPS_3 Misfit layer chalcogenides $\text{MM}'\text{X}_3$ and $\text{MM}'_2\text{X}_5$
Layered halides	MX_2 , Nb_3Cl_8 , MX_n n=3-6

The formation of layered materials is spontaneous with certain compositions, which presents a natural and the most common way of classification. It is based on the primary forms that are available in nature, like clays and silicates, or obtained by direct synthesis. These primary forms are sometimes called layered precursors, especially for zeolites, to differentiate from derivative materials produced by post-synthetic modification. The primary composition classes can include a single compound or be quite broad including those with no practical limits to compositional variations. Further grouping of

compositional classes can be carried out according to different criteria, e.g. layer charge – neutral, positive or negative.^{1,17} Table 1 presents the major classes of layered materials based on the division into insulators and redox materials as applied by Schöllhorn.⁵ There is another type of division based on the thickness of constituent layers, which distinguishes 3 classes.¹⁹ Class I comprises materials with one atom thick mono-layers (graphite, boron nitride - BN), class II – a few atoms, class III – many atom thick layers. This concept is relevant here because layer thickness can be related to its rigidity and generation of controlled porosity, which is the primary concern of this review, requires rigid layers. The rigid class III layered materials are found primarily in the insulator group. There are apparent exceptions on both sides – the insulator layered double hydroxides and redox AMO_2 are comprised of relatively thin layers. Both appear to be quite rigid and capable of forming well defined layered derivatives. The classification in Table 1 includes recent additions, namely 2D zeolites and lanthanide metal hydroxide. As for the major layered classes in Table 1, the listing is quite universal and similar compilations can be found in other sources dedicated to this topic.^{1,4,6}

The study, development and reporting of different classes of layered materials has been progressing mainly along the compositional lines with not very much crossover/overlap. This is justified because of differences in their chemical reactions and what they might offer in terms of functionality. Nonetheless, there are studies on preparation of mixed systems composed of different types of layers, e.g. negative oxides and positive layered double hydroxides.²⁰ This can be accomplished by combination of appropriate colloidal suspensions. At one level, neglecting chemistry and looking at 2D materials as collection of separable rigid layers, one might expect that all classes should be able to produce similar structures and types of materials. How to get there would be dictated by the particulars of their compositions and chemistry, which is determined by the chemical nature of the surface. Aside from the possible stability issues, one can imagine that other factors, such as the mentioned flexibility-rigidity differences, can make such across-the-board similarity of all layered solids impossible. On the other hand, it may be very useful to consider why certain analogues among various classes should or possibly cannot exist. This might lead to better understanding and new findings, which might not be contemplated when considering only a particular group. The comparison of various silica forms: clays, silicates and zeolites can provide an excellent case for such study. At this point there are many differences between them in terms of interlayer chemistry, which are most likely determined by particular features or functionality on the layers.

3. Layered zeolites and unification of 2D and 3D framework structures

Each of the compositional layered classes is of great interest on their own and often offers special practical benefits. The recent discovery and expansion of 2D layered zeolites appears as a particularly significant development.²¹⁻²³ It expands the concept of layered materials by adding a new level from combining 2D and 3D materials. The following points justify this as new ground breaking development:

1. Zeolites were perceived as model 3D structures, inconceivable as 2D solids. As a whole class they now comprise both 3D and 2D materials, which is quite unique.

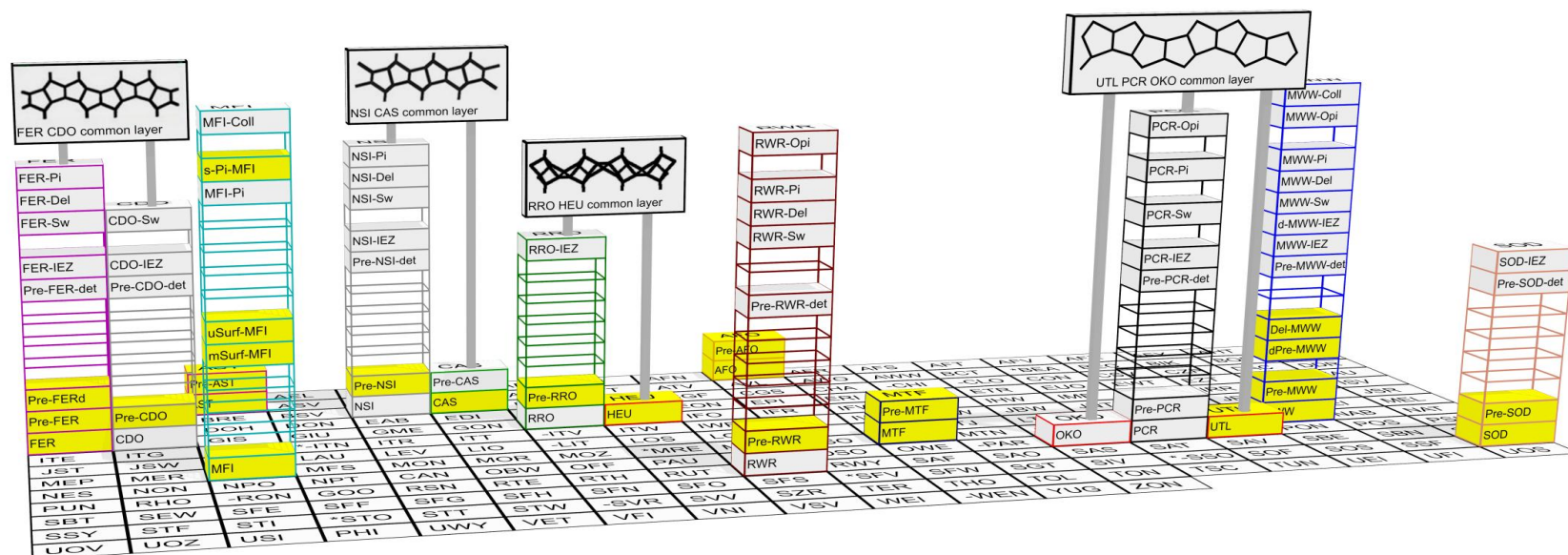
2. Zeolites and layered materials such as clays have been often competitors in catalysis, ion exchange and adsorption application and each had something different to offer (e.g. structural rigidity vs. flexibility; different activity; cost), thus complementing each other.
3. Zeolite layers contain intrinsic strong acid centers. The generally lower activity of the other types of layered materials made them less competitive in catalysis.
4. Zeolite layers can contain cavities and internal pores, including through/across the layers, which may offer additional benefits in sorption and catalysis. Porous layers can be also adapted for membrane application. The stability and rigidity of zeolite layers is also a great advantage.
5. There are additional types of structural transformation with layered zeolites (Figure 1) like the congruent joining of the layers affording 3D ordered, fixed structures. This is exemplified by the interlayer expanded zeolites (IEZ) and the normal 3D frameworks themselves. There are no equivalent materials yet with the other 2D classes.

Taking into account different types of structures and inorganic/organic composites reported for 2D zeolites and including the 3D framework there are already about 15 distinct layered forms that can be formally distinguished.²⁴ For each of these forms there are as-synthesized (uncalcined) and calcined pairs, which further increases the overall number of material types to be considered. Not all of them are structurally unique, especially among the calcined products, and some may appear trivial like the calcined swollen precursor. The 3D zeolite forms are evidently unique and historically viewed as separate opposites of layered solids.^{5,6} They are considered in this classification for completeness as derivatives, at least conceptual, of the corresponding layered structures. 3D frameworks can be viewed as a special, end form of layered structures, i.e. layers fused congruently and completely. This definition does not seem to have a particular practical significance but can be recognized formally as logical extension of the 2D concept. In fact, it may stimulate taking another look at various conventional layered materials from the standpoint of possible fusion into ordered 3D framework. Layered silicate illerite is the case in point. It has been extensively studied and modified as model layered silicate²⁵ but was recently discovered to produce 3D zeolite framework, denoted RWR.²⁶ It is therefore a layered zeolite precursor. In fact it is the first one synthesized²⁷ although not recognized as such until the area became more developed with other zeolites and precursors.

There are over 200 unique zeolite structures officially recognized by the IZA Structure Commission with assigned 3 letter code. So far about 15 have been found to have layered representative. Many more possibly all zeolites are anticipated to produce 2D precursors or other layered species.¹⁵ This may not be provable one way or another but any framework can be envisioned as composed of layered components. Many of the different derivative layered zeolite forms, e.g. swollen, pillared, delaminated and others, were modeled on the previously known examples from the other compositions like clays. Some of the structure types obtained for zeolites have no recognized counterparts among the known 2D layered materials and may be even impossible or unimaginable, like the 3D framework themselves. On the other hand, as proposed above, this may be the basis for consideration if and how some of the layered structures obtained with zeolites can be replicated with other 2D composition classes.

Like for most classes of layered materials there are also extensive recent reviews of the 2D zeolite area. The existing formal system for recognition and compilation of zeolite frameworks administered by the

IZA prompted the idea for its extension to include the various layered forms as well. It was proposed as an expanded concept of zeolite structures represented by a 2-dimensional table/graph.^{24, 28} In one direction there is the listing of frameworks as the primary structures and the various 2D forms, defined as secondary structures are listed in the perpendicular direction. This can be displayed, identifying species already known for a given type/framework, in different graphical forms for example as a table²⁴ or as shown in Figure 1. The proposed classification and notation are preliminary and subject to verification, validation and approval as the area continues to advance and develop. Some categories can be considered as trivial, especially the apparently collapsed structures. Similar materials were probably already encountered with the other layered materials but not considered as separate category or being meaningful. This is exemplified by the de-templated layered zeolite precursors. There are good reasons for their recognition as separate class: their powder X-ray diffraction pattern (XRD) distinct from the precursor with intercalated organic between layers, different reactivity towards swelling with other organics and production of so-called sub-zeolites upon calcination. Swelling of the precursors with the original template between the layers may be difficult or impossible, e.g. as shown by NSI.²⁹ After detemplation by acid treatment and conversion into protonic (detemplated) form, the precursor shows facile swelling with amines and other bases. Detemplated precursor often collapse upon calcinations into poorly ordered products with the repeat d-spacing lower than the condensed zeolite structure. For that reason they were dubbed Sub-zeolite structures. Special attention is justified to the interlayer expanded zeolites (IEZ)³⁰ that had no recognized counterparts among layered solids. They are described in detail in section 5 discussing special contribution to the 2D solid area from zeolites.



Symbol, structure	Layered form type, description	FER	CDO	AST	MFI	NSI	CAS	RRO	HEU	RWR	AFO	MTF	OKO	PCR	UTL	MWW	SOD
ZEO-Coll	Colloidal suspension	-	-	-	31	-	-	-	-	-	-	-	-	-	-	31	-
ZEO-Opi	Organic pillared	-	-	-	-	-	-	-	-	32	-	-	-	33	-	34	-
s-Pi-ZEO	Self-pillared	-	-	-	35	-	-	-	-	-	-	-	-	-	-	-	-
ZEO-Pi	Pillared zeolite	36	-	-	37	-	-	-	-	-	-	-	-	40	-	41	-
ZEO-Del	Delaminated swollen precursor	36	-	-	-	42	-	-	-	43	-	-	-	-	-	44	-
ZEO-Sw	Swollen precursor	36	45	-	-	29, 38	-	-	-	46, 47	-	-	-	48	-	41	-
d-ZEO-IEZ	Stabilized disordered precursor	-	-	-	-	-	-	-	-	-	-	-	-	-	-	49	-
ZEO-IEZ	Stabilized ordered precursor (IEZ)	30	30	-	-	50	-	51	-	-	-	-	-	52	-	53	54
Pre-ZEO-det	De-templated precursor; sub-zeolite	45	55	-	-	29, 38,	-	-	-	46	-	-	-	48	-	57	58
						56											
uSurf-ZEO	Unilamellar precursor with surfactant	-	-	-	59	-	-	-	-	-	-	-	-	-	-	-	-
mSurf-ZEO	Multilamellar precursor with surfactant	-	-	-	60	-	-	-	-	-	-	-	-	-	-	-	-
Del-ZEO	Monolayer; delaminated	-	-	-	-	-	-	-	-	-	-	-	-	-	-	61, 62	-
dPre-ZEO	Disordered multilayer precursor	-	-	-	-	-	-	-	-	-	-	-	-	-	-	63	-
Pre-ZEOd	Ordered multilayered prec. → incomplete 3D	64	-	-	-	-	-	-	-	-	-	-	-	-	-	-	-
Pre-ZEO	Ordered multilayered prec. → complete 3D	65	66, 67	68	-	69-71	72	73	-	74-76	77	78	-	52	-	79-81	82, 83
ZEO	3D Framework	84	66, 67	85	86	69, 70	87	73	88	26	89	90, 91	52, 92	52	82, 93	94, 95	96

Figure 1 Zeolite frameworks approved by the IZA Structure Commission in alphabetical order and their known layered forms with proposed nomenclature and references to the first reported and notable examples; status at the end of 2014 with 229 structures. Yellow boxes designate materials obtained by direct synthesis. Positions of the following frameworks pairs were switched for clarity: OKO ↔ PAU, UTL ↔ PSI,

RRO \leftrightarrow GOO, NSI \leftrightarrow CAN, CDO \leftrightarrow FRA, SOD \leftrightarrow *-SSO. Order of frameworks in the table/legend based on drawing from left to right Two drawings for a structure (in table) represent as-synthesized and calcined forms. The arrows ' \rightarrow ' in the description of Pre-ZEO and Pre-ZEOd refer to formation of a complete and incomplete (with uncondensed silanols) 3D structures upon calcination.

4. Overview of transformations of layered materials with layer structure preservation

The outstanding and particularly valuable characteristic of the layered materials is the possibility of their modification, structural and chemical, with preservation of the layer integrity. There are two basic chemical processes: host-guest reactions, i.e. intercalation or formation of inclusion compounds, and surface modification (topotactic). The latter typically requires presence of some distinct sites that can be chemically functionalized, e.g. surface hydroxyl groups. Intercalation is more universal and has been studied extensively for all classes with various compounds, mainly organic. This subject has been thoroughly reviewed and updated on a regular basis with regard to preparation, characterization and applications. Intercalation is the primary process for layer separation with the eventual goal of generating hierarchical layered materials with porous structure, but it is usually reversible. To achieve permanent structural modification the layer separation by intercalation must be accompanied or followed by additional action or events. Pillaring of clays by ion exchange of Al_{13} -oxo-Keggin ions ($[\text{AlO}_4\text{Al}_{12}(\text{OH})_{24}(\text{H}_2\text{O})_{12}]^{7+}$) exemplifies pillaring through intercalation but in practice requires activation and fixing at high temperature.

Table 2 Basic information about synthesis and structure of the layered materials discussed in this review.

2D class	Formula, composition	Availability, typical synthesis	Layer thickness, nm	Charge or H/OH density per nm^2
Clays ¹³	(Basic, no substitution ²)	Natural, hydrothermal		
1:1 Kaolin	$\text{Al}_4\text{Si}_4\text{O}_{10}(\text{OH})_8$		0.74	0
2:1 Smectite	$\text{Al}_4\text{Si}_8\text{O}_{20}(\text{OH})_4$		0.96	0.9-2.6
Vermiculite				2.6-3.9
Mica				~4.3
Brittle mica				~8.7
Zr phosphates ¹³	$\alpha\text{-Zr}(\text{HPO}_4)_2 \cdot 2\text{H}_2\text{O}$ $\gamma\text{-Zr}(\text{PO}_4)(\text{H}_2\text{PO}_4)_2 \cdot 2\text{H}_2\text{O}$	Reflux Zr salts with phosphates	0.76 1.16-1.22	4.2
Oxide nanosheets ¹⁷	$\text{M}_x\text{Ti}_{1-y}\text{O}_2$ MO_2 (Mn, Ru) $\text{KCa}_2\text{Nb}_3\text{O}_{10}$ $\text{Cs}_4\text{W}_{11}\text{O}_{36}$	Solid state, 800-1300°C (polycrystalline product)	0.75 ⁹⁷ 0.45 1.45 2.2	6.25 ²⁰ 6.7
Layered double hydroxides ¹⁷	$\text{M}_{1-x}^{2+}\text{M}_x^{3+}(\text{OH})_2\text{A}_{x/n}^{n-} \cdot m\text{H}_2\text{O}$	1. Coprecipitation (gel, low crystalline) 2. 'Homogeneous' coprecipitation (+ urea or $(\text{CH}_2)_6\text{N}_4$)	0.48 ¹⁷	4.1 for $\text{Mg}_2\text{Al}^{98}$ 3.2 for Mg_3Al
Rare earth ¹⁸	$\text{Ln}_8(\text{OH})_{20}\text{A}_{4/q}^{q-} \cdot n\text{H}_2\text{O}$	1. Homogeneous precipitation + $(\text{CH}_2)_6\text{N}_4$, reflux 2. Ln salts + NaOH, R_3N , hydrothermal	0.93 ¹⁷	4.1-4.4 ⁹⁸
Silicates ¹⁴		Hydrothermal, natural	(Basal spacing)	
Kanemite	$\text{NaHSi}_2\text{O}_5 \cdot 3\text{H}_2\text{O}$		1.0	5.6 ⁹⁹
Illerite, RUB-18	$\text{Na}_2\text{Si}_8\text{O}_{17} \cdot 9\text{H}_2\text{O}$		1.1	3.7 ¹⁰⁰
Magadiite	$\text{Na}_2\text{Si}_{14}\text{O}_{29} \cdot 11\text{H}_2\text{O}$		1.5	
Zeolite precursors		Hydrothermal with organic SDA	(Layer thick.)	¹⁰¹
MWW			2.5	1.12
FER			0.9	1.85
PCR/OKO			0.9	2.30
10 others				

The generation of porous materials from layered precursors has been focused predominantly on the oxide-based compositions, mainly from the insulator group and the redox AMO_2 oxides. They seem to provide suitable layer rigidity, which enables layer manipulation and generation of well-defined porous structures resulting in more or less structurally robust tractable products. The additional attributes of these types of layers that are required for application in sorption and catalysis include chemical and thermal stability, although in general these properties show a broad range of variability.

The principal transformations of layered precursors are illustrated based on 2D zeolites in Figure 2. Zeolites were chosen because they provide the broadest platform and diversity of structural modifications. The other classes considered in this review produce many but not all of the forms, both among the as-synthesized and modified materials. In some cases, such as swelling and exfoliation, the transformation of layered zeolite precursors seems to be particularly difficult and demanding. The reasons for that are not fully elucidated and maybe inherent. Alternatively it may be the novelty of layered zeolites that is the reason and with time wider range and milder conditions may be found.

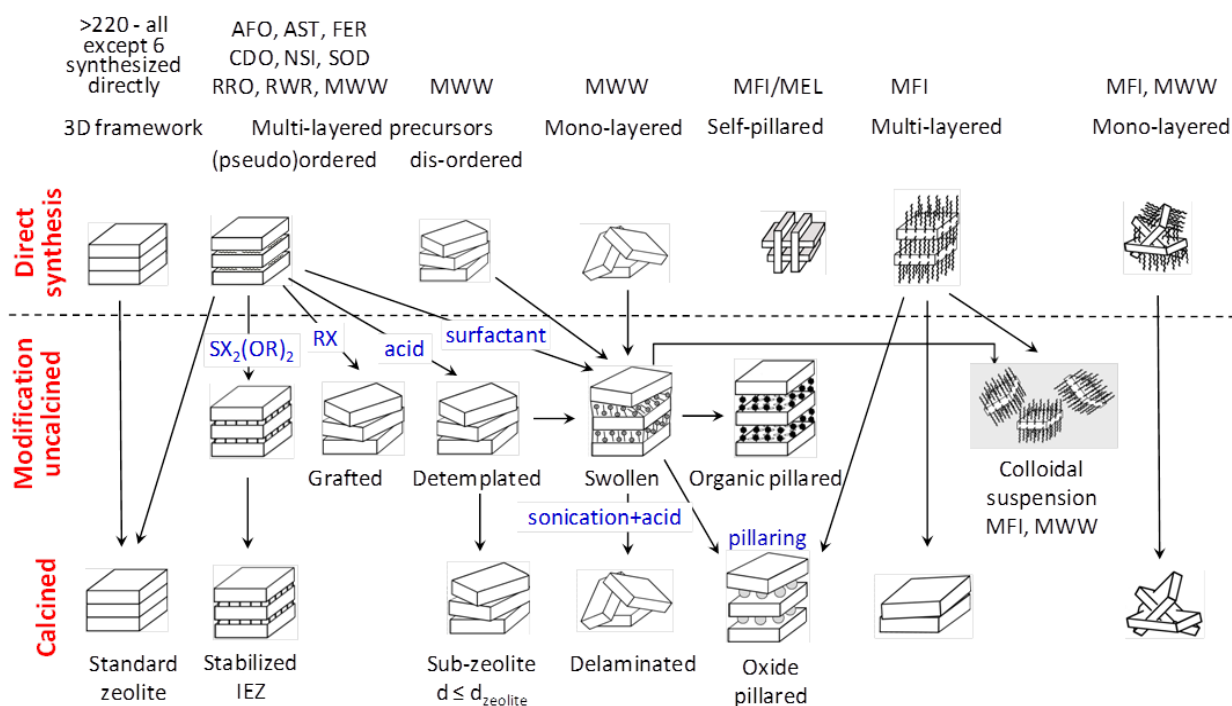


Figure 2 Principal modifications and structural transformation of layered materials exemplified by 2D zeolites. The representatives for selected layered form are specified with the 3 letter framework code.

Among the various types of materials shown in Figure 2 the prominent representatives of hierarchical porous materials can be readily identified as the pillared and delaminated species. They are the most common final goal of modification of the layered materials discussed here. Their preparation often entails intermediate steps like swelling and 'liquid exfoliation'. This makes the corresponding swollen and exfoliated forms also very important. Before focusing on these modifications we would like to

return to zeolites to consider their special contribution of various layered precursor forms that are unmatched by the other layered classes.

5. Special contributions from zeolites to the layered materials

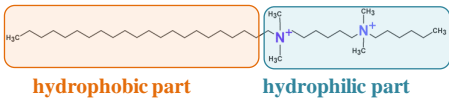
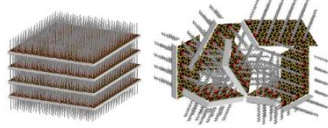
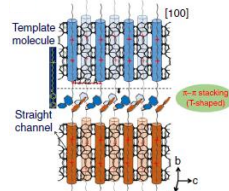
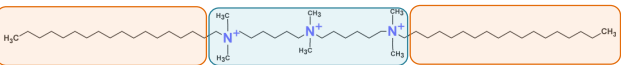
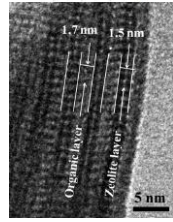
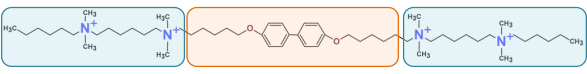
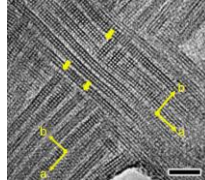
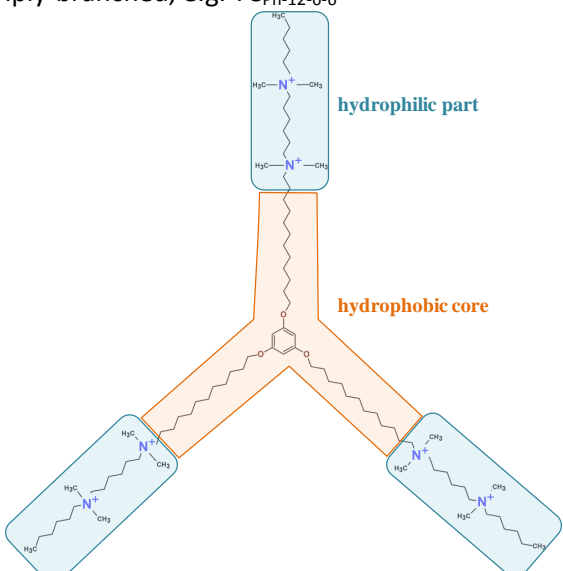
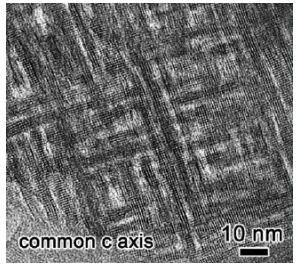
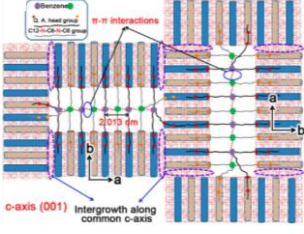
Layered zeolites precursors were discovered when many of the other classes of 2D solids were well known and developed. The 2D solid area was quite mature and often served as the template for expanding the layered zeolites. The discovery of 2D zeolites was an unexpected fundamental breakthrough although the underlying layered nature of zeolite structures and their possible formation via layered intermediates were contemplated prior to its 'reduction to practice'.¹⁰² One of the main efforts after the discovery of layered zeolite precursor was to replicate the known chemistry of the conventional 2D solids such as intercalation, swelling, pillaring and delamination. This has proven to be successful. On the other hand, zeolites revealed new phenomena and possibilities that were novel or unnoticed with the previously established 2D materials.

5.1 *New layered zeolites by design of novel structure-directing-agents*

The discoveries of layered forms of zeolites were in most cases accidental when trying to synthesize new 3D frameworks. The standard approach relies on using organic structure directing agents (SDA) as templates. Many of the preparations involved conventional organic SDA molecules like derivatives of cyclic amines, quaternary ammonium cations and others. In some cases one SDA molecule can lead to both 3D and 2D form of the same zeolite, like in the case of MWW, and it depends only on the chemical composition of the initial gel or/and synthesis conditions. This illustrates the unpredictability of the formation of layered zeolites in the case of common SDA molecules, which may simultaneously direct three-dimensional frameworks.

This situation inspired ideas of designing SDA molecules capable of directing exclusively layered zeolitic materials. The pioneering work was done by Ryoo and co-workers⁶⁰ who developed a strategy for designing bi-functional SDA molecules acting as micropore- and mesopore-porogenic agents. The suitable SDA molecules consist of two parts. First, the hydrophilic part presented by quaternary ammonium groups directs micropore formation similarly as conventional organic SDAs. It promotes the interaction with charged silica species in a gel and consequently formation of a crystalline zeolitic framework. The second part, hydrophobic one, prevents the uniform crystal growth by blocking propagation in the 3rd dimension.

Table 3 Different types of layered MFI materials prepared with designed structure directing agents (SDAs). The blue and orange rectangles indicate hydrophilic and hydrophobic parts of the molecule, respectively. Structure images reprinted by permission from Macmillan Publishers Ltd: Nature (**461**, 246-249), copyright 2009, and Nature Communications (**5**, 4262), copyright 2014 and from Chemistry of Materials, **26**, 7183-7188. Copyright 2014 American Chemical Society.

Organic structure directing agent (SDA)	Zeolite product	Structure
Single-alkyl-tail, e.g. C ₂₂₋₆₋₆  <p>hydrophobic part hydrophilic part</p>	Multilamellar and unilamellar MFI ^{59, 60}	
Single-aromatic-tail, e.g. C _{Ph-Ph-10-6} 	Single-crystalline mesostructured zeolite nanosheets (SCZN-1) ^{103, 104}	
Gemini, e.g. C _{18-N3-C18} 	Single-pore-zeolite ¹⁰⁵	
Bolaform, BC ₆₋₆₋₆ 	MFI nanosheets joined with a 90° rotational boundary (SZCN-2) ¹⁰³	
Triply-branched, e.g. TC _{Ph-12-6-6}  <p>hydrophilic part hydrophobic core</p>	Mesoporous ZSM-5 material with intercrossed nanosheets (MZIN) ¹⁰⁶	 <p>common c axis 10 nm</p>  <p>Intergrowth along common c-axis</p>

The design of new organic molecules enabling formation of thin nanosheets, or micro- and mesoporous hierarchical materials, has been attracting increasing attention. The concept of designed SDA was further progressed by the inventors and later other groups continued following this direction. Some among the novel SDAs have produced various nanomorphous materials with hierarchical porosity, not only 2D solids, but here we will focus only on those directing layered zeolites as relevant to this review.

The first designed SDAs containing one long carbon chain was referred to as a single-alkyl-tail SDA. The representative molecule is $C_{22}H_{45}-N^+(CH_3)_2-C_6H_{12}-N^+(CH_3)_2-C_6H_{13}$, for brevity designated C22-6-6 (Table 3). Its use led to the first synthesis of zeolite MFI in the form of nanosheets.^{60, 107} This was considered as a remarkable breakthrough because MFI is the second most important zeolite used in industrial catalytic applications.¹⁰⁸ In principle, the ammonium head templates crystallization of MFI layers while the long hydrophobic carbon chain prevents growth of the lamellae in the third dimension. As a consequence, MFI nanosheets are well-developed along a-c plane while being very thin with thickness of about 2.5 nm corresponding to about one unit cell along b-axis. The layers are composed of three pentasil layers with two parallel zigzag channels (in a-c plane) and one direct perpendicular channel (along b-axis). The nanosheets are stacked in a regular arrangement denoted as multilamellar with alternating inorganic (MFI) and organic layers.⁶⁰ The d-spacing repeat is equal to about 6 nm. Unlike in the typical layered zeolites, e.g. MCM-22P, PreFER and others, the removal of organic SDA from the multilamellar MFI does not produce complete three-dimensional framework. The high temperature combustion of organics (calcination) causes the collapse of nanosheets onto each other but only with partial condensation because of apparent layer mismatch and misalignment. This results in some void spaces between the nanosheets with overall BET up to $\sim 500 \text{ m}^2/\text{g}$, total pore volume $0.5 \text{ cm}^3/\text{g}$.⁵⁹ Alternatively, the as-synthesized layered MFI can be pillared, which is discussed in the corresponding section below. The synthesis of MFI nanosheets by using single-alkyl-tail SDA is sensitive to chemical composition of the initial gel and synthetic conditions can change spatial arrangement of the lamellae even for the same SDA. The presence of Na^+ promotes formation of multilayered crystals but under alkali free conditions, using the C22-6-6 hydroxide, the nanosheets are randomly assembled in an arrangement denoted as unilamellar.⁵⁹ The aluminum content impacts the synthesis time and the preferred arrangement. With increasing Al content the synthesis time generally increases and the multilamellar ordering is inhibited.³⁷ The unilamellar MFI preserves large interlayer space volume after calcination as the disordered nanosheets support each other like in a house-of-cards with possible contribution from some intergrowth. The calcined unilamellar material has large surface area (BET up to $\sim 700 \text{ m}^2/\text{g}$) and significant external surface as well as high total pore volume (up to $1.2 \text{ cm}^3/\text{g}$).⁵⁹ The mesopore size distribution is usually broad (5-25 nm) due to the random arrangement of the nanosheets.

The thickness of layers prepared with a single-alkyl-tail SDA (in both multi and unilamellar arrangements) can be controlled within a certain range by changing the number of ammonium groups in the SDA.¹⁰⁷ The ammonium group linked directly to the long carbon chain appears not to contribute to zeolite formation. It is postulated that the attached hydrophobic chain repulses charged silica species in the gel and thus prevents their interaction with the closest ammonium group.¹⁰⁷ The number of ammonium groups involved in the MFI nanosheet formation is the total number of ammonium groups (n) minus 1, i.e. $n-1$.¹⁰⁷ Hence, the minimum number of ammonium groups required is 2 like in C22-6-6.

It also explains why simple surfactants like hexadecyltrimethylammonium have not been very effective in directing zeolite synthesis.

The C22-6-6 SDA was also used in a dual template strategy in combination with tetrapropylammonium hydroxide (TPA-OH). By including TPA-OH in the synthetic gel the textural and catalytic properties of MFI nanosheets that are primarily templated by C22-6-6 can be tailored.¹⁰⁹ Under certain conditions the co-templating effect leads to a hybrid lamellar-bulk MFI (HLBM) zeolite with the bulk core and lamellar shell. The hierarchical nature of the hybrid material can be modulated by changing gel composition (e.g. C22-6-6 concentration) and synthetic conditions (synthesis time and temperature).¹¹⁰

Other MFI nanosheets similar to multilamellar ones reported by Ryoo et al. were prepared using single-aromatic-tail SDA containing naphthalene or biphenyl rings (see Table 3).¹⁰³ The single-crystalline mesostructured zeolite nanosheets (SCZN-1), as they are referred to, have similar characteristic to multilamellar MFI nanosheets being 2.7 nm thick along b-axis. More interestingly, the calcination of SCZN-1 leads to condensation of the MFI nanosheets by forming new Si-O-Si bonds. It indicates that using single-aromatic-tail SDA can lead to more ordered and/or less distorted nanosheets than those synthesized with single-alkyl-chain SDA as full condensation has never been achieved in the latter case. Detailed study on the influence of SDA structural parameters, like the number of benzene rings or the chain length, on the formation of SCZN-1 material was published later.¹⁰⁴ The single-aromatic-tail SDA contains only one ammonium group, therefore it does not follow the rule observed for single-alkyl-tail SDA (discussed above) where at least two ammonium groups are required for the formation of MFI nanosheets. One can speculate that the interacting hydrophobic aromatic-tails do not repulse the charged silica species to such an extent as micelles formed by alkyl tails, and thus enables MFI crystallization.

Another type of MFI layers was obtained with gemini type SDAs having two alkyl hydrophobic chains and the hydrophilic part (ammonium groups) located in between them (Table 3). The typical gemini SDA is $C_{18}H_{37}-N^+(CH_3)_2-C_6H_{12}-N^+(CH_3)_2-N^+(CH_3)_2-C_6H_{12}-C_{18}H_{37}$, designated for brevity as C18-N3-C18. This SDA produced even thinner zeolitic nanosheets consisting of only two pentasil layers with one parallel zigzag channel.¹⁰⁵ The layer thickness is approximately equal to 1.5 nm, which corresponds to about $\frac{3}{4}$ of the b lattice parameter in MFI unit cell). In this case the exact assignment of the framework type as a known zeolite topology MFI is not possible. The proposed designation is a single-pore zeolite or generally 10-ring zeolite nanosheets.

More changes in the stacking patterns of MFI layers and consequently new type of hierarchy were achieved by further modification of the SDA. One such example is the bolaform SDA which consists of aromatic-tail (with rigid biphenyl group) terminated on both ends by quaternary ammonium groups that can template MFI nanosheets (Table 3).^{103, 111} Biphenyl (or naphthyl) rings in the tail stabilize the lamellar structure via aromatic-aromatic (π - π) stacking interaction. Besides micelle formation via long alkyl chains this is another type of packing with a bulky hydrophobic barrier, which prevents the regular three-dimensional crystal growth. Theoretically, using the bolaform type of SDA with alkyl-tail in the middle should not be effective because it would not be able to form micelles or other packing that could prevent the regular crystal growth. The general formula for a bolaform SDA is BCX-Y-Z where X stands

for the length of the head alkyl group, Y for the chain between two ammonium groups and Z for the length of the middle aromatic chain.

The group of Hongxia Xi studied the effect of the aromatic chain length ($Y = 6, 10, 12$) and the length of the head alkyl group ($X = 4, 6, 8$) on the hierarchical nature of the final material.¹¹¹ The spacing between two ammonium groups was fixed by the C_6H_{12} chain (C6), i.e. BCX-6-Z. It was found that all such biphenol-bolaform SDAs lead to formation of multilamellar MFI nanosheets similar those reported by Ryoo.⁶⁰ However, by modifying the SDA structure one can control regularity of the nanosheets arrangement, their morphology and final textural properties. The representative material prepared with BC6-6-12 SDA exhibits BET surface area over $500 \text{ m}^2/\text{g}$ (with more than half of it assigned to external surface) and total pore volume $0.38 \text{ cm}^3/\text{g}$.¹¹¹ Based on the textural properties it is very close to the multilamellar MFI prepared by single-alkyl-tail SDA C22-6-6.

The group of Shunai Che investigated the same type of bolaform SDA containing biphenol group.¹⁰³ They fixed the length of the head group (C_6H_{13}) and the distance between two ammonium groups (C6) and modified only the aromatic chain length, i.e. BC6-6-n where $n = 4, 6, 8, 10, 12$. Unlike the Xi's group results they found that with a certain aromatic chain length of the SDA, particularly BC6-6-6 and BC6-6-8, MFI nanosheets are joined with a 90° rotational boundary. With shorter or longer chain the amount of intergrowths decreases significantly. This new hierarchical MFI denoted as SCZN-2 (single-crystalline zeolite nanosheets) exhibits high BET surface area up to $660 \text{ m}^2/\text{g}$ and total pore volume about $0.5 \text{ cm}^3/\text{g}$ with relatively narrow mesopore-size distribution centered around 2.4 nm .¹⁰³ Nevertheless, the authors acknowledge that calcination of MFI nanosheets prepared with this kind of bolaform SDA usually leads to either collapse of the lamellar structure forming bulk zeolite, or produce randomly stacked nanosheets, which under favorable conditions can be intergrown structures.

The same group of Shunai Che further developed this strategy when they designed a triply branched SDA (Table 3). The benzene ring is substituted at positions 1, 3, 5 with alkyl chains terminated with diquatery ammonium head.¹⁰⁶ This combines again the dual stabilization effect of diquatery ammonium head groups with strong π - π interactions in the hydrophobic core, which is said to enable micellar organization. A clear dependence of MFI crystallization and its hierarchical nature on the chain length was observed.¹⁰⁶ It was found that triply branched SDA with shorter alkyl chain, i.e. TcPh-10-6-6, enables crystallization of a single-crystalline mesoporous ZSM-5 (denoted as SCMZ). It contains sheet-like mesopores along a- and c-axis with thickness about 2 nm and lengths varying in the range $5\text{-}50 \text{ nm}$. More interestingly, the increase of alkyl chain length by only two carbons, i.e. to TcPh-12-6-6, affects the crystal arrangement in such a way that MFI is preferentially formed as $2\text{-}4 \text{ nm}$ thin nanosheets that are 90° intercrossed. This mesoporous ZSM-5 material with is abbreviated as MZIN. Its mesoporosity is preserved after calcination due to the nanosheets interconnection. This material exhibits a surface area of $\sim 550 \text{ m}^2/\text{g}$ and mesopore volume $0.37 \text{ cm}^3/\text{g}$.¹⁰⁶ The authors tried to explain the described phenomena of SCMZ or MZIN formation based on the size of micelles postulated to form in the first stages of crystallization. The shorter alkyl chain affords smaller micellar size, which enables crystal growth also along the b-axis and thus connects the crystalline domains. On the other hand, the larger micelle diameters favor formation of thin intercrossed nanosheets.¹⁰⁶

The above materials derived from the MFI framework are very important because the corresponding 3D parent is the second most useful and valuable zeolite, widely used in many catalytic processes. The layered forms have been reported to show advantages in applications such as methanol-to-gasoline and catalytic conversions of bulky molecules.⁶⁰ Their use in practice will depend on overcoming some the barriers that are discussed at the end of this review.

5.2 Hierarchical layered structures by direct synthesis

Layered materials are highly valued from the perspective of hierarchical structures because of the possibility of post-synthesis design and modification. On the other hand, for convenience and larger scale use it is desirable to minimize the number of modifications steps and direct synthesis is ultimately the preferable option. One such case was already mentioned above – the unilamellar MFI composed of single layers in random packing with possible intergrowth.⁵⁹ A completely different example is provided by the material called self-pillared-pentasil (SPP) containing zeolite MFI and MEL nanosheets.³⁵ Surprisingly it is obtained with relatively simple SDA, tetrabutylphosphonium cation (TBP), which induces formation of zeolite nanosheet intergrowths. TBP appears to contribute to anisotropic growth leading to single-unit cell nanosheets. The SPP is described as MFI nanosheets of one-unit cell thickness (along b-axis, 2 nm) that are intergrown with their 90° twins or as nanosheets that are rotational intergrowths having a common c-axis. The MFI nanosheets may be connected through threads of MEL zeolite. This is a remarkable new and low-cost method for the synthesis of hierarchical micro-/mesoporous zeolites. It appears to be limited to zeolite frameworks capable of anisotropic growing as thin layers or to zeolites supporting branching at certain acute angles.

The formation of intersecting zeolites layers was also achieved with faujasite but the layers are multi-unit cell thick. These layer-like zeolites are described in detail in Section 12.

The methods described above have been successful in producing mono-layers only with one framework, MFI. The design relies on having pores perpendicular to layers, which limits the number of suitable frameworks. The microporogenic centers in all reported cases are tetraalkylammonium cations. The presence of other amine-based head groups (related to pyridine, pyrrolidine etc.) may extend the application of the designed SDA to other frameworks. The introduction of bulkier components (like phenyl rings) into SDA structure already led to new kinds of mesoporous materials with beta or MTW topology,^{112, 113} however, they are generally described as nanosponges.

5.3 Top-down preparation of novel layered precursors from zeolites

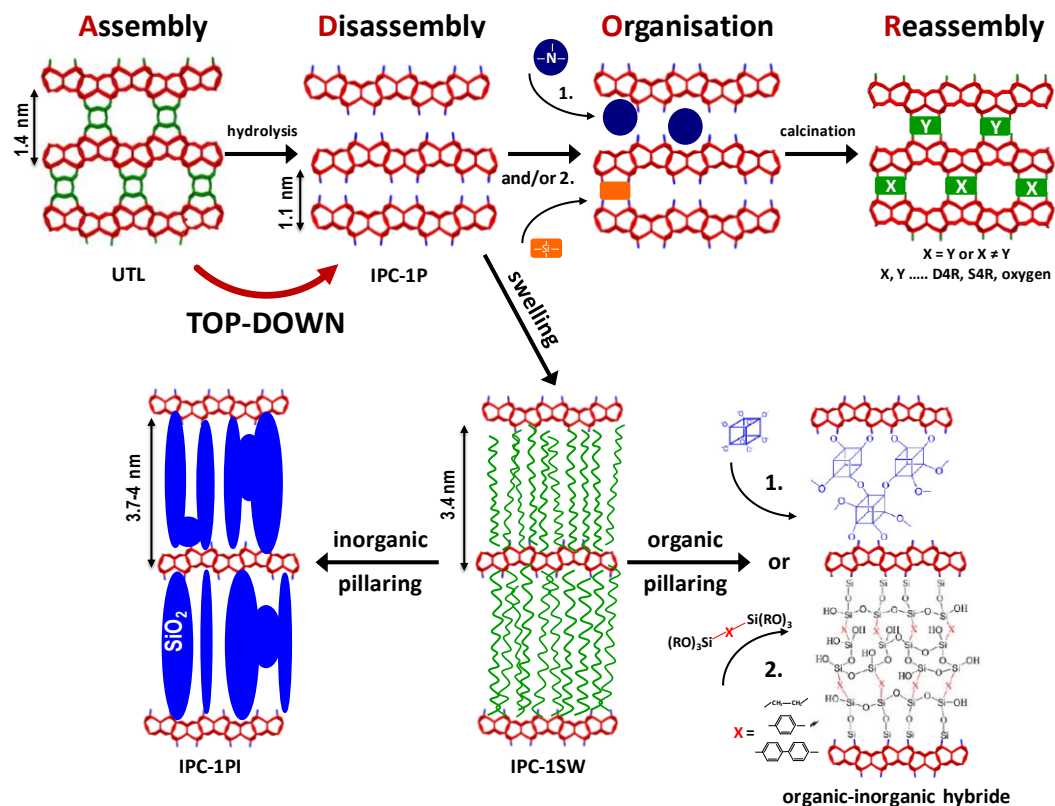


Figure 3 The general scheme of the ADOR method involving top-down synthesis of the layered IPC-1P material from the UTL zeolite. The precursor IPC-1P can be transformed into new zeolites with controllable pore size (the A-D-O-R pathway) or expanded by swelling and pillaring leading to materials with increased pore sizes and void volumes.

The basic primary layered materials, both natural and synthetic, are obtained by direct synthesis, (assembly) from mixtures of ingredients. This is a bottom-up approach starting from a gel that is converted into more complex crystalline solids, usually under solvothermal conditions. Formally it can be defined as going from 0-dimensionality to 2D. The top-down pathway, from 3D to 2D has been rarely considered, not only because the opposite direction from 2D to 3D appears like a more rational goal and is often the actual objective. First, there is the problem with feasibility of going from full 3D connectivity down, especially if wanting to do so in a controlled way. Second, practical merits of such degradation may be questioned. While both of these issues are valid a top-down approach has been demonstrated and showed attractive features. Specifically, it produced layers with previously unknown internal structures and revealed new phenomena and interlayer chemistry, such as layer ordering upon intercalation of organics.¹⁰¹ The top-down approach is based on structural degradation of a three-dimensional system into two-dimensional lamellas by post-synthesis treatments. It is not completely new as prior examples of ‘selective extraction processes’ applied to other types of materials have been known. For instance, thermal extraction of Si atoms from SiC single crystals produces epitaxial growth of graphene.¹¹⁴ In another case, the synthesis of 2D transition metal oxides was enabled by selective

leaching out of alkali cations from their three-dimensional salts.¹¹⁵ Similarly 2D early transition metal carbides and carbonitrides called MXenes can be prepared by the selective etching of elements like Ti, Nb, Mo, V, etc. from carbides and nitrides.^{116, 117}

These examples give a clue, which materials are suitable for the application of the 3D to 2D method. Their common feature is the presence of some elements, or more specifically bonds, which are under certain conditions more sensitive or susceptible to leaching out of the framework than the others might be. The perspective by Morris and Čejka discussed materials containing some built-in weak sites.¹¹⁸ They focused on materials with regioselective weakness, i.e. those with weak bonds specifically located in the framework. Using selected as examples MOF and zeolite structures it was pointed out how this regioselective weakness can be turned into advantage. Weak bonds can be selectively broken or remade to influence the properties of a solid. This is the guiding principle of the top-down method developed for the preparation of 2D layered zeolites from 3D frameworks. These new 2D materials can be transformed by the conventional approaches into expanded hierarchical structures.⁴⁰ They also revealed a new potential for re-assembly into new frameworks and hierarchical materials by the process designated ADOR.^{52, 119}

So far the number of layered zeolite materials represents less than 10% of all frameworks and all of them, except the case now being discussed, have been obtained by the bottom-up approach. The top-down method was first recognized with germanosilicate UTL.⁴⁸ The class of germanosilicate zeolites has experienced a great expansion from the beginning of 2000s.¹²⁰ Germanium was found to favor formation of small rings, like double-four-rings (D4R), single-three-ring (S3R) or double-three-rings (D3R).¹²¹ The inclusion of germanium in synthetic gels, sometimes in combination with fluoride anions as a mineralizing agent, enabled the discovery of more than 20 new frameworks. Many of them are characterized by large or extra-large pore channel systems and low-density frameworks. This attracts a lot of attention due to their potential catalytic application including reactions of bulky molecules. The major drawback of germanosilicates is their overall decreasing hydrothermal stability with increasing germanium content. The germanium oxide bonds are susceptible to hydrolysis even by air moisture. However, this was recently recognized as a possible advantage enabling transformation of 3D frameworks into 2D materials with new layer structures and representing a top-down method of preparation.

Germanium in zeolite UTL is located almost exclusively in D4R units which act as pillars separating rigid nonporous layers. By hydrolysis under mild acid conditions (0.01-1M HCl at 85-100°C), these D4Rs units can be removed yielding stacks of silica layers bonded only via hydrogen bonds.^{40, 48, 52, 122} This top-down process afforded novel layered zeolite called IPC-1P by the regioselective hydrolysis. This new layered material turned out to be the precursor to a new framework PCR, not known at that time, but obtained later from this precursor. Similarly results were demonstrated with other germanosilicates like IWW, ITH, IWR, ITR, containing enough germanium atoms in D4R units to be selectively removed by hydrolysis.^{123, 124} The top-down method for generating zeolite layers was further developed into a more complex strategy called ADOR. The abbreviation stands for Assembly-Disassembly-Organization-Reassembly. In principle it means first to synthesize the parent 3D zeolite (Assembly), thereafter hydrolyze it into a 2D layered material (Disassembly), subsequently organize the layers into a suitable

position with respect to each other (Organization) and finally calcine the material to obtain a novel 3D zeolite (Reassembly), see Figure 3.

This methodology is novel in two respects: it is the first top-down method for synthesis of new layered zeolites and it enables preparation of new zeolites with predictable topology and controllable porosity. Moreover, the top-down mode offers another advantage in comparison to a bottom-up approach. It is related to the use of a 3D zeolite with known topology as the starting material. The weaker germanium bonds can be regioselectively removed without disrupting the remaining framework. Therefore, the topology of obtained lamellae is the same as in the parent zeolite and consequently it is relatively easy to identify. In the case of the bottom-up synthesis the structure of a new product is unknown and its determination can be very complicated and time consuming.

As layers can be used as basic hierarchical units, by their subsequent manipulation the hierarchical nature of the final solid can be 1) further developed/preserved by the conventional approaches through modification of the interlayer space; or 2) modified in a non-traditional way by condensation of the layers forming novel 3D zeolites and other frameworks, e.g. not 4-connected (see Fig. 1). The second procedure is exemplified by formation of new connective units between the layers like single oxygen bridges, single-four-rings (S4R), or even double-four-ring (D4R), using varying hydrolysis conditions and optionally intercalation chemistry.^{52, 125, 126} For more details readers are referred to the recent review paper devoted to the ADOR strategy.¹⁰¹ Different connecting units give rise to distinct channel systems. For instance, with single oxygen bridges between the layers the reassembled zeolite PCR (also denoted IPC-4) has 10-8-ring channels; with S4R units the zeolite (denoted IPC-2) has 12-10-ring channels. More importantly, it is possible to direct the overall distribution of new connections to have 100% of the layers with one type of connection or the combination of two different layer connections in the final material in range 0-100%. In this manner two unique zeolites were prepared containing two types of layer connections. Zeolite IPC-6 has about 50% layers interconnected via oxygen bridges and 50% with S4Rs. These two types of connecting units constructed two independent channel systems, 10-8-ring and 12-10-ring, respectively. Similarly, it is with IPC-7 zeolite, which has about 50% of layers connected with S4Rs and 50% with D4Rs leading to two independent channel systems with sizes 12-10-ring and 14-12-ring.³¹ Both IPC-6 and IPC-7 zeolites can be considered for hierarchical materials (in broader sense of definition) because they were prepared by post-synthetic manipulation with the layers (as basic hierarchical units) and they contain two different levels of porosity, although both in micro scale.

In summary, the ADOR method provides a new synthetic tool to prepare various materials having a common topology of the layers but differing in the layer connectivity. It is achieved by a top-down generation of zeolitic layers and subsequently by their spatial manipulation using various post-synthetic modifications.

5.4 Interlayer expanded zeolites (IEZ)

The key observation leading to the discovery of layered zeolite forms was contraction of the as-synthesized precursor upon calcination by about 0.2 nm or more. It was evident based on the differences in the XRD patterns and was caused by removal of interlayer template and condensation of silanols from the opposite layers. The opposite observation, namely the absence of the expected

contraction upon calcination of as-synthesized precursors, was the basis for the discovery that appeared to have no obvious counterpart among the non-zeolite based 2D solids.⁵³ It was initially referred to as 'stabilization of (expanded) layered precursor' but the corresponding products are now called interlayer expanded zeolites, IEZ. They are formed when silanol pairs on opposite layers become bridged by an $=\text{SiR}_2$ moieties, R= organic or OH, which substitute the silanol protons. Instead of the oxygen $-\text{O}-$ connecting the layers as part of the framework there is now the $-\text{O}-\text{SiR}_2-\text{O}-$ bridge as a discrete pillar preserving the 3D periodic structure. This produces an expanded zeolite-based framework, which is not a formal zeolite, with interlayer pores increased by two Si–O links and expanded pore size by about 0.2 nm. Novel circumstances occur when the bridging groups are close and can couple together forming additional Si–O–Si connections parallel to the layers. It was reported first for IEZ-ferrierite.¹²⁷ In the case of the PCR precursor, IPC-1P, there are four such bridges close to each other. Their condensation produces a complete zeolite structure, IPC-2, which was also produced by an alternative route and recognized as framework OKO (COK-14).⁹² The expanded IEZ materials can show increased uptake metals with benefits for catalysis and this further discussed in the section on activity (number 13). The formation of IEZ analogues with the non-zeolitic layered materials has not been explored and is yet uncertain.

5.5 Layered material AMH-3

This silica-based layered material deserves a special mention because of its zeolite like 8-ring pores in all 3 directions in the layer, including perpendicular.¹²⁸ This is the first such materials reported. It may produce hierarchical layered structure with transport through the layers. The layers have the possibility of condensing into two 4-connected frameworks, still hypothetical, i.e. not synthesized yet, which makes AMH-3 a potential layered zeolite precursor. It is prepared from the mixture of alkali, strontium and titanosilicate by hydrothermal synthesis at 473 K. The structure collapses at 773 K. AMH-3 can be swollen from 1.14 to 4.1. nm d-spacing by combined treatment with DL-histidine and dodecylamine. The swelling with quaternary ammonium surfactants, dodecylamine by itself and other intercalating reagents was tried but found to be ineffective.^{129,130} Successful swelling was accompanied by partial silica condensation and structural changes of the layers. Accordingly, the product was pronounced to be a new material not an AMH-3 intercalate. The swollen material was combined with a polymer to form a nanocomposite, which showed improved selectivity for hydrogen/carbon dioxide separation in comparison to the pure polymer.¹²⁹ Swelling of AMH-3 with diamine was reported to preserve its pore structure.¹³¹ Functionalization with octyl(methyl)dimethoxysilane increased hydrophobicity of the surface increasing the potential for more effective incorporation in polymer membrane materials.¹³²

5.6 Layered metal-organic-frameworks (MOF)

MOFs are inorganic-organic frameworks with extended structures consisting of metal or metal cluster centers interconnected by coordinating organic molecules called linkers.¹³³ There has been an explosion in the interest and the number and varieties of MOFs. They are investigated fundamentally and for applications as porous and catalytically active materials. MOFs are known predominantly as solids with 3D connectivity but also afford 2D layered forms.¹³⁴ By analogy to zeolites the existence of layered precursors that can produce corresponding 3D frameworks can be also imagined. The principal question concerning 2D MOFs is their potential for layer manipulation like it is possible with the other layered solids. This possibility has not been systematically explored and in practice there are complications

related to large void spaces inside MOFs structure. The porous nature of potential MOF layers maybe be beneficial while majority of the other 2D classes have no pores in the layers. However, MOFs have propensity for interpenetration of networks,¹³⁵ which might be undesired for exploiting through-the-layer porosity. MOFs are also less chemically and thermally stable than typical oxide solids, especially zeolites. Several types of MOF materials with 2D structure are presented in Figure 4.

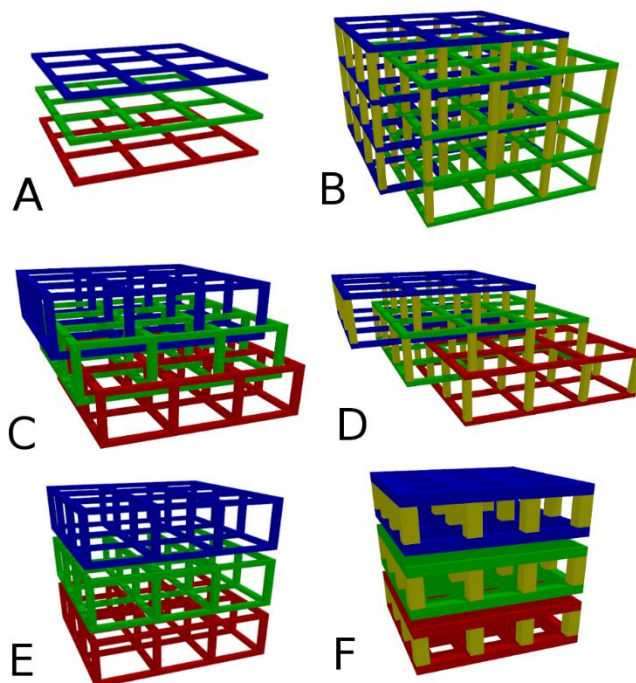


Figure 4 Schematic representation of 2D MOF structures. A-monolayers; B,C,D-pillared monolayers; C,E-bilayers. B, C, D are interpenetrated structures. F - porosity introduced by pillaring of impermeable layers. Specific examples are discussed in the text.

The simplest type of layered MOF is the case of frame-like monolayers that are stacked together¹³⁶⁻¹⁴⁰ (Figure 4A). They can be modified to build classic 3D,¹⁴¹ interpenetrated 3D (Figure 4B),¹⁴²⁻¹⁴⁶ separated¹⁴⁷ and interpenetrated bilayers¹⁴⁸ (Figure 4 F and D, correspondingly). On the other hand a 3D structure can be disassembled into 2D layers.¹⁴⁹ If the linker is bent and long enough even monolayers can be interpenetrated.¹⁵⁰

There are examples where bilayers are formed during primary synthesis in both interpenetrated¹⁵¹ and stacked¹⁴⁷ modes (Figure 4C and E, correspondingly). Further modifications of stacked layers are possible which may lead to intercalation of even long molecular chains.¹⁴⁷ Some of 2D Metal-Organic-Frameworks undergo reversible structural and sorption capacity tuning,¹⁵² for others small amount of alcohol may lead to shift of gate opening for CO₂ to lower p/p^0 values.¹⁵³

6. Separating layers in 2D materials – general trends

The transformation of 2D layered precursors into hierarchical porous materials depends on their ability to allow layer separation and subsequent or concomitant structural and chemical modification. The layers, considered to be separated by definition, in practice are usually present as assemblies or agglomerates with various degrees of adhesion imposing a specific structure. An even more important factor, that is usually not considered explicitly, may be the intergrowth of layers or particles. The preexisting arrangement of layers can be changed in terms of interlayer distances and orientation by exploiting the intercalation potential of 2D materials. It is strongly dependent on the nature of both the layered host and potential guest molecules. As one of the most prominent features of layered materials, the intercalation has been regularly reviewed and updated. With regard to separation of the layers two specific situations with practical consequences can be distinguished: swelling, i.e. significant increase in volume and/or interlayer distance, and complete separation of the layers into independent entities usually in some dispersing medium like liquid. The latter process is called delamination or exfoliation. Both terms are often used interchangeably to denote layer separation in general¹⁵⁴ but sometimes are explicitly applied to describe different phenomena.

Before continuing with specific discussion, the layer separation ability of various classes will be briefly overviewed for comparison. There are two basic practical questions concerning the separation, expansion and modification of layers in 2D materials: how easy it can be accomplished and whether the starting precursor needs to be transformed first into a more reactive and expandable form. An exchange of the originally present cations or organic molecules by treatment with appropriate acid is a common form of activation. The 2:1 clays provide possibly the most convenient option. They can be expanded with concomitant pillaring and exfoliated into single sheets in water in some of their Na⁺ and Li⁺ forms.¹⁵⁵ The 1:1 clay kaolin has layers connected via hydrogen bonding, which can be disrupted by small polar molecules.¹⁵⁶ Expansion to more practically meaningful dimensions is possible by substitution with larger guest compounds.¹⁵⁶ The layered Zr(IV) phosphates and related compounds are exfoliated by treatment with a water/acetone mixture and amines.¹³ It exposes all layers to subsequent reactions and processing. There are many direct approaches to expanding and exfoliating layered double hydroxides,¹⁴ which can be considered as being quite easy. Layered transition metal oxides can be also conveniently and readily modified to achieve dispersion into single layers.^{17, 97, 157, 158} This is frequently preceded by conversion into protonated forms by contacting the original cation containing substrate with an acid until the exchange reaches satisfactory level. Tetraalkylammonium hydroxides or amines are then used to produce the desired interlayer expansion. Layered silicates can be also expanded by direct exchange of the alkali with large organic cations or with amines upon conversion into layered silicic acids. This is illustrated by exemplary systematic studies in this area by Lagaly et al.^{159, 160} So far layered zeolites proved to be rather difficult to expand.^{16, 41} There is a significant difference between them and most of the other layered solids, namely their as-synthesized forms contain organic structure directing agent embedded between layers. The intercalated SDA molecules must be usually removed first by acid treatment and the resulting protonic form can then be reacted with appropriate intercalating/swelling agent. Swelling requires basic pH and therefore adds another complication, which is the possibility of partial layer dissolution. Layered silicates and zeolites are also more difficult to convert into the exfoliated state in a liquid. Whether this is due to intrinsic factors or simply because more convenient methods have not been found yet remains to be seen.

7. Synthesis of pillared layered materials

Pillaring is a “process by which a layered compound is transformed in a thermally stable micro- and/or mesoporous material with retention of the layer structure.”¹⁶¹

The concept of pillared materials started with tetraalkylammonium exchanged clays.¹⁶² They demonstrated expanded interlayer space and permanent microporosity but had limited thermal stability because of organic nature of the pillars. The stability problem was solved by incorporation of inorganic pillars by the treatment of clays with solutions containing Al-oxo oligomers.^{163, 164} Aluminum Keggin ion $[\text{Al}_{13}\text{O}_4(\text{OH})_{24}(\text{H}_2\text{O})_{12}]^{7+}$ is usually considered as the representative species that is substituting smaller cations between clay layers. It expands interlayer galleries producing basal spacing increase from 0.96 to ~1.8-1.9 nm.^{13, 165} Upon calcination the intercalated Keggin cations fuse with layers and are no longer exchangeable. The pores generated between layers are in the micropore range but many are greater than in zeolites like FAU, i.e. >0.7 nm. The BET surface area is also increased reaching values up to 500 m²/g. The primary incentive for production of Al-pillared clays was to have active materials for catalytic cracking with pores larger than provided by zeolites. They were promising but suffered two disadvantages: increased coke production and insufficient hydrothermal stability. The alleviation of these deficiencies has been one of the primary drivers for the subsequent studies of both different pillar compositions and the other classes of 2D materials. A wide variety of pillared layered materials has been produced as the result.

Clays have turned out to be one the easiest layered solids to pillar. Consequently they have been reported with a great diversity of pillar compositions and forms.¹⁶⁵ First, the similarity between Al and Ga was exploited to produce the Al-Keggin ion partially substituted with Ga as well as all-gallium form for pillaring. The oxo/hydroxo clusters of others metals like tetrameric zirconium, octameric iron with organic ligands, dimeric and hexameric chromium and others were used for pillaring. Another approach entailed mixed compositions with the Al polymers as the principal component. The most common combinations were Al with Fe and Ga, then with Zr, Cr, Cu, Ge, Mo, Ru, lanthanides. Other reported combinations comprised of tri-metallic pillar compositions with and without Al as well as binary without Al, e.g. Fe with Cr and Zr. Most of these products were expected to end up as calcined oxo/hydroxo materials but other pillaring agents that were not as thermally stable have been also investigated. To this group belong the hexameric chlorocomplexes of Nb, Ta and Mo, organometallics like Cp₂Ru, and coordination compounds with organic ligands. It was also possible to incorporate between the clay layers much bigger entities like metal oxide sols and the tubular aluminosilicate (imogolite), which has diameter 2.3 nm.¹⁶⁶ The corresponding composite with montmorillonite has d-spacing 3.4 nm.

Aside from the goal to overcome the stability and coking problems of the original Al-pillared clays the diversification effort also sought to tailor compositions to a particular catalytic functionality and increasing height of the interlayer space, i.e. basal spacing.

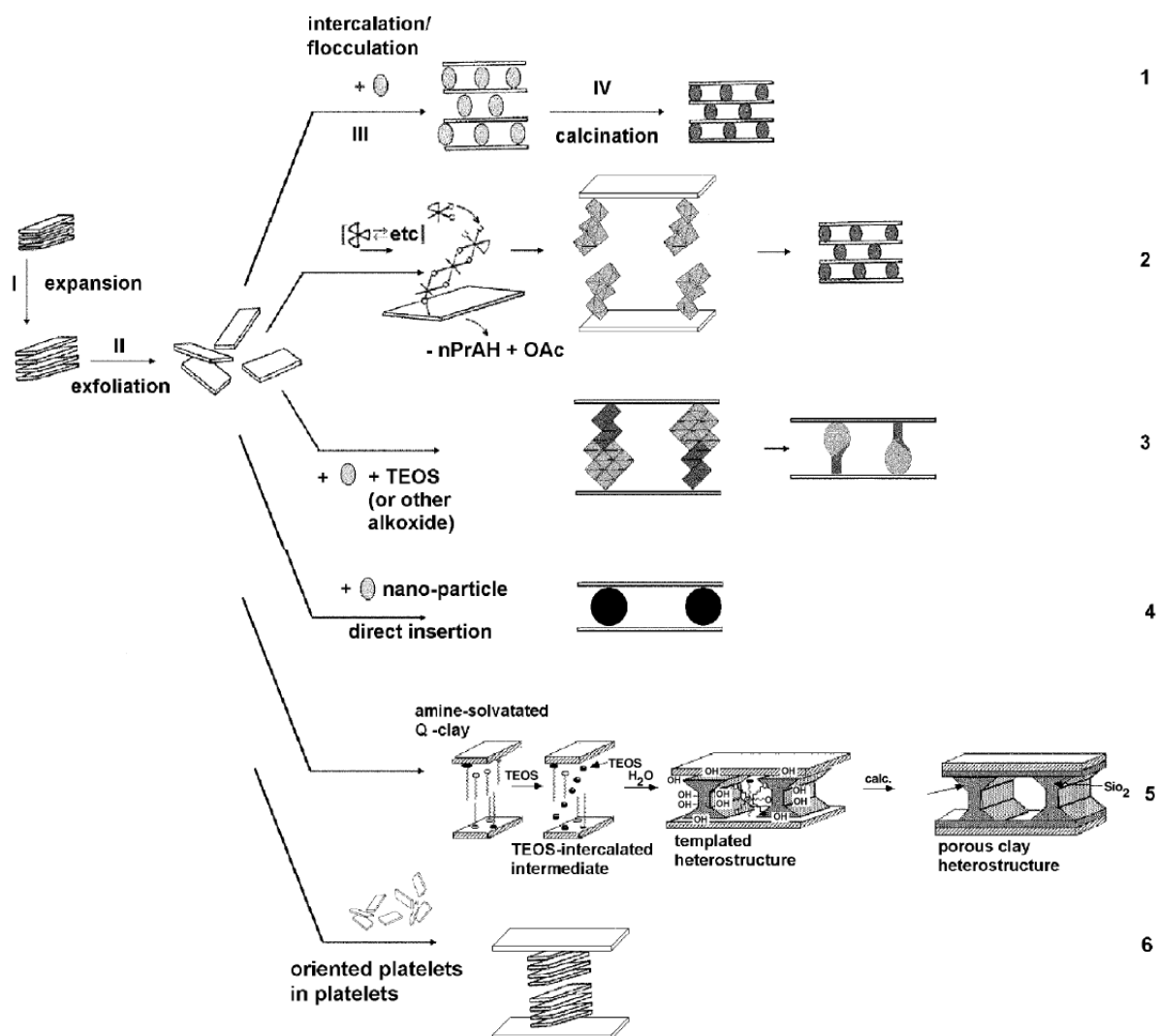


Figure 5 Different methods for pillaring clays (from top to bottom):¹⁶⁷ 1. The traditional Al-Keggin ion route; 2. Surface hydrolysis and polymerization of oxide precursor; 3. Sol-gel intercalation; 4. Intercalation of nano-particles; 5. Porous clay heterostructures; 6. Platelets as pillars (Reprinted from *Catalysis Today*, Vol. 114, pp. 126-141, A. De Stefanis and A. A. G. Tomlinson, Towards designing pillared clays for catalysis, Copyright 2006, with permission from Elsevier).

A new class of expanded clay materials called porous clay heterostructures was obtained by combining two novel strategies reported in the early 1990: the use of surfactants to generate ordered mesoporous structures^{168, 169} and pre-swelling of layered oxides before treatment with pillaring reagents.¹⁷⁰ The synthesis involved expansion of the clay by reaction with a cationic quaternary ammonium surfactant and long chain amine as co-surfactant.¹⁷¹ The isolated swollen intermediate was treated with the

pillaring silica precursor such as tetraethylorthosilicate, TEOS, followed by calcination. The obtained products exhibited much higher basal spacing than those prepared conventionally by the ion exchange approach. This is exemplified by expansion to d-spacing up to 4 nm, correspondingly greater pore dimensions, ca. 2.5 nm and BET surface area of the order of 900 m²/g. This method of pillaring was applied to the other layered classes e.g. kenyaite and titanosilicate.^{172, 173} The silicate kenyaite swollen with dodecylamine and pillared with TEOS was expanded to basal spacings 5-5.5 nm resulting in BET close to 900 m²/g.

The use of Al-oxo clusters as well as other potentially pillaring compositions that was developed with clays has been extended to the other layered classes like silicates,¹⁷⁴ zirconium phosphates¹⁷⁵ and transition metal oxides.¹⁷⁶ In these cases high charge density of the layers favored dense packing of the pillaring particles like the Al-Keggin ion in the galleries. Frequently this left little void space resulting in low porosity of the final products. Nonetheless, there are many reports describing various types of layered materials with diverse pillar compositions.

Zirconium phosphates were initially pillared by procedures resembling those from the clay area.¹⁷⁵ The starting layered precursors were intercalated or exfoliated with amine. Then they were combined with the oxide precursor solution such as the Al-Keggin ion, other metals and mixtures, and heated. The textural properties of the products obtained after calcination varied depending on composition, i.e. types of metals and ratios, and conditions. The expansion to d-spacing as high as above 4 nm (as-synthesized) and 3 nm calcined, and BET up to 700 m²/g were reported.¹³ The overall quality of the pillared products seemed not to be as high as with clays. This is illustrated by the general characterization articulated as follows:¹³ "The difficulty with pillaring of the layered metal phosphonates is the inability to control the synthesis reactions to obtain predictable structures. Furthermore, the structures obtained are noncrystalline or poorly crystalline."

The known lability of hydrogen phosphate groups in γ -M(VI) phosphates inspired another type of pillaring that involves substitution with organic phosphonates.¹³ The presence of organic part results in reduced thermal stability but is notable as an example of ordered/periodic pillaring, which so far is quite rare (another example is provided by interlayer expanded zeolites). The substitution is carried out by treatment of exfoliated γ -zirconium phosphate, e.g. in acetone-water mixture, with biphosphonic acid. Low concentration of the latter ensures crosslinking of the opposite layers. Porous structure is created if density of the bridging groups is appropriately low. The strategies for pore generation were not limited to judicious selection of crosslinking biphosphonates and conditions of the preparation. The density of 'pillars' has been controlled by the presence of smaller moieties, like phosphites, which are referred to as spacers. The methods of introduction include the use of mixed pillaring compositions of bisphosphonate crosslinking ligand with monophosphonate spacer or a second biphosphonate with hydrolysable organic moiety, which can be removed. Another benefit of the pillared Zr(IV) phosphonates is the ability to functionalize the organic fragments. For example aromatic part of the pillar can be functionalized with SO₃H groups generating strong acidity. Another variation involves the use of linear organic bridges combining acetylene groups linking phenyl rings. This is be considered 'analogous to the isorecticular extension of ligands in MOFs'.¹³

Pillaring of the other layered compositions, namely metal oxides and silicates, with Al-Keggin ion and related substances presented similar problems like the Zr(IV) phosphates. The isolated products were reported to show expanded interlayer spacing and increased porosity but overall seem to be poorly crystalline and not particularly well defined. The higher charge density compared to clays was blamed as the primary factor for low porosity but other chemical reasons could also play a role. Better control over synthesis conditions and the properties of the products was clearly needed.

The pillaring of layered oxides of titanium and manganese with Al-Keggin ion was approached from a new direction.^{177,178} The suspension of Ti/Mn oxide nanosheets can produce pillared nanocomposites upon mixing with the solution of Al-Keggin ion. A double-layer pillared structure is obtained, d-spacing 2.3 nm with high concentration of the pillar and single-layer, d-spacing 1.4, with lower concentration. The pillared titanate had BET $\sim 300 \text{ m}^2/\text{g}$ while the standard pillaring produces 100-200 m^2/g . The Mn analogue had BET of $\sim 200 \text{ m}^2/\text{g}$.

The intercalation of negative polyoxometalates (POM), e.g. Keggin anions, between positive LDH layers could be viewed as reverse pillared clays.¹⁷⁹ The typical products show low microporosity due to high charge densities and formation of nanocomposites. There are also problems with preparations and stability due to adverse effects such as leaching of cations from the layers in acidic and neutral solutions and instability of the POMs themselves.

A novel approach to pillaring allowing better control over the outcome was developed in the early 1990s.¹⁷⁰ It was a multi-step procedure referred to as a 'method for preparation of molecular sieves from dense, layered metal oxides'. The first step involved expansion of interlayer space, swelling, by intercalation of long chain polar organic molecules. The swollen product was isolated and treated with soluble inorganic oxide precursors, especially TEOS. Subsequent calcination created permanent oxide props supporting the layers and producing void space between them. The procedure was illustrated by the prepared layered silicates and alkali titanates. Using octylamine as the swelling agent the interlayer expansion up to 2 nm was achieved, while BET surface areas were increased from negligible to about 300 and 600 m^2/g for titanates and silicates, respectively. Another outstanding benefit of the method was the ability to control the interlayer expansion and consequently the pore system by simply choosing the size (length) of the swelling agent. The authors illustrate this by the swelling of $\text{Na}_2\text{Ti}_3\text{O}_7$ with a series of alkylamines with increasing length: propyl, hexyl, octyl and dodecyl. The d-spacings increase gradually to 2.1 nm and BET surface area to 470 m^2/g .

This approach can be used as a general strategy. It was quite effective and enabled close monitoring of the interlayer expansion and its permanent propping by X-ray diffraction. Pillaring with TEOS proved to be relatively easy when the swelling was successful. The drawback of TEOS is its lack of catalytic activity, which prompted efforts to incorporate more active heteroatoms and functional groups in the pillars. The use of alternative, potentially more active pillar precursors like alkoxides of aluminum, titanium and other metals, affected the quality and porosity properties of the final products. TEOS appears to have suitably slow kinetics of hydrolysis, which enables penetration into the interlayer region and depositing as pillaring oxide precursor. Not much is known about this process in detail.

The discovery of layered zeolite precursors^{79, 80, 95} was recognized as an opportunity to produce pillared materials combining large pores and strong acid sites. The direct synthesis of zeolites with pores larger than 12-ring and high catalytic activity was not known at that time. The pillaring of layered zeolites having strong acid sites was an alternative for circumventing these problems. Swelling became a key issue and since the known traditional methods failed, it required an innovative approach. The desired interlayer expansion allowing pillaring with TEOS was achieved by swelling with cationic surfactant in hydroxide form. In the first reported case,⁴¹ the precursor MCM-22P, with the framework structure MMW and layer thickness 2.5 nm was swollen with hexadecyltrimethylammonium hydroxide (HDTMA-OH) to d-spacing above 5 nm. Complete swelling required high pH but was also affected by the presence of smaller cations, which apparently could compete with HDTMA⁺ and prevent layer separation.^{180, 181} Layer dissolution was also a possibility and had to be considered especially since the solubilized silica could produce surfactant templated mesoporous phases and give false signs of pillaring.¹⁸² This swelling method was also adopted later for the preparation of delaminated materials.⁴⁴ The evidence of successful production of the pillared zeolite product, MCM-36, factored in all of these possibilities.⁴¹ It was based on X-ray powder diffraction, TEM microscopy and high sorption of hydrocarbons. Dynamic sorption measurements confirmed absence of contamination with a mesoporous phase. MCM-36 showed superior performance to MCM-22 in isobutene alkylation despite containing up to 50% w/w of inert silica as pillars. This proves that it is qualitatively a different type of a material. Layered silicate NU-6(1), later shown to be the precursor to zeolite framework NSI, was swollen and pillared by the same approach.²⁹ The described pillaring method was also applied with ferrierite (ITQ-36)¹⁸³ and PCR.⁴⁸

Most of the layered zeolite precursors identified to date have relatively low Al content and catalytic activity. They attracted some interest but not as much as the layered forms of the MWW family, which are readily synthesized in various 2D forms and with high Al content with Si/Al down to around 10/1. The ZSM-5/MFI nanosheets can be also made with significant Al content and show promising performance in catalytic processes. They are synthesized directly as nanosheets separated by surfactant chains, i.e. formally being swollen, with the organics partially integrated into the layers. This allowed pillaring to be carried out directly on the isolated as-synthesized precursor. The use of excess TEOS afforded pillared MFI with conventional amorphous silica as pillars.¹⁸⁴ Smaller amount of TEOS was reported to result in pillars with MFI structure.³⁷ The idea of crystalline pillars is very attractive because the traditional ones made of amorphous silica are catalytically inactive, i.e. represent an inert filler, and are less stable hydrothermally. The actual nature of pillars, i.e. silica distribution between layers is an enigma. The pore structure can be probed by the standard adsorption methods but as far as geometric properties of the pillars like size, shape, distribution, etc. nothing is known, not even if these characteristics are definable.

The convenience and effectiveness of silica pillaring with TEOS makes it an excellent first choice for 'proving the principle' while functionalization to increase or modify catalytic properties emerges as the next logical challenge/opportunity. So far such studies have been limited. This may be caused in part by lower quality of the products indicated by their textural and structural properties. An illustrative example is provided by the study of pillaring MCM-22 precursors using aluminum oxide dissolved in NaOH by itself and with addition of Ba and Mg.^{185, 186} The pillaring treatments were carried out with both

swollen MCM-22P (at 90 °C for 4 h) and after it was reacted TEOS (at 40 °C for 6 h) to introduce silica pillars. The former products had low BET below 400 m²/g and the latter up to 750 m²/g. For comparison the unmodified zeolite MCM-22 and the TEOS pillared MCM-36 had BET equal to 432 and 711 m²/g, respectively. These treatments modified activity properties and included higher number of acid sites at the pore mouth or at the outer surface of the layers, additional and stronger Brønsted acid due to silica–alumina clusters in the galleries, while Mg and Ba were the source of basic sites. Functionalization is also possible by using mixtures exemplified by TEOS with tetrabutylorthotitanate (TBOT) with ratios as low as 5:1. The obtained pillared MCM-22 materials showed BET area above 700 m²/g and after acid treatment became active for cyclohexene epoxidation.¹⁸⁷

As said at the beginning the concept of pillaring of layered materials started with intercalation of organic compounds but subsequent effort was focused on preparation of thermally stable inorganic pillars. As diverse systems and compositions were being explored later on the studies were again extended to pillaring of layered silicates with organic pillars. The incorporation of biphenyl-containing perpendicular organic supports into illerite was carried out by first expanding its protonic form by intercalation of hexylamine.³² The product was reacted with bis(triethoxysilyl)biphenyl (BESB) and after isolation treated with acid. The interlayer spacing was expanded from 0.74 nm to 1.94 nm and BET surface area increased to 616 m²/g. The structural stability of this product depended on formation of pairs of the biphenyl 'pillars' due to reaction between their SiO groups in addition to connecting to the layer. The follow up study involved analogous bridging compounds but with gradual substitution of the ethoxy groups attached to silicon atoms with methyl groups (-CH₃), which are not reactive and could not form the dimers as supports. This resulted in the loss of structural rigidity and was described as transformation from pillared to nanocomposite system.¹⁸⁸ Related forms of organic-inorganic hybrids have been obtained by using bridged silsesquioxanes as pillars: in magadiite¹⁸⁹ and layered zeolite precursors IPC-1P³³ and MCM-22P.³⁴ As mentioned above, organic pillared zirconium phosphonates can be obtained by direct synthesis in many varieties in terms of composition and interlayer structures.

The as-synthesized multilamellar MFI described in section 5.1 was utilized in another way while still containing template in the pores. It was turned into an acid-base catalyst just by the combination of mild acid treatment and ion-exchange with ammonia solution.^{190,191} The authors postulated that the basic sites were present as SiO⁻ species and OH⁻ anions. Since the C22-6-6 SDA was still present in the micropores, only acid sites located on external surface were available for catalytic reaction. This organic-inorganic catalyst was tested in the tandem deacetalization-Knoevenagel condensation.¹⁹¹ Interestingly, when bromide counteranions in the template were replaced by iodide anions, the MFI material was highly efficient in cycloaddition catalysis of carbon dioxide and different epoxides.¹⁹⁰

8. Delaminated layered materials

The separation of layers is described in the literature as exfoliation or delamination, often used interchangeably, resulting in frequent ambiguity as to what is exactly being reported. Both terms have been also used in reference to intercalation and or swelling. Gardolinski and Lagaly¹⁵⁴ proposed the

following distinction for clay minerals: "Exfoliation is defined as the decomposition of large aggregates (booklets) into smaller particles; delamination denotes the process of separation of the individual layers of the particles". Based on this delamination can be considered as a higher order process producing materials such that each sheet is effectively a separate entity. This is a rarely achievable situation since even in the case of highly efficient delamination, like dispersion in liquids, the population is not 100% mono-layers and includes multi-layer aggregates. It may also change with time due to re-agglomeration. There is additional complication that for a given sample only a small fraction may be truly delaminated and the yield of mono-layers can be quite low. The exact information about these properties is often not provided introducing considerable uncertainty about true nature of 'delaminated/exfoliated' samples that are reported. The above proposed distinction between exfoliation and delamination will not be adopted here as there is no way to reevaluate the published accounts.

The ultimate delamination can be envisioned as dispersion of individual nanosheets in a liquid producing colloidal suspension. This is a subject of considerable interest and has been recently reviewed for the conventional layered materials.¹² The title of the review 'Liquid exfoliation of layered materials' is not in line with the differentiation suggested above. Table 4, summarizes the reported results according to techniques used for achieving exfoliation. These liquid systems are not hierarchical in the sense used herein but are of enormous significance, both fundamental and practical, for hierarchic materials. First of all, obtaining dispersion in a liquid demonstrates the ability for complete delamination, which should not be taken for granted for all 2D solids. Second, a dispersion can be used as a source of layers for preparation of hierarchical.⁹⁷ Figure 6 shows several types of 'nanoarchitectures' that can be produced from colloidal dispersions of solid layers. Some are explicitly designed to generate hierarchical porous materials. The 'nanocomposite' case in Figure 6 represents pillaring.

Table 4 Methods for liquid exfoliation of layered solids.¹²

<i>Layered composition type</i>	<i>Formula/Sub-group</i>	<i>Exfoliation/delamination method</i>				<i>Special approach</i>
		<i>In surfactant solution</i>	<i>In solvents</i>	<i>In polymer solutions</i>	<i>Intercalation</i>	
Graphite		sonication	sonication	sonication		graphene oxide
Hexagonal-BN		sonication	sonication	sonication		
M dichalcogenides	Metal-X ₂ (MoS ₂)	sonication	sonication	sonication		
M trichalcogenides	Metal-X ₃				ion	
	Metal-PX ₃				polymer	
Metal halides	MX ₂				ion	
	MX ₃				ion, polymer	
	MX ₄ , MX ₅ , MX ₆				ion	
Oxides	Ti, Nb				ion	
	Mn	sonication			ion	
	V				polymer	
	MO ₃				ion, polymer	
	2D trirutile phases				H-form, ion	
	Perovskites and niobates				H-form, ion, sonication	
Oxy-chalcogenides and -pnictides		not reported yet				
M oxyhalides					ion	
III–VI semiconductors	GaX, InX (S, Se, Te)	surfactant			ion	
Zr phosphates and phosphonates			1. water/acetone; 2. water/amine		polymer	
Clays	2:1 (Na ⁺ , Li ⁺) 1:1 (kaolinite)		dispersion in water CH ₃ O grafting,		polymer	
Layered double hydroxides		surfactant	1. in DMF; 2. functionalize, + solvent		1. intercalation; 2. surfactant + guest	
Layered silicates					Na-C ₁₂ H ₂₅ sulfate	
Layered zeolites					ion (C ₃ H ₇) ₄ N-OH) ¹⁹²	swell + extrude with polymer, + solvent, gradient centrifug., + acid ¹⁹³
Transition metal carbides, nitrides						M(Al,Si)(C,N) _x + HF

Clays such as the 2:1 type montmorillonite are one of the easiest layered materials to delaminate when they contain strongly hydrated cations Na^+ and Li^+ . In contact with water their interlayer region expands due to adsorption of the solvent.¹⁹⁴ The interlayer distance can increase continuously, due to osmotic swelling, forming clay suspensions. The dilute suspensions are stable and do not agglomerate. Relatively high concentrations, around 3 % of clay, form gels due to interparticle interaction and agglomeration. These processes are governed by electric double layer and are strongly influence by the medium, e.g. presence of electrolytes, pH, etc.

The α - and γ -zirconium phosphates are also easy to delaminate into colloidal state. The former and VO-phosphate disperse into individual layers in water when intercalated with some short-chain alkylamines. The γ -zirconium phosphate was shown to disperse reversibly in 30-90 % acetone in water at temperatures above 50 °C.¹⁹⁵

Delamination of LDH is also relatively easy and has been carried out by variety of ways. The examples of transparent homogeneous dispersions with stability of weeks to months were summarized by Schwieger with conditions for preparation.¹⁴ Delamination can be facilitated by some anions like dodecylsulfate, amino acids, lactate or borate that are incorporated during synthesis or by substitution. High boiling organic solvents can cause delamination at elevated temperature (butanol, formamide) but in some cases room temperature stirring and sonication were sufficient. Delamination in water was also reported for Mg/Al-lactate but it took 12 hrs at 60 °C while in an appropriate organic solvent it could be instantaneous.

Delaminated LDH suspensions usually produce crystals with restacked layers rather than mono-layer assemblies when they are separated from the liquid. An actual "large-scale synthesis of highly dispersed layered double hydroxide powders containing delaminated single layer nanosheets" was reported as a step-out advance.¹⁹⁶ In this approach, termed aqueous miscible organic solvent treatment (AMOST), the LDH are prepared by the conventional co-precipitation procedure. The solid isolation step involves redispersion in an aqueous miscible organic (AMO) solvent resulting in delamination, which persists all the way to the final product. Multiple instrumental techniques and treatments were applied to corroborate the mono-layer nature of this material. Conceptually it may be similar to the zeolite monolayer materials MCM-56⁶² but there are many differences between them, which may warrant further evaluation and comparisons.

Colloidal suspensions of transition metal oxides with various layer thicknesses, depending on a particular composition, can now be generated quite readily.^{17, 97, 157} The as-synthesized polycrystalline solids are first contacted with an acid and the obtained hydrated protonic form is contacted with a solution of organic base such as tetrabutylammonium hydroxide. One of the phenomena described for these systems is the extreme swelling with for example 100 times expansion of the galleries.¹⁹⁷ It is not complete delamination because the layers are not behaving independently. The primary practical focus of these types of 2D materials has been electronics, optics and related advanced fields but they obviously can be used to prepare porous structures^{177, 178}

The delamination of most classes of layered solids is quite easy and therefore the attention can be shifted to further processing to make functional products. With silicates and layered zeolites delamination is still the hard part. There are some published procedures but a routine delamination is still not possible, which may be a temporary situation and in the future general facile procedures may become available. Some of the reasons that have been mentioned as possibly increasing difficulty of layer separation include high layer charge density and strong hydrogen bonding between silanols from opposing layers as well as with hydrated interlayer cations.⁹⁹

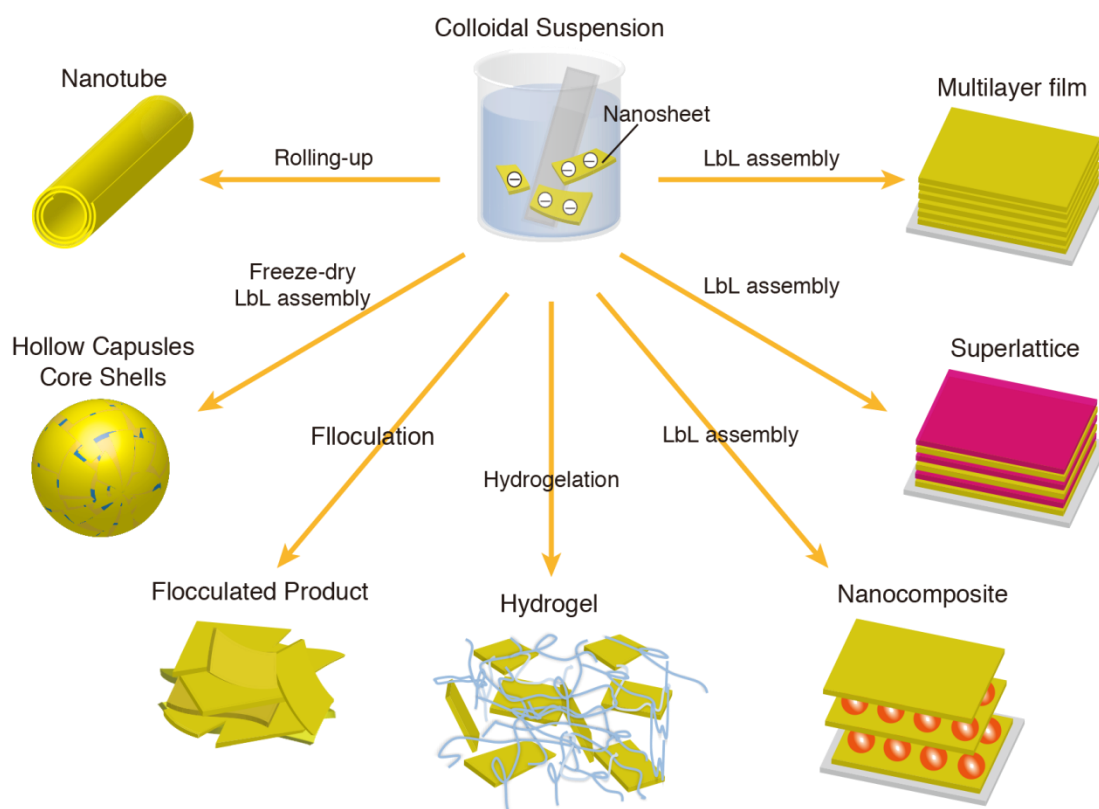


Figure 6 Examples of different nanoarchitectures that have been produced from colloidal suspension of nanosheets. (Reprinted by permission from Macmillan Publishers Ltd: *Polymer Journal* (**47**, 89-98)⁹⁷, copyright 2015).

The investigation of layered crystalline silicas (typical representative $\text{H}_4\text{Si}_{20}\text{O}_{42} \cdot x\text{H}_2\text{O}$) produced unusual result during interaction with the anionic surfactant sodium dodecylsulfate, SDS, which was found to intercalate between layers together with the counterion.¹⁹⁸ This produced increase in the layer separation "...to such an extent that the crystals disarticulate in a fan-like manner or delaminate into thinner packets of layers or smaller aggregates." Removal of the intercalants by washing reconstituted the parallel layer orientation and lead to "re-aggregation of the packets and fragments."

Layered silicate octosilicate, which is precursor to zeolite RWR, was exfoliated by two methods. In one its surface was modified with butylimidazolium groups after being swollen with hexadecyltrimethylammonium (HDTMA) chloride by ion exchange.¹⁹⁹ It was said to be "fully exfoliated into monolayer

nanosheets in water". The layers had thickness of 1.9 nm confirmed by both AFM and XRD. The layer identity as octosilicate was verified based on the XRD peak at 0.19 nm assignable to the (400) reflection. The second example is provided by dodecyldimethylammonium-exchanged octosilicate.⁴³ It was stirred in pentane and exfoliated upon ultrasonication. The method may be applicable to other similar materials.

Delaminated zeolites have been recognized as very valuable materials "combining the benefits of zeolites and mesoporous materials for catalytic uses".^{44, 200} Zeolite layers are unique by offering strong acid sites on the surface, which can be accessed by bulky reactant molecules. They are also known for physical and chemical robustness. The additional beneficial feature with some frameworks is to have channels through the layers, which should further diversify and facilitate diffusion throughout the particle. The first zeolite delamination was performed⁴⁴ on the MCM-22P swollen like reported earlier for pillaring.⁴¹ It was sonicated in the mother liquor, acidified, isolated and calcined. The obtained product ITQ-2 had a high BET surface area equal to 900 m²/g and other characteristics indicating delamination. Edge-to-face type structure was proposed. Analogous technique was applied to delaminate precursors to zeolite FER and NSI (without template removal) and MCM-47, designated ITQ-6,¹⁸³ ITQ-18⁴² and ITQ-20, respectively. The delamination of layered zeolites was found to be complex and influenced by many factors especially the Al content. For two MCM-22P with initial Si/Al 50/1 and 20/1 the latter showed smaller surface area increase upon delamination²⁰¹ (BET 1010 and 600 m²/g, respectively after 10 hrs of sonication; the former was in fact a mesoporous MCM-41 type material produced due to destruction of zeolite. The study of MCM-22 precursor swelling at ambient temperature concluded that "high temperature swelling and ultrasonication to produce ITQ-2 is essentially a fragmentation process resulting in exfoliated and other fragments".²⁰² In contrast, MCM-22P swollen at room temperature with layer preservation "cannot be exfoliated simply by ultrasonication in water to produce ITQ-2."²⁰² The influence of various parameters on delamination via the swelling/ultrasonication/acidification procedure was investigated with the layered silicate magadiite, which can be considered equivalent to low-Al zeolite.²⁰³ The highest BET obtained was 553 m²/g with wet magadiite, swollen with HDTMA-TPA-OH, filtered, sonicated in water, acidified, dried and calcined. The comparison between sonicated/acidified magadiite in mother liquor versus treated in water was carried out too. Starting with the dried magadiite, the separation from mother liquor after swelling resulted in higher surface area (386 vs. 150 m²/g when sonicated in mother liquor). The isolated high surface area material was described as made of crumpled silicate layers not the 'house-of-cards' structure typically attribute to delaminated layered materials. An opposite effect regarding the ultrasonication/acidification treatment in mother liquor vs. solid redispersed in water was reported with high-Al disordered form of MCM-22P, MCM-56.²⁰⁴ It is obtained by direct synthesis⁶² and characterized as composed on MWW layers arranged face-to-face⁴⁴ while ITQ-2 is viewed as edge-to-face.⁴⁴ The study of MCM-56 was aimed to explore its potential for transformation into the edge-to-face ITQ-2 like structure after swelling at room temperature.²⁰⁴ It was sonicated in the swelling mother liquor and in water with and without acidification (4 samples). Only in one case was BET increased – MCM-56 acidified in mother liquor suggesting that the porosity gain was from some mesoporous phase forming from the dissolved silica and surfactant in solution.

A mild approach to delamination of MCM-22P adopted the treatment with surfactant HDTMA-Br, and tetrabutylammonium fluoride and chloride.²⁰⁵ The prepared material UCB-1 was concluded to be delaminated based on several techniques including XRD, microscopy, NMR and FTIR spectroscopy and nitrogen physisorption. In comparison to MCM-22 both UCB-1 and ITQ-2 showed reduced adsorption in the very low pressure region $10^{-7} < p/p^0 < 10^{-4}$, which is expected due to loss of interlayer 10-rings resulting from delamination. At the pressures above $10^{-4} p/p^0$ the uptake shown by UCB-1 is much lower than ITQ-2 and similar to MCM-22. It was explained by proposing that ITQ-2 consists of larger micropores and mesopores originating from amorphous silica which is also responsible for hysteresis observed in the adsorption/desorption branches.²⁰⁵ The lack of amorphization due to mild reaction condition was emphasized as particularly beneficial. Another favorable effect attributed to this approach was retention of heteroatoms. i.e. active centers in the framework.²⁰⁶ Delamination was also proposed to occur upon simple $\text{Al}(\text{NO}_3)_3$ treatment of the boron containing MWW precursor, ERB-1. The method was characterized as "single-step delamination (...) under mild conditions without surfactant and sonication".²⁰⁷ In addition to physical characterization, acylation of 2-methoxynaphthalene was used as the model reaction to confirm the catalytic benefits of delamination by the used procedure.

The particular significance of zeolite lies in their potential for providing monolayers with perpendicular channels allowing diffusion through them. This can be exploited for application of membranes: alone or in nanocomposites. So far there is no evidence that procedures described above could produce delaminated layers suitable for use in membrane application. The only reliable method presently known consists of 6-7 steps including zeolite synthesis.³¹ It is complicated but essentially the only one yielding pure suspensions of zeolite layers.¹⁹³

9. The role of X-ray diffraction and microscopy in the identification and structure characterization

The identity and structure of layered materials are investigated by powder X-ray diffraction (XRD) as the primary characterization tool. Single crystal determinations are not possible in most cases because of the generally small particle size, usually not greater than a few microns, and more importantly, the loss of 3D periodicity occurring during most of the modifications. The typical feature of patterns for layered samples are broadened peaks resulting from various effects like stacking faults, misalignment and limited thickness. The last, i.e. small crystal size, has dramatic effect on XRD peaks, causing streaking and appearance of non-Bragg reflections,²⁰⁸ which is exemplified by some of the MWW zeolite materials.^{209, 210} Peak positions on the low angle side are used to estimate interlayer distances. It is also possible to make a judgment about relative order/disorder. As the standard and routine tool, powder XRD is very useful and informative but it has significant limitations, both intrinsic and due to the nature of products. The general lack of atomic 3D periodicity rules out exact structure determination. There are no adequate quantitative theories and algorithms for describing disorder in general and its specific embodiments. Consequently only some layer arrangements that are not 3D ordered can be verified by model calculations.^{31, 211} More advanced quantitative characterization of disorder by X-ray diffraction has been undertaken with clays.^{212, 213} It has not been extended to the other layered materials for general identification and structure validation.

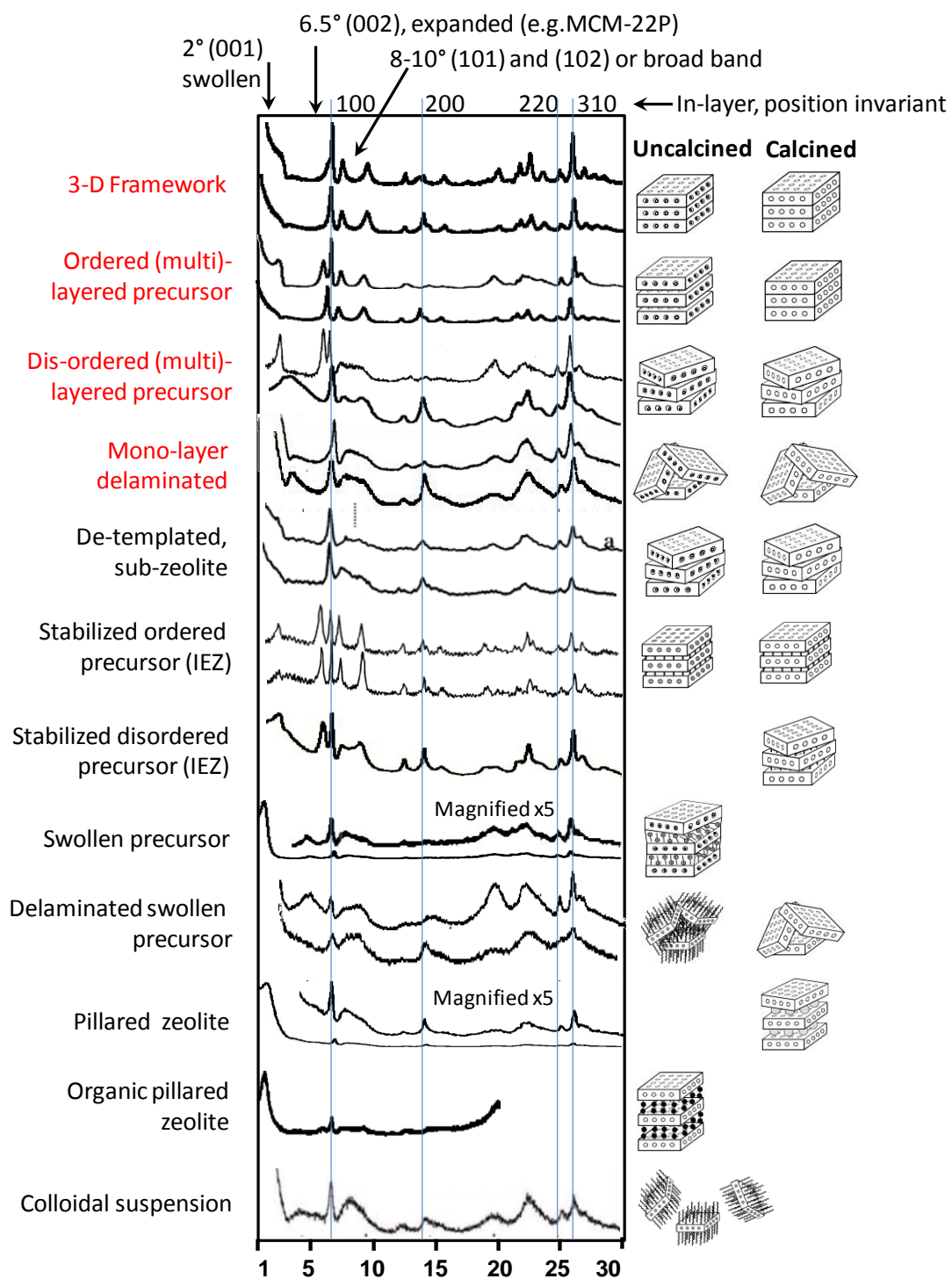


Figure 7 X-ray diffraction patterns for MWW zeolite materials with different structures. The in-layer ($hk0$) reflections do not change positions. Interlayer distances are indicated by reflections below $7^\circ 2\theta$, which are in some cases merged with the (100) at $7.1^\circ 2\theta$. The region $8\text{--}10^\circ 2\theta$ with either resolved or merged (101) and (102) reflections indicates order or disorder, respectively. Materials obtained by direct synthesis are in red.

The structure of most layered precursors is known reasonably well and can be linked to specific diffraction peaks in the X-ray pattern. This way structural changes resulting from various treatments, especially interlayer expansion, can be monitored and verified. Zeolite MCM-22 and its various layered forms are an example of the application of this approach based on the behavior of various intra- and interlayer reflection in the XRD pattern.²⁸ More than 10 different layered forms of the MWW framework have been recognized and assigned based on the X-ray pattern.²⁴ Nitrogen adsorption and determination of pore volume and surface area are used as additional tools to validate the proposed structures. In the case of the MWW family there are particularly favorable circumstance – XRD peaks that allow evaluation of the interlayer distances and lateral disorder are well resolved and positioned below about $10^\circ 2\theta$ (Cu K α radiation).⁶³ Furthermore, the higher symmetry of the framework, i.e. not mono- and triclinic means that interlayer reflections, e.g. with (hk0) indices, maintain their position despite changing interlayer architecture. Figure 7 shows X-ray patterns of various MCM-22 materials and their structure assignments. No analogous analysis has been presented yet for other layered zeolites. A more complex situation is expected with the lower symmetry cases where the shifting of intralayer peaks may present additional complication. The layered zeolite MFI illustrates another complication because most of its prominent peaks are intralayer reflections. The interlayer peaks, which could be used to diagnose structural changes, are not easy to assign due to dominance of the intralayer ones. This is clearly a subject requiring more thorough and systematic inquiry but its general effectiveness remains to be proven.

Due to limitations of X-ray crystallography in dealing with layered materials the direct visualization by microscopy is frequently indispensable for confirming nature of novel products and their features. The review of modern electron microscopy techniques by Liu et al.²¹⁴ points out the invaluable role of electron diffraction (ED), high resolution transmission electron microscopy (HRTEM) and scanning electron microscopy (SEM) in revealing different structural information: layer packing, average periodic structure, structural defects and surface selective information. Most of these data could not be obtained by other techniques. Electron microscopy is particularly important for zeolite materials to distinguish between standard 3D products and expanded layered modifications. High resolution images were often instrumental in combination with powder X-ray diffraction to corroborate the breakthroughs like the first pillared zeolite MCM-36 and the synthesis of MFI nanosheets by design.

The former case, MCM-36 is particularly instructive as it demonstrates both the power and limitations of TEM imaging exemplified by the calcined, i.e. organic-free samples shown in Figure 8a. First, there are extensive sections where MWW layers are seen evenly spaced at 2-2.5 nm, except minority domains where swelling/pillaring must have been unsuccessful. The spaces between layers are apparently filled by pillars, which must have ill-defined structure because they are invisible.

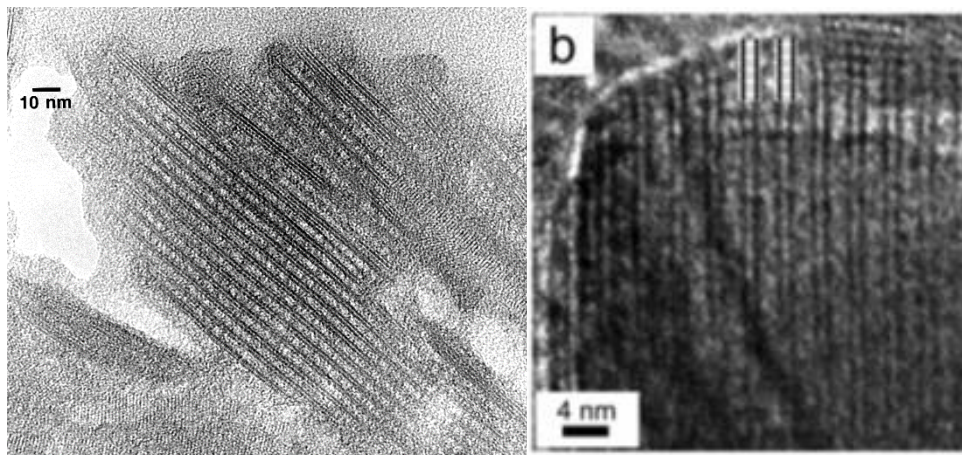


Figure 8. HRTEM images of (a) MCM-36 after swelling at 100°C , (b) MCM-22P precursor after swelling at room temperature (Reprinted with permission from J. Am. Chem. Soc. 2008, 130, 1507-1516. Copyright 2008 American Chemical Society).²⁰²

10. Porosity of hierarchical layered materials

Porosity characterization of lamellar materials or those derived from layered precursors have been addressed in several reviews^{13, 2, 215-217} therefore in this work we will focus only on these porosity aspects that are directly related to the hierarchical layered structures.

Low temperature adsorption (i.e. physisorption) of N_2 or Ar is a standard method for porosity characterization. The adsorption isotherms exhibit distinct features related to different aspects of porosity, allowing determination of the characteristic parameters and relations. However, as hierarchical layered materials usually comprise micropores and mesopores (both intra and interparticle) as well as large surface area, the corresponding isotherms are usually combination of type I, II and IV ones, therefore these features are often superimposed and sometime difficult to be noticed and interpreted (Figure 9).

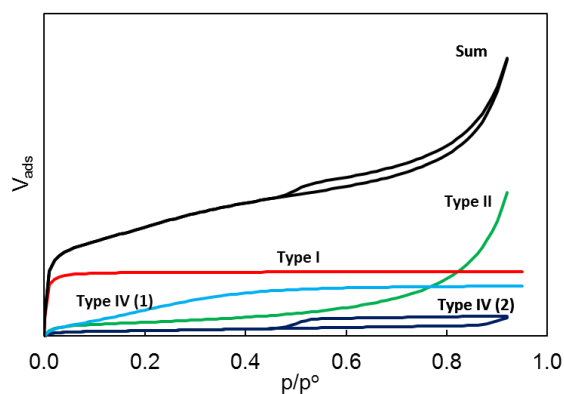


Figure 9 Sample adsorption isotherm, typical for hierarchical layered micro-mesoporous material constructed as linear combination of type I (Langmuir function), II (BET function) and IV (BET + logistic function) isotherms.

There are numerous methods for analysis of the adsorption-desorption data, developed for determination of specific surface area and pore volume (either micropore, mesopore or total) as well as micro- and mesopore size distributions. Before short discussion of these methods and their relevance in porosity characterization of hierarchical layered solids, a qualitative overview of a typical adsorption isotherm will be given. This seems important, as it allows proper identification of the studied material and may help in choosing the appropriate data reduction methods.

Initial sharp increase of the adsorption volume, observed in the low pressure range ($p/p^0 = 10^{-5} - 10^{-2}$) results from filling the micropores. These data are used for calculation of the micropore size distribution. If this range is not covered in the measurement, only the micropore volume may be found from the offset of the isotherm. Non-zero slope in the range of 0.05-0.25 indicates considerable surface area (external and/or mesopore). A step (with an inflexion point) in the intermediate part of the isotherm due to filling narrow mesopores may be difficult to be spotted, especially in the case of their broad size distributions. Decreased slope of the isotherm, observed in the range of 0.50-0.75 is related to the external surface area, which may be much lower than the total surface area, including that of the mesopore. Long and narrow adsorption-desorption hysteresis loop (type H4), does not provide any information about genuine porosity of the material, as it is attributed to capillary condensation in the interparticle mesopores, formed between the plate-like crystallites.

Values of the micro- and mesopore volume as well as the specific mesopore and external surface area are often calculated using the comparative methods (t-plot or α_s -plot). These methods are based on transformation of an adsorption isotherm by replacing pressure with a quantity corresponding to some standard isotherm. In the t-plot method this quantity is the statistical thickness of the layer (film) adsorbed on the surface, usually expressed as the Harkins-Jura function, while in the α_s -plot methods this is a normalized experimental isotherm obtained for nonporous material with similar surface chemistry. Linear segments in the t-plot or α_s -plot indicate the occurrence of unrestricted multilayer adsorption. From the slopes and intercepts of these linear sections the values of surface area (being covered) and pore volume (already filled) may be calculated, respectively (Figure 10)

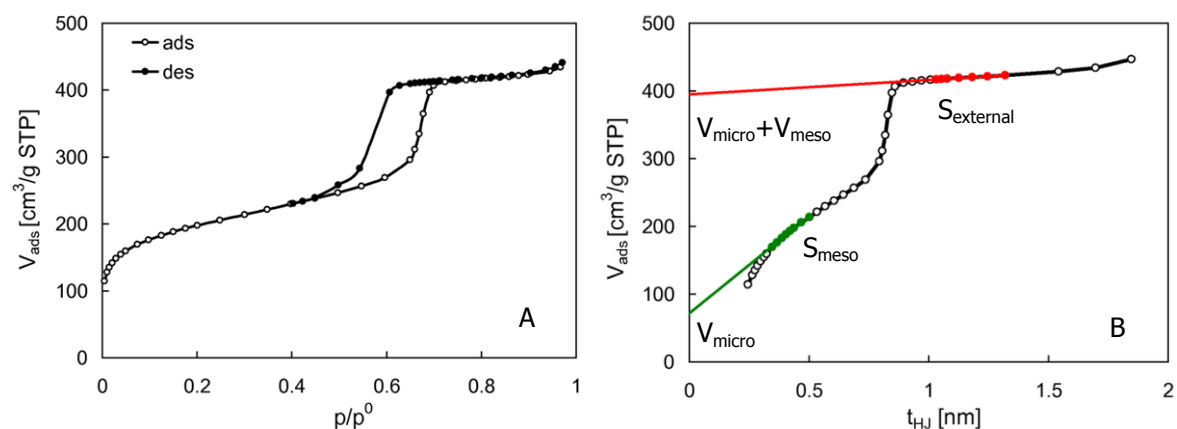


Figure 10 Illustration of the t-plot method: A) sample isotherm for the model micro-mesoporous material (SBA-15 silica), B) t-plot with the linear segments indicated and extrapolated.

However, for microporous solids containing also small mesopores (2 nm) with broad size distribution (such as pillared layered zeolites), this approach may lead to incorrect results (Figure 11). Application of the t-plot method in the range recommended for zeolites²¹⁸ ($p/p^0 = 0.056-0.4$; $t = 0.33-0.57$ nm) for analysis of the simulated isotherm from Figure 9 drastically underestimates values of the micropore volume (by 75% in Figure 11A). Shifting the linear fit to larger t-range gives more reasonable values of the combined volume of micropores and small mesopores (underestimated by 15% in Figure 11A). Very similar effects were observed in the experimental data for the pillared MCM-56 zeolite (Figure 11B). These examples indicate that for detailed characterization of microporosity of such of materials the measurements in the low pressure range ($p/p^0 = 10^{-5}-10^{-2}$) and determination of the micropores size distribution are necessary.

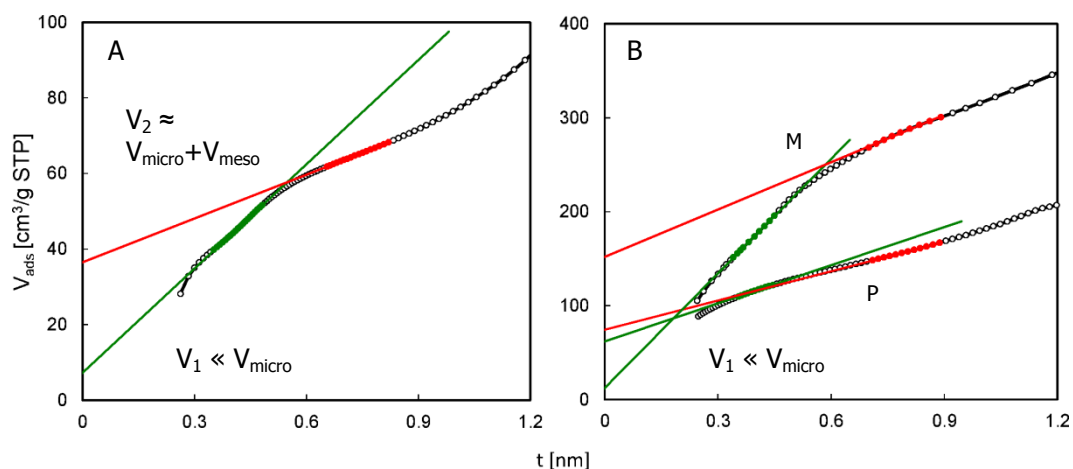


Figure 11 Application of the t-plot method in adsorption data analysis for hierarchical micro-mesoporous materials: A) simulated isotherm from Figure 9, B) experimental adsorption data for MCM-56 zeolites: parent (P) and modified by swelling with hexadecyltrimethylammonium-OH/Cl and pillaring with TEOS (M).²¹⁹ The corresponding adsorption isotherms are shown in Figure 10A.

Another common method for the determination of specific surface area is the BET method. In the standard BET procedure a linear equation is fitted to the experimental data (for $p/p^0 = 0.05-0.25$), transformed according to the linearized BET equation.²¹⁸ This procedure almost always results in very good fit, even for microporous materials that do not meet assumption of the BET model, as unlimited multilayer adsorption is not consistent with the mechanism of filling the micropores. This is shown in Figure 12, where N₂ adsorption isotherms observed for two MCM-22 zeolites (P: parent and M: modified by swelling with HDTMA-OH/Cl solution and pillaring with TEOS)²¹⁹ are plotted together with the theoretical BET functions, resulting from the calculations. Despite very good linearity of the transformed data (Figure 12B), values of the BET surface area obtained for both zeolites (686 and 413 m²/g for zeolite M and P, respectively) are much higher than the corresponding t-plot values (259 and 160 m²/g). The BET surface values have little physical sense for zeolitic materials, since they do not represent real

geometrical surface, but they combine contributions from the micropore volume and external surface area.

In the case shown in Figure 12 the theoretical BET isotherm obtained for the modified zeolite is in good agreement with the experimental data, but for the parent zeolite a completely unrealistic trend is found (Figure 12A, the red line) due to negative value of the C constant. This flaw may be corrected by adjustment of the fitting range to lower pressure values ($p/p^0 = 0.03-0.12$) according to the recommendation of Rouquerol,²²⁰ but even then the BET surface area remains unreasonably high (442 m^2/g).

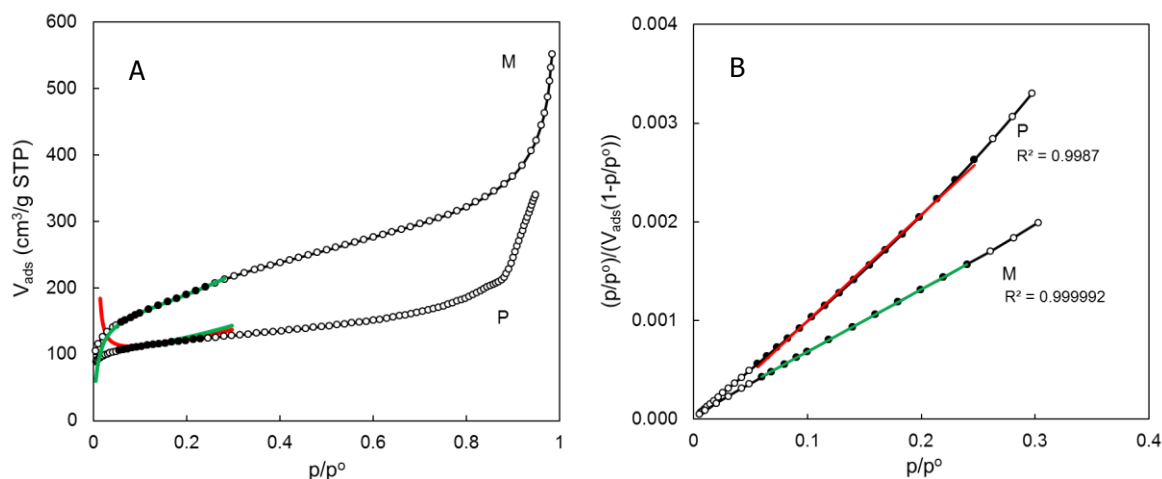


Figure 12 Application of the BET method for determination of the specific surface area of MCM-56 zeolites: parent (P) and modified by swelling with HDTMA-OH/Cl and pillaring with TEOS (M).²¹⁹ Red points denote the data used in calculation, green or red line – the resulting BET functions (A: nonlinear, B: linearized) calculated from the fitting parameters.

Determination of the pore size distributions (PSD) of hierarchical layered materials is usually a difficult task, as they typically contain both micropores and mesopores. The PSD methods most often used are the HK (Horvath-Kawazoe),²²¹ derived for slit-like micropores in carbon materials and the BJH (Barrett–Joyner–Halenda),²²² developed for cylindrical mesopores in silica. Despite their limitations as well as numerous variants and improvements²²³⁻²²⁶ proposed as alternatives in the literature, the HK and BJH remain the standard industry methods²²⁷ and are widely used in research. However, these methods (or any other ones developed specially for micro- or mesopores) cannot be used for porosity analysis of materials containing the intermediate pores (of ca. 2 nm in size), such as porous clay heterostructures or pillared zeolites. Only the methods based on density functional theory (DFT)²²⁸ may cover the whole range of the pores involved in physisorption of N_2 or Ar. Although they were successfully applied in characterization of pillared clays^{229, 230} and zeolites,²²⁸ they are rarely used in research.

Another problem concerning determination of PSD for materials containing micropores results from relatively strong quadrupole interactions of N_2 molecules with ions or dipoles present on their surface. Due to these interactions the profiles of filling the micropores with N_2 molecules do not reflect their size distribution. Therefore for polar microporous materials like zeolites the use of Ar as adsorbate in

physisorption measurements is recommended.²³¹ Some of the material classes are discussed individually below.

10.1 Clays

Unmodified clays exhibit little porosity, as they contain no intrinsic micropores within the layers and the layers are closely held together by electrostatic interactions. Typical N₂ adsorption data for the pristine clays resemble low intensity type isotherms II (Figure 9), sometimes with long and narrow H4 hysteresis loop, corresponding to the mesopores formed between the plate-like particles. Usually they have low BET surface area (2-30 m²/g), while larger values (up to 300m²/g) are observed for highly dispersed clay particles.²³²

Porosity of clays changes considerably upon modifications. Acid treatment may lead to delamination of the original layered crystals, resulting in huge increase of the specific surface area (e.g. from 21 to 335 m²/g) and formation of large mesopores, generated by smaller packets of layers arranged disorderly.²³³ Pillaring with metal cation oligomers followed by calcination introduces metal oxide species between the layers, thus generating the interlayer pores (supermicropores and narrow mesopores) as described above. Porosity of such systems depends on many parameters, including type of the clay (especially charge density of the layers), type and content of the metal as well as chemistry of oligomeric cations used for pillaring (see Figure 13).

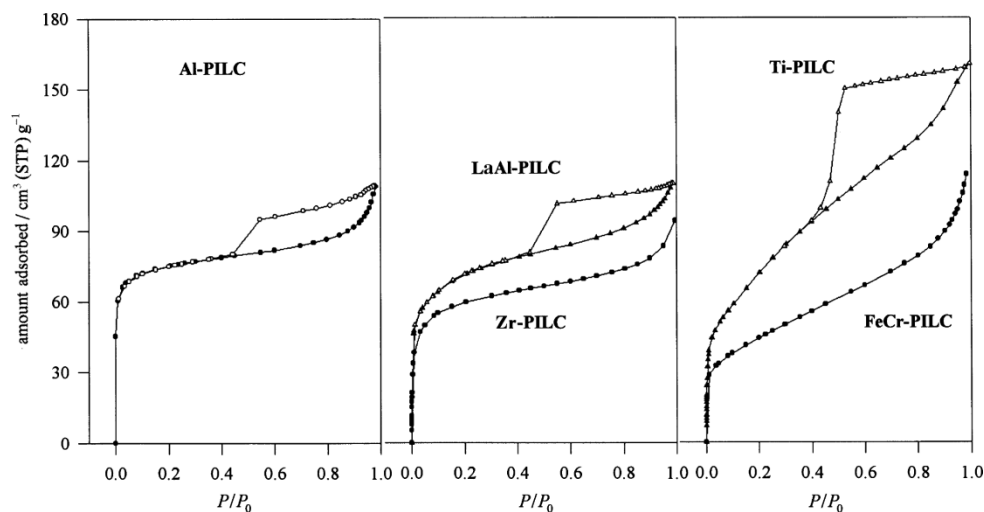


Figure 13 Examples of N₂ adsorption isotherms for montmorillonite pillared with different metal oxides.²³⁴

N₂ adsorption isotherms typical for the pillared clays (Figure 13) may be regarded as combinations of types Ib and IIb. The initial step of the isotherms indicates presence of considerable micropore volume (the highest for alumina pillared clays, Al-PILC), while the slope of the intermediate parts reveals relatively high external surface area (especially for Ti-PILC and FeCr-PILC). Large hysteresis loops resulting from irreversible adsorption and desorption in the interparticle mesopores reflect hierarchical structure of these materials.

Typical values of the BET surface area for pillared montmorillonites are in the range of 220-380 m²/g,^{235, 236} but the external surface areas are smaller (30-70 m²/g).²³⁴ Values of the micropore volume do not exceed 0.15 cm³/g.²³⁵ Pore sizes, generally limited by the interlayer separation (gallery height) and pillar-pillar distances, are usually equal to 0.8-0.9 nm.^{234, 235} For some metals oxides as pillars (e.g. TiO₂ or Fe₂O₃-Cr₂O₃) larger micropores (1.4-1.7 nm) have been found.^{235, 237}

Porous clay heterostructures (PCH) are formed by pillaring with silica, formed by hydrolysis TEOS, of layered clay precursors (natural or synthetic) that were treated (pre-swollen) with a cationic surfactant. This swelling procedure is more efficient in terms of interlayer separation, as is not controlled by charge density of the layers. Typical gallery height in PCH is about 1.5-3 nm and this is also the size range of pores formed between the layers.

N₂ adsorption isotherms characteristic for PCH materials are qualitatively similar to those observed for pillared clays. However, their gas uptake is much higher indicating larger pore volume and surface areas of these materials. Typical BET surface area values for PCHs are about 500 - 1100 m²/g and the total pore volumes are about 0.50 - 1.00 cm³/g.²³⁸⁻²⁴⁰ Moreover, in addition to the initial steps at very low pressure corresponding to adsorption in the micropores, there is considerable increase of the sorbate uptake in the p/p^0 range 0.02 - 0.25, which indicates presence of small mesopores.

Figure 14 illustrates difficulties in pore size analysis of micro-mesoporous materials like PCHs. The PSDs calculated from the isotherms using both the Horvath-Kawazoe and BJH methods, confirm presence of micropores and mesopores as well as continuity of their size distribution. However, drawing conclusion about the actual pore sizes based on these plots is problematical due to well know drawbacks of the HK and BJH methods, hence for precise pore size analysis using Ar as adsorbate and application of the NLDFT method would provide more realistic values.

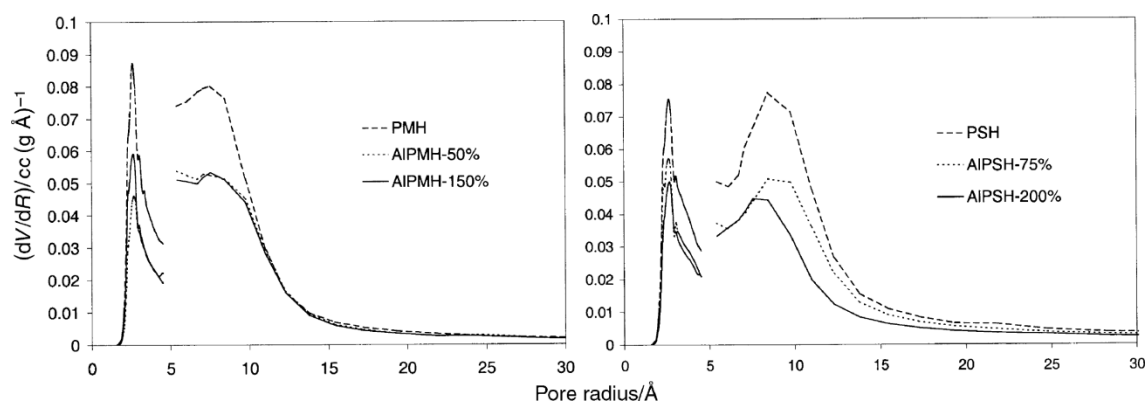


Figure 14 PSDs calculated using the HK and BJH methods of the PCH materials synthesized from montmorillonite (PMH) and saponite (PSH) and their derivatives with Al grafted on the surface.²³⁸

10.2 Hierarchical layered zeolites

Hierarchical materials derived from lamellar zeolitic precursors like MCM-22P exhibit more complex porosity than pillared clays or porous clay heterostructures, due to intrinsic microporosity of the individual layers. However, this complexity is not always evident. N₂ adsorption isotherm obtained for

the 3D MCM-22 zeolite obtained by calcination of the lamellar MCM-22P precursor is very close to type Ia, characteristic for microporous materials.^{215, 241} The only divergence from this typical profile is the step with hysteresis loop, observed in the high pressure range ($p/p^0 = 0.8-1.0$), corresponding to the capillary condensation in the interparticle mesopores. The isotherm obtained for the delaminated ITQ-2 material is more complex. In addition to the micropores and interparticle mesopores it suggests presence of narrow mesopores resulting in a step at $p/p^0 = 0.5$, with large surface area and volume. Porosity of ITQ-2, with BET surface area $840 \text{ m}^2/\text{g}$ and mesopore volume of $0.853 \text{ cm}^3/\text{g}$ is considerably enhanced in comparison of MCM-22 (with of $453 \text{ m}^2/\text{g}$ and $0.169 \text{ cm}^3/\text{g}$, respectively).²⁴¹

Another example of hierarchical zeolites from MWW family is the pillared zeolite MCM-36, synthesized in a similar way as PCHs.²⁴² Adsorption isotherms of N_2 and Ar for this material (Figure 15) are slightly similar to those found for ITQ-2, but lower slope of the isotherm and step in the low pressure range corresponding to narrow mesopores indicate smaller mesopore volume and surface area (of $0.26 \text{ cm}^3/\text{g}$ and $586 \text{ m}^2/\text{g}$, respectively).

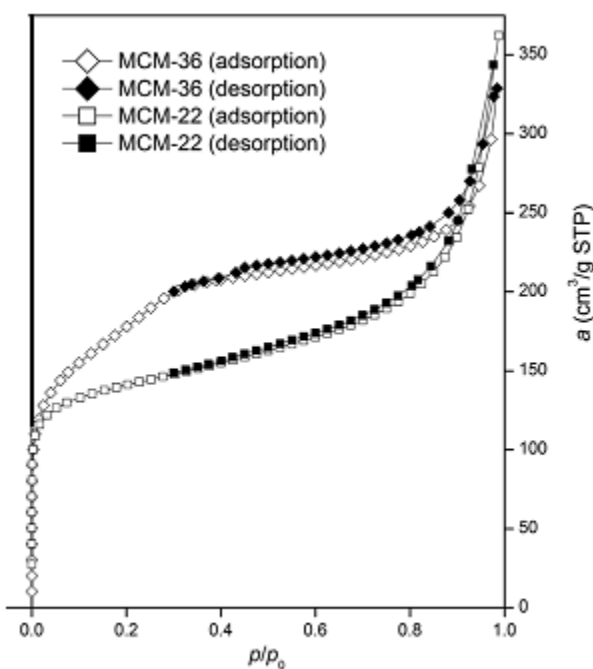


Figure 15 Ar adsorption isotherms observed for MCM-22 and MCM-36 zeolites, adopted from ref.²⁴²

High resolution pore size distributions, calculated using state-of-the-art NLDFT method from Ar adsorption isotherms for the pillared MWW zeolites, confirm presence of uniform micropores within the zeolitic layers as well as larger pores, which exhibit much broader spread of sizes, extending from the wide micropore to the narrow mesopore range.

Another family of hierarchical layered zeolites is based on MFI nanosheets, synthesized with use of special templates, preventing formation of 3D zeolitic framework. In addition to the micropores, both materials exhibit high surface area and mesopore volume ($505 \text{ m}^2/\text{g}$ and $0.57 \text{ cm}^3/\text{g}$ for the non-pillared material, $615 \text{ m}^2/\text{g}$ and $0.44 \text{ cm}^3/\text{g}$ for the pillared one).³⁷ For the pillared nanosheets

remarkably uniform mesopores were observed, while non-pillared material exhibit much broader size distribution due to disordered pore structure.

10.3 Non-conventional pore characterization methods

The above methods based on static gas adsorption are not sufficient for complete characterization of systems with complex pore structures, which are often generated in hierarchic materials. Alternative approaches have shown in the past to answer questions that could not be resolved by the conventional techniques. Dynamic adsorption of hydrocarbons is one of them and was applied to characterization of zeolites with different pores sizes.²⁴³ It was found to be very useful in confirming the nature of MCM-36 as the pillared zeolite without contamination with mesoporous MCM-41-like phase.⁴¹

Another useful technique called quasi-equilibrated desorption employs normal and isoalkanes as well as cycloalkanes as probe molecules for porosity characterization. Based on thermodesorption profiles (exhibiting features attributed to the micropores, mesopores and external surface) it is possible to calculate values of the micro- and mesopore volume, as well as the mesopore size distributions.²⁴⁴ By using specially chosen probe molecule (2,2-dimethyloctane) the amount of surface 12-ring cups in hierarchical MWW zeolites could be quantified.²¹⁹

11. Characterization by IR spectroscopy and catalytic reactions

The layered materials discussed in this review are of practical interest because of their acid/base or redox activity, which may be inherent or introduced during modification. Hierarchic materials are prepared for the purpose of improving of the original properties of the primary layered products, especially deficiencies like catalyst deactivation due to confined space, constrained molecular diffusion efficiency, or poor accessibility for bulky molecules. There is also the potential for adverse effects associated with the creation of more open structures like the possibility diminished stability of the active sites and structures.

11.1 Clays

The specific structure of different clays imposes several types of acidities. The interlayer cations are hydrated and autodissociation of coordinated water gives rise to weak Brønsted acidity (presence of hydronium ions). Metal atoms within the clay layers, such as Al, Mg or transition elements may be coordinatively unsaturated, and act as Lewis acid sites. Because of their acidity, clays have been used as industrial catalysts, especially as petroleum cracking catalysts, for many years²⁴⁵ but have been replaced with zeolites as the principal active components. In recent decades clays were mainly investigated for their application in acid-catalyzed reactions such as:²⁴⁶ ethylation, alkylation, isomerization, esterification, hydrodealkylation, hydro-dehydrogenation, ring opening, etc. A second main area of use is for polymerization and as polymer additives. Other applications include NO_x abatement, Fischer-Tropsch reaction, cracking of waste plastics, selective oxidation, and synthesis of fine chemicals.²⁴⁶

The first attempts to increase surface area and thus accessibility of the active centers of the original clays involved acid treatment to produce formation of pores by dissolution. This results in exposure of the central layer, thus increasing availability of different cations located in that layer. The Si-OH-Si

groups can sporadically have Al-for-Si substitutions, generating strong Brønsted acid groups and, after dehydroxylation, strong Lewis acid sites. All of these features result in relatively high catalytic activity of the modified clay catalysts²⁴⁷. The acid treatment of clays was difficult to control and other methods of generating strong acidity and increased porosity have been developed. Pillaring with the Al-Keggin ion, $\text{Al}_{13}\text{O}_4(\text{OH})_{24}(\text{H}_2\text{O})_{12}^{7+}$ that was introduced in the 1970s²⁴⁸ generated high porosity and new catalytically active sites.

The intercalation of clays with solutions containing two or more cations can lead to formation of pillared layered clays (PILC) with improved thermal, adsorptive, and catalytic properties. The first, easily polymerizing cation is usually Al. The second is added in small quantity and includes Ga, La, Si, Fe, Cr, Mn, Ti. Such mixed-cations PILC were used for numerous reactions, starting with isomerization or disproportionation, requiring the presence of acid sites of relatively mild strength, through more demanding alkylation and cracking reactions, and finally application in some deep oxidation reactions.²⁴⁹

Acidity of PILC was usually measured by ammonia-TPD or IR techniques (pyridine, ammonia adsorption^{250,251}), and showed the presence of both Brønsted and Lewis acid sites, in different proportions. Generally, it is believed that Brønsted acidity is mainly coming from structural hydroxyl groups in the clay layer, while Lewis acidity is attributed to the metal oxide pillars.²⁵² For pillared Ga-Al hectorite, it was showed by pyridine adsorption, that besides strong Brønsted sites, there were two different types of Lewis-acid sites: weaker ones on the surface of the exposed clay layers, and stronger on the surface of pillars.²⁵³

IR spectroscopy has been also the method of choice, very often in combination with TPD, for investigating the dehydration and dehydroxylation of clays and pillared clays.²⁵⁴ The analysis has been focused in the stretching O-H region ($3900\text{--}3300\text{ cm}^{-1}$), bending OH characteristic of molecular water (ca. $1630\text{--}1650\text{ cm}^{-1}$) and in the skeletal region (below 1200 cm^{-1}). IR, together with NMR spectroscopy can be used to follow the mechanism of rearrangement of Al-octahedra as part of pillar formation during high temperature treatment.

Metal-containing PILCs were used for the wet oxidation of waste in water using H_2O_2 as oxidant,²⁵⁵ which is the reaction occurring through the Fenton (or Fenton-like) mechanism. They show good rate of conversion of the pollutants and negligible leaching of the cations.²⁵⁶ Although it is said that addition of pillars is enhancing the catalytic activity of the parent clays, Centi²⁴⁶ points out that PILC-based materials are used as commercial catalysts only in few cases and clays, not pillared clays are preferential additives for commercial cracking catalysts.

In the work of Bagshaw et al.²⁵⁷ surface acidities of alumina-, zirconia-, and titania-pillared clays (montmorillonite, synthetic mica-montmorillonite, rectorite) together with their un-pillared parent forms were studied using FTIR method with pyridine as the probe molecule. The authors found that Lewis acid sites were present on the pillar surfaces, while Brønsted sites were present both on the pillar surfaces and the layers of the parent clay. While alumina-pillared clays exhibited both Lewis and Brønsted acidity (associated with the pillars), zirconia- and titania-pillared clays had Lewis acidity and Brønsted sites located on the exposed clay surfaces and pillar-to-clay layer bonding sites. The overall acidity of alumina-pillared rectorite was the strongest of the pillared clays studied, while the acidity of zirconia-pillared montmorillonite was the weakest.

The review by Tomlinson²⁵⁸ gives an overview of different techniques for characterizing the properties of clays, pillared clays and metal(IV) phosphonates. Apart from the results from IR (acidity) and Si or Al MAS NMR (local environment of the Si or Al atoms) measurements, the range of catalytic test reactions (catalytic activity) is presented^{259, 260}. One of the most commonly used reaction for discrimination of the relative Brønsted acidity (activity) is cracking/isomerization of heptane or m-xylene disproportionation. Other reactions, discriminating between the presence of Brønsted and Lewis acid sites are isopropanol or ethanol decomposition.²⁶¹

11.2 Layered double hydroxides (LDH)

Layered double hydroxides (LDH), the most common of which is hydrotalcite (HT), possess positively charged dense layers with compensating anions in the interlayer space. The following cations can be present in the layer $M^{2+} = Ca^{2+}, Mg^{2+}, Zn^{2+}, Ni^{2+}, Mn^{2+}, Co^{2+}$ or Fe^{2+} and $M^{3+} = Al^{3+}, Cr^{3+}, Mn^{3+}, Fe^{3+}, Ga^{3+}, Co^{3+}$ or Ni^{3+} .²⁶² These materials occur in nature but are mostly synthesized in the laboratory. During thermal treatment hydrotalcites transform through amorphous oxide to a crystalline spinel-like oxides. These last oxides reveal a memory effect and during catalytic reaction they may convert to a structure similar to the starting HT.²⁶³

Spectroscopic methods are very useful for characterization of the LDHs. Braterman et al.²⁶⁴ recommended strongly the use of IR spectroscopy as a routine method of characterization for application directly after the synthesis: using the framework absorption bands to check quality of the material and following the characteristic IR bands to confirm presence of the anion. The level of hydration and the status (the mode of bonding) of interlamellar water as well as the presence of hydroxyl groups may be also conveniently studied by this method. IR can be also used to follow intercalation of anions, both organic and inorganic, to determine not only their presence, location and quantity but also orientation, form, and symmetry may be investigated.

Anionic clays (LDH) are usually synthesized by the co-precipitation method. Prinetto et al.²⁶⁵ investigated the influence of the type and ratio of M^{2+} and M^{3+} cations, the type of interlayer anions, and activation conditions on the acidity/basicity of LDHs and their derived mixed oxides with the materials obtained by the sol-gel route. LDHs containing the most common cations, divalent Mg^{2+} or Ni^{2+} and trivalent Al^{3+} , were studied. The authors used the parallel study: TPD together with FT-IR spectroscopy with the same molecules (CO_2 and NH_3). They showed that in all cases the sample possessed both basic (O^{2-} atoms and $M^{n+}-O^{2-}$ pairs) and Lewis-type (Al^{3+} in Mg-containing materials and Al^{3+} and Ni^{2+} in Ni-containing materials) acidic sites of medium-high strength. They proved that relative amounts of basic and acidic sites strongly depend on the nature of the divalent cation: Mg-containing mixed oxides had higher amount and strength of the basic sites. The authors followed also the influence of the synthesis method (sol-gel vs. co-precipitation) on the acid-basic properties of the resulting LDHs, showing that sol-gel method gives materials with higher concentration of the basic sites but increased amount of defects. Higher activation temperature resulted in decrease of the surface basicity mainly due to segregation of alumina phases and/or the formation of inverse spinel domains. The nature of the interlayer anions, decomposing during thermal treatment pointed to higher basicity of mixed oxides obtained by decomposition of carbonate-exchanged LDHs and detrimental effect of Cl^- anions, able to substitute for lattice oxygens.

Intercalation is applied to introduce or change the chemical, electronic, optical, and magnetic features of parent LDH materials, which are used more as the layered carriers for active components than as active material themselves. Various anions have been intercalated into LDH including halides, OH^- , CO_3^{2-} , SO_4^{2-} , ClO_3^- , $\text{SiO}(\text{OH})_3^-$, phthalocyanines, various polyoxometalates and numerous anionic complexes. The synthesis and characterization of polymer intercalated LDH was reviewed by Leroux and Besse.²⁶⁶ The intercalation of biologically active materials has been recently reported in the literature including porphyrins,²⁶⁷ nucleotide phosphates,²⁶⁸ and therapeutic agents.²⁶⁹

In catalysis, several commercial catalysts for partial oxidation and steam reforming of hydrocarbons, alcohol synthesis, methanation reaction and Fischer-Tropsch synthesis are based on hydrotalcite materials.²⁷⁰ Catalytic potential of LDH comes from the presence of intrinsic basic and redox(metal) sites and can be tailored to fit a specific reaction. Both functionalities may exist at the same time, thus hydrotalcites are potential bifunctional redox-base catalysts.

11.3 Layered zirconium phosphates

Crystalline zirconium phosphates of the general formula $\text{Zr}(\text{HPO}_4)_2 \cdot \text{H}_2\text{O}$ ²⁷¹ differ from clays in high concentration of P-OH groups located on the surface of layers (1 POH per 0.24 nm²). For α -zirconium phosphate the P-OH groups extend perpendicular to the layers and are hydrogen-bonded to water. The layers are held together only by van der Waals interactions. In γ -zirconium phosphates, two different phosphate groups are present, one fully deprotonated and one which retains two protons. Water forms continuous network of hydrogen bonding with the hydroxyl groups of the layers. In both cases the protons, although acidic, are not directly used as acid centers for catalytic reaction due to insufficient free space between the layers (2.6 Å) and all catalytic activity stems from the external surfaces. For catalytic purposes, layered Zr-phosphates have to be functionalized first, e.g. pillared.

Wan et al.²⁷² pillared the α -zirconium phosphates with organic molecules (phenyl, diphenyl and dimethylphenyl). They found that the BET surface areas increased with the increasing size and number of organic groups in the interlayer space. α -Zirconium phosphate pillared by diphenyl adsorbed isopropanol, which was undergoing decomposition that took place mainly in the interlayer region of this catalyst. The dehydration of isopropanol to propylene was the primary reaction for all of the investigated catalysts. Layered phosphates pillared with aluminium, chromium, zirconium and silicon oxides were catalytically active for many reactions, such as dehydration, polymerization, cracking, dehydrogenation and selective oxidation.²⁷³ Pillared α -zirconium phosphates were also obtained with mixed oxides of Al-Si, Cr-Si and Fe-Si. They were thermally stable up to 773 K with interlayer spaces between 1.39 and 1.55 nm, BET areas of 152–243 m²/g and pore volumes 0.075–0.115 cm³/g. Due to their high surface acidity equal to 0.79–1.64 mmol/g (tested by NH₃-TPD method) they were active in acid-catalyzed reactions such as isopropanol dehydration and toluene disproportionation.²⁷³ Quite recently²⁷⁴ alkyl/aryl functionalized porous pillared-zirconium phosphates with BET ~600 m²/g, pore volumes 0.46–0.96 cm³/g, and total acidities equal to 2.45–2.90 mmol/g were tested for alkylation of hydroquinone and esterification of lauric acid in liquid phase showing not particularly high activity.

11.4 Layered transition metal oxides

The layered metal oxides are exemplified by manganate ($\text{Na}_4\text{Mn}_{14}\text{O}_{26}\cdot x\text{H}_2\text{O}$), titanates ($\text{Na}_2\text{Ti}_3\text{O}_7$, $\text{K}_2\text{Ti}_4\text{O}_9$), niobates (KNb_3O_8 , $\text{Ca}_2\text{Nb}_3\text{O}_{10}$) and titanoniobate (KTiNbO_5).²⁷⁵ They can afford pillared derivatives that are porous and possess high surface areas. Similarly to pillared clays, the pillars can introduce new functionalities and at the same time retain the original chemical properties of the layers. It was observed that Al-pillared derivatives generally had higher acidity than either the Si-pillared or non-pillared layered compounds.²⁷⁶

Takagaki et al.²⁷⁷ used HTiNbO_5 , HTi_2NbO_7 , and HTiTaO_5 nanosheets to catalyze esterification of acetic acid and hydrolysis of ethyl acetate, which are reactions running on the Brønsted acid sites, and the performance was better than HZSM-5 zeolite and comparable with that of the niobium acid $\text{Nb}_2\text{O}_5\cdot n\text{H}_2\text{O}$. ^1H MAS NMR data attributed catalytic activity of these nanosheets to strong Brønsted acid sites: $\text{Ti}(\text{OH})\text{Nb}^{5+}$ or $\text{Ti}(\text{OH})\text{Ta}^{5+}$. Such strong acid sites were formed exclusively on the surface of the nanosheets prepared by exfoliation-aggregation of the protonated-layered transition-metal oxides. By ^1H MAS NMR and TGA it was found that the concentration of strong acid sites $\text{Ti}(\text{OH})\text{M}$ on HTiNbO_5 , HTi_2NbO_7 , and HTiTaO_5 nanosheets was equal to 0.39, 0.36, and 0.37 mmol/g.

11.5 Layered silicates

One of the most characteristic features of layered silicates (known also as metal silicate hydrates) is the fact that the number of $\equiv\text{Si}-\text{OH}$ groups on the layer surface is independent of the number of the $\equiv\text{Si}-\text{O}-\text{Si}\equiv$ bridges inside their dense layer. The density of surface $\equiv\text{Si}-\text{OH}$ groups determines many properties of layered silicates as all chemistry of these materials is taking place in the interlayer space. A silicate layer can consist of one sheet of $[\text{SiO}_3\text{OH}]$ tetrahedra or may be produced by condensation of several such tetrahedral mono-layers. The complete layers can be held together by electrostatic forces, hydrogen bonds and van der Waals forces, since Si-OH groups, metal cations and water molecules are occupying the interlayer space. Acidities of surface Si-OH groups are rather moderate (in comparison to zeolites), and have been measured²⁷⁸ by the adsorption of Hammett indicators, showing H_0 values in the range -5 to 1.5 (equivalent 75% and 0.2% H_2SO_4). It should be pointed out that dye molecules used as indicators cannot penetrate the interlayer galleries and thus only the surface acidity of the crystals was measured.

Layered silicates may be intercalated, swelled and delaminated, regardless of their layer thickness or charge density. Nature of the swelling agent, pH and temperature play an important role in all these processes.¹⁹⁸ Intercalated layered silicates are being investigated for other than catalysis-related applications, for example, selective adsorption of Zn^{2+} from seawater²⁷⁹ and highly selective adsorption of CO_2 .²⁸⁰

11.6 Layered zeolites

The discovery of layered zeolite precursors was recognized as the opportunity to combine the well-known high activity of traditional 3D zeolites with the structural flexibility of layered materials. The particular goal was the preparation of highly active materials, which now are called hierarchical, combining high activity and mesopores. The pillared MCM-22 precursor denoted MCM-36 provided the first example. Layered zeolites were expected to solve the problem of limited usefulness of 2D solids in catalytic applications because of weak acid activity of the layers, poor hydrothermal stability and complex preparation methodology^{15, 275}.

Hierarchical layered zeolites require special methods of characterization to distinguish their standard activity from that arising from enhanced external surfaces. This has been approached using carefully chosen probe-molecules for FTIR spectroscopy and test reactions in order to distinguish centers located inside from those located outside of the microporous network. There are three bulky probe molecules that are usually applied for this purpose in the FTIR spectroscopy – 2,6-di-tert-butylpyridine (2,6-DTBP), 2,4-dimethylquinoline (2,4-DMQ, occasionally substituted by the less bulky 2,6-DMQ) and 2,4,6-trimethylpyridine (2,4,6-TMPy, γ -collidine). All of these molecules are not able to penetrate the micropores with the diameter 0.5-0.6 nm and below, and have specific IR maxima when protonated or interacting with Lewis acid sites. For quantitative studies, the values of absorption coefficient of the specific bands have been used, and the available data are listed in Table 5. For 2,6-DTBP the absorption coefficients of pyridine IR bands²⁸¹ are often used²⁸².

Table 5 Absorption coefficients based on intensities or integrated intensities of IR maxima characteristic of bulky probe molecules that are used to study adsorption on external acid sites.

Molecule	Frequency, cm ⁻¹	Absorption coefficient, ϵ
2,4-DMQ ²⁸³	1647	3.3 \pm 0.2 cm/ μ mol
2,6-DMQ ²⁸³	1547	0.5 \pm 0.1 cm/ μ mol
	1649	2.2 \pm 0.6 cm/ μ mol
2,6-DTBP ²⁸⁴	1630	0.5 cm/ μ mol 5.3 cm ² / μ mol
2,4,6-TMPy ²⁸⁵	1632–1648	10.1 cm/ μ mol
2,4,6-TMPy ²⁸⁶	1635	0.62 cm ² / μ mol 8.1 cm/ μ mol

The same bulky molecules are also used, due to their basic characters, to selectively poison external acid sites during investigation of catalytic reactions. For poisoning studies the range of molecules that can be useful is much wider, since the requirement for appropriate spectroscopic properties are no longer applicable and it is more important to ensure that base molecules remain chemisorbed at the reaction conditions.

Hierarchical materials derived from layered zeolites are very promising because of the high acidity and catalytic activity of their parent zeolite frameworks. The excellent case study is provided by the framework MWW, which is found in many forms with high Al content and activity. Majority of the layered forms of other zeolite frameworks have very low Al content. The pillared zeolite obtained from the MCM-22P layered precursor, designated MCM-36, was the first example of expanded zeolite structure.⁴¹ The layers are separated by about 2.5 nm by amorphous silica pillars that contain neither strong Brønsted acid sites nor Lewis acid sites. Despite that MCM-36 performance as catalyst in the very demanding alkylation of isobutane/butane is much superior to the parent zeolite MCM-22. Detailed characterization of the acidity of MCM-36 samples was carried out by Laforge et al.²⁸⁷ The authors identified acidic OH groups located in supercages (IR band at 3621 cm⁻¹) and in sinusoidal channels (IR band at 3608 cm⁻¹). The amount of the former was ca. 7 times smaller for MCM-36 than MCM-22 (parent sample), which is consistent with extensive interlayer separation. It was also shown that 60 to 75% of the protonic acid sites of MCM-36 should be located in the surface cups, with majority being

open to the mesopores and/or supermicropores created by pillaring. This paper was also the first to suggest that frequency of the IR bands of Si-OH-Al groups are different when located in full supercages between condensed layers from their analogues present in the half-cup (pocket) at the external surface of the layer. The concentration of Brønsted acid centers decreased but there was no corresponding increase of the Lewis site concentration. Other publications²⁸⁸ showed that pillaring was having no effect on the concentration of Lewis acid sites, while decreasing the total concentration of Brønsted sites and increasing the amount of the Brønsted sites located at the external surfaces of the pillared zeolite (probed with di-tert-butylpyridine). He et al.²⁸⁹, used 2,2,4-trimethylpentane as the probe molecule for IR studies and showed that with MCM-36 about 10% of the present Brønsted acid sites interacted with 2,2,4-TMP, compared to ca. 1% for MCM-22. This indicated that even if only a fraction of the overall acid centers was accessible through the mesopore interpillaring space it was still improvement in comparison to the conventional zeolite MCM-22.

Recent publication by Liu et al.²⁹⁰ reported quantitative comparisons of the reaction rates per active site at the external surfaces. For this purpose, the MWW and MFI zeolites as well as their pillared or self-pillared forms, were tested using the liquid phase parallel catalytic conversions of benzyl alcohol: etherification to dibenzyl ether and alkylation to 1,3,5-trimethyl-2-benzylbenzene. It was observed that enhancement of the external surface structure altered substantially the reaction rates and selectivities, pointing to the importance of external Brønsted acid sites for the course of both reactions. Both of the parallel reactions occurred exclusively on the external surface of pillared MWW catalysts with alkylation being favored over etherification. In the case of pillared MFI, etherification was favored and occurred on both internal and external surface, while alkylation occurred exclusively on the external surface. The authors also concluded that "the methodology can be extended to other zeolite types and may lead to finding even larger differences of external surface reactivity for reactions of bulky molecules."

Pillared MWW material obtained from MCM-56 (Si/Al = 12/1), was investigated by Zhang et al.²⁹¹ The pillaring produced decreased concentration of Al (Si/Al=26), decreased concentration of both Brønsted and Lewis acid sites detected with pyridine, and increased BET area of 834 m²/g.

Maheshwari et al.²⁰² presented swelling procedure that would result in reduced loss of crystallinity and dissolution of the crystalline phase. The method was based on swelling of MCM-22(P) at room temperature. The treatment did not disrupt the framework connectivity present in the parent material. By extensive washing with water, the low-temperature swollen material gave a new ordered layered structure, for which the HRTEM images showed well-ordered layers with an expanded interlayer distance relative to MCM-22(P). Low-temperature swelling was reversible, restoring MCM-22(P) by acidification of the sample. The swollen material could also be pillared to produce MCM-36 which retained the long range order. The Si/Al ratio for new swollen material was 43.2, which was about the same as for the parent sample (46.7) and much better than for high-temperature swollen zeolite (11.8). Interestingly, it was shown that the room temperature swollen material could not be delaminated by ultrasonication to produce ITQ-2. Room temperature swelling is also inadequate for MCM-22P with high Al content, which is critical for maximizing catalytic activity.²⁹² In contrast, MCM-56 with comparable high Al content but proposed to be unilamellar, swells readily not only at ambient temperature²⁹³ but

using NaOH as the source of high pH needed for swelling.²⁹² IR measurements confirmed high acid site concentration in MCM-56 but the swelling and pillaring result in their reduction by about 30%.²⁰⁴

Another key hierarchical layered material is identified as ITQ-2 - delaminated MWW with proposed house-of-card structure⁴⁴ but it was also stated that "the inherent structural complexity of ITQ-2 poses many problems when attempting to provide an all-encompassing, quantitative model of its structure". It is generally accepted that idealized ITQ-2 material should consist of thin MWW sheets (2.5 nm thick) randomly dispersed in 3D, with large external surface area. Such 'all surface' material may be vulnerable to dealumination at all stages of production (especially calcination). Additionally, Narkhede et al.²⁹⁴ showed, by using pair distribution function (PDF), that ITQ-2 sheets are usually curved and curled, which results in poor periodicity of the nanosheet, and limited structural coherence. All these factors strongly influence not only the total amount of acidic sites but also ratio between Brønsted (BAS) and Lewis (LAS) centers. The acidities reported for ITQ-2 in literature vary considerably: Si/Al=50 - 193 $\mu\text{mol/g}$ (BAS+LAS, Py-IR)²⁹⁵; Si/Al= 12.2 - 409 $\mu\text{mol/g}$ by NH_3 -TPD and 203 $\mu\text{mol/g}$ (BAS only, Py-IR); Si/Al= 19 - 0.62 mmol/g by NH_3 -TPD and 110 (BAS) + 125 (LAS) $\mu\text{mol/g}$ (Py-IR)²⁹⁶; Si/Al=15 - 0.81 mmol/g by NH_3 -TPD and Si/Al=30 - 0.53 mmol/g by NH_3 -TPD;²⁹⁷ Si/Al= 15 - 69 (BAS) + 33 (LAS) $\mu\text{mol/g}$ (Py-IR).²⁹⁸

Catalytic activity was measured in n-decane cracking and experiment showed similar rate constants for MCM-22 and ITQ-2 (Si/Al= 50) and also in reactions of more bulky molecules (di-isopropylbenzene and vacuum gasoil) where the beneficiary role of the enhanced external surface was more prominent (ITQ-2 was reported to be more active and selective than the MCM-22, yielding more of the gasoline and diesel products and less gas and coke).

Rodrigues et al.²⁹⁹ and Kikhtyanin et al.³⁰⁰ studied the formation of coke in the comparative studies of MCM-22, pillared MCM-36 and delaminated ITQ-2. In both studies it was found that the hierarchization of the structure prevented excessive coke formation and the catalyst life-time was substantially increased. Two types of coke is generally formed during most of the acid-catalyzed reactions, so-called 'soluble' (light) and 'insoluble' (polyaromatic, heavy) coke. Rodrigues showed, using ^{13}C NMR spectroscopy, that formation of the heavier, polyaromatic coke occurred mainly inside the micropores, blocking the internal active sites and causing loss in conversion. Kikhtyanin carried out oxidation of the coked catalyst, which showed that lamellar hierarchical zeolites accumulated more of the light coke (easier oxidizing) than their 3D counterparts. The evaluations were also carried out with re-used samples. The furfural conversion over re-used (coked and washed with ethanol before reaction) MCM-36 samples decreased to about 5-7% from about 30-35% obtained over the fresh catalysts while for re-used MCM-22 and MCM-49 conversion dropped to 33-38% from the original 55-60%. The authors suggest that the formation of coke that is poorly soluble in ethanol occurred in the cups located on the external surface of MWW monolayers and in the mesoporous pillared space. This mechanism is opposite to the one proposed by Rodrigues.

There are some interesting features that are connected with the formation of ITQ-2. Góra-Marek et al.³⁰¹ investigated the acidity of MCM-22 and ITQ-2 of Si/Al = 15 and 50, obtained from the same precursors by means of IR spectroscopy, using CO , N_2 and NH_3 as probe-molecules and compared the results with NH_3 -TPD experiment. They found 4.0 $\text{H}^+/\text{u.c.}$ for ITQ-2 with Si/Al=15 (theoretical $\text{H}^+/\text{u.c.}$ =4.5) and 1.3 $\text{H}^+/\text{u.c.}$ for ITQ-2 with Si/Al=50 (theoretical $\text{H}^+/\text{u.c.}$ =1.4). What was interesting is that the value of

absorption coefficients for Si-OH-Al groups with IR maximum at $3620\text{--}24\text{ cm}^{-1}$ changed from $3.29\text{ cm}^2/\mu\text{mol}$ for MCM-22 to $1.02\text{--}1.04\text{ cm}^2/\mu\text{mol}$ for ITQ-2. Such change in the value of the absorption coefficient implies some important change in the chemical and/or geometrical environment of the acidic center. Onida³⁰² compared ITQ-2 with MCM-22 and showed that no substantial loss in Brønsted acidity took place as a result of exfoliation (total acidity measured by ammonia sorption remained unchanged). At the same time the intensity of the IR band at 3624 cm^{-1} was much lower than expected for such acidity. Authors proposed conversion of the bridged Si-OH-Al exposed at the external surfaces into AlOH acidic species.

Turning now to the IEZ forms of layered zeolites, the study of Inagaki et al.³⁰³ showed, by NH_3 -TPD that all types of IEZ-MWW materials obtained by silylation in the ammonium salts solutions retained the original acidity (in terms of the overall concentration of acid sites) of the parent MCM-22 zeolite (0.46 mmol/g), in the range $0.35\text{ to }0.41\text{ mmol/g}$. The acid strength of Al-IEZ-MWW was ca. 154 kJ/mol , quite close to that of Al-MWW (156 kJ/mol).³⁰⁴

The syntheses of interlayer expanded zeolites are usually carried out in acid solutions with a silylating agent, DEDMS (diethoxydimethylsilane), which becomes anchored between the layers. The acid environment causes dealumination decreasing the concentration of acid sites and consequently affecting catalytic activity. One of the first method of preventing dealumination was vapor phase silylation of Al-MWW(P) with dichlorodimethylsilane³⁰⁵, and preparation of Al-YNU-1 from deboronated MWW.³⁰⁶

Quite recently, two new methods of silylation have been published, both leading to a material with preserved acidity. The first one was a “two-step” silylation treatment with DEDMS, first in 0.1 M HNO_3 and then in $1.0\text{ M NH}_3\text{aq}$ or water³⁰³. In the second method, silylation was conducted under weakly acidic conditions (pH 5 to 7) in aqueous solutions of various ammonium salts³⁰⁴. This method resulted in crystalline MCM-22-IEZ zeolites with increased BET area ($460\text{--}505$ vs. $381\text{ m}^2/\text{g}$ for MCM-22) and preserved acidity ($0.35\text{--}0.41$ vs. 0.46 mmol/g in MCM-22). The IEZ materials did not exhibit superior catalytic performance in the acylation of anisole and subsequent acid treatment (resulting in some dealumination) was necessary to improve their catalytic activity. It was suggested that acid treatment led to the change in distribution of Al species in the framework, forming catalytically active sites that improved the performance. The authors applied ^{27}Al MQMAS NMR technique to attribute each cross-section in the ^{27}Al MQMAS NMR spectrum to a specific T-site, but to date the clarification of the relationship between Al distribution and catalytic performance is still under investigation.

Other examples of silylation of layered zeolite precursors include the SOD precursor RUB-51 reacted with tetrachlorosilane (SiCl_4)³⁰⁷ and RUB-39 precursor to RRO.³⁰⁸

The preparation of IEZ materials with elements other than silica can introduce additional activity but is not as easy to carry out successfully. The formation of --O--Fe--O-- bridges was tried by adding iron(III) salt ($\text{FeCl}_3\cdot 6\text{H}_2\text{O}$) to the layered precursor material aiming at incorporation of Fe as isolated, catalytically active sites linking the layers of a zeolite precursor.³⁰⁹ The procedure is applicable to both purely siliceous and Al-containing precursors with ferrierite layers, resulting in materials IEZ-type materials designated COE-4/Fe or Al-COE-4/Fe. Both materials show similar d-spacing of 11.7 \AA compared to 11.2 \AA in the layered precursor and the iron content of ca. 0.5 wt\% , with UV-Vis band characteristic for

isomorphously substituted Fe in the framework positions. Acidity of the resulting samples is negligible (pyridine adsorption followed by IR): BAS concentration 4 $\mu\text{mol/g}$, LAS concentration 21 $\mu\text{mol/g}$ for COE-4/Fe and 23 $\mu\text{mol/g}$ BAS, 32 $\mu\text{mol/g}$ LAS for Al-COE-4/Fe and comparable with the non-expanded sample. The structure analysis and refinement supported the suggestion of Fe occupying mostly the newly incorporated –O-Fe-O– interlayer bridges.

12. Miscellaneous preparations of porous materials based on 2D layers

12.1 Restructuring of layers into ordered mesoporous materials

The reaction of layered silicate kanemite with hexadecyltrimethylammonium in basic solution produced material³¹⁰ similar to the hexagonal mesoporous silica MCM-41.¹⁶⁸ It was postulated that this process involved solvent-mediated recrystallization of kanemite and formation of the product by ‘liquid-crystal-templating’.³¹¹ The alternative Folding-Sheet-Mechanism suggested bending of the silicate sheets to form the honeycomb-like pattern³¹² but it is now suggested to involve layered intermediates composed of fragmented silicate sheets and alkyltrimethylammonium cations.³¹³ The formation of another novel material, KWS-2, that was obtained from alkyltrimethylammonium intercalated kanemite, is likely to involve layer bending. The product has unidimensional square channels that are formed upon mild acid treatment of the intercalate.³¹⁴

12.2 Mesoporous synthetic clays

These materials are prepared by direct hydrothermal synthesis of a clay in the presence of polymers, e.g. for 2 days under reflux.³¹⁵ The product is a polymer-clay nanocomposite with a proposed ‘house of cards’ structure consisting of randomly packed ‘single or small stacks of layers’. The polymer can be removed by calcination producing a mesoporous structure. A representative product properties are 20% of polymer in the solid, 250 m^2/g BET surface area and average pore sizes 4-9 nm but with relatively narrow distribution.³¹⁶ These properties can be tailored by changing the amount of polymer in the synthesis mixture (to 30%) and nature of the polymer. Catalytic testing showed good performance as support in hydrodesulfurization.³¹⁷

12.3 Layer-like zeolites

The preparation of layered hierarchical materials is usually carried out by modification of available layered precursors. Another type of effort aims to produce layered form of materials with known useful properties. It is exemplified by zeolites FAU/EMT and MFI. The former structures are constructed from the same hypothetical layer propagated with different stacking related by translation and center of inversion.³¹⁸ This is similar to other framework pairs with the difference that the layered precursors are already known and the stacking relationship is translation and a mirror plane.³¹⁹ These frameworks are FER/CDO, NSI/CAS and RRO/HEU. The particular interest in FAU is dictated by its second to none preeminence in zeolite catalysis, where its primary crystal form is cuboidal. The formation of FAU multilayered, i.e. many unit cells, nanosheets was observed with organic additives such as the organosilane 3-(trimethoxysilyl)propyl hexadecyl dimethyl ammonium chloride (TPHAC).³²⁰ The particles exhibited a cotton-ball appearance with nanosheets intergrown in the triangular arrangement. The

particle size was around 9 micron and their characterization by nitrogen sorption revealed mesopores with average dimension equal to 7 nm. It has been shown recently that similar crystal habit and morphologies can be also induced by additives like Li_2CO_3 and zinc nitrate.³²¹ Such organic-free syntheses are very attractive because of cost and scale-up potential. Khaleel et al. reported study of FAU-nanosheets forming cuboctahedral assemblies by electron microscopy.³²² It was postulated that EMT domains within FAU nanosheets were responsible for the observed morphology.

13 Application opportunities and barriers

Both the primary layered materials and their hierarchical derivatives show practical benefits as catalysts and sorbents in diverse applications, which is well documented including very recent reviews providing detailed up to date advances.^{13, 14, 16, 97} The expected practical value and potential of these hierarchical materials arises from the proven usefulness of porous materials in general. The modifiable 2D solids are particularly valuable because their porosity can be enhanced allowing better access and diffusion for larger reactants and guest molecules. This is regarded as advantage in comparison zeolites, which the layered materials are expected to complement in practical uses.²⁰⁰ The additional benefit from the modification of layered materials is the potential for tailoring of properties over wide range of compositions and different structures. Overall the outlook for the applications of layered materials is very promising but the benefits are usually associated with additional synthesis effort and cost, which may offset gains in performance. With this in mind the discussion will focus on those applications and materials that may seem most viable for practical implementation in the near future. Before looking at the benefits it is useful to consider first the barriers as they are most likely to determine the practical prospects.

The most significant barrier is presented by the additional processing steps during synthesis and the fact that the enhancement of performance is often achieved with reagents that may be exotic, expensive and not readily available. This is rarely an important factor when trying to 'prove the principle' but must be a priority if practical implementation is seriously considered. In such cases the designed SDA molecules are frequently very difficult or impossible to use for reasons of unavailability in reasonable quantities, cost or handling issues. The high material and labor cost make proper validation of the perceived benefits particularly important. Literature reports usually provide sufficient evidence to show that a hierarchical product is useful for some application and is better in some respect than the starting layered precursor. However, the standard of proof becomes much higher in the case of high cost and potential production problems. The comparison should be made with the state of the art materials as well as alternatives that may be conceived with the knowledge of the improved 2D material. Such validation may be difficult because the best materials are often proprietary and unavailable for evaluation. Sometimes commercial or industrial samples are available but may not be the best for a particular use. There are many grades of the same material, even among zeolites, that are tailored to specific use and choosing a proper benchmark is essential.

It is evident from the consideration of the barriers that low cost and simple preparation are the key to practical use of new hierarchical layered materials, at least in the near term. This is because there are many varieties of porous materials and frequently good alternatives can be found. Clays provide a good

illustration of this points. First are the pillared clays prepared by intercalation of the Al-Keggin ion. The synthesis has essentially one additional step and the reagent is not particularly expensive. Practical implementation could have been possible but the product failed because of very severe conditions of the process in which they were used, i.e. cracking. Another example is provided by the organo-clays, which are used as plastic reinforcement. The organic component may represent a significant cost increase but the clay additive is only a small part of the product hence the economics are still favorable.

Layered zeolites are among the most attractive candidates for practical use because their 3D forms are already widely used as catalysts and sorbents. Since conventional zeolites are manufactured in large quantities the preparation of layered precursors is expected to be readily scalable. Taking into account preparation simplicity these forms that can be made in one-step synthesis like the SPP MFI and layer-like FAU 2D are of great interest. At the present time the MWW zeolites are particularly attractive as essentially the only layered forms available with high Al content, which is critical for high activity. The traditional 3D crystals of MWW are already used in commercial process like aromatic alkylation. The layered form MCM-56, which appears to be unilamellar has shown higher activity than the commercial catalysts for the mentioned aromatic alkylation.¹⁶ The disordered multilayered form UZM-8,³²³ which is structurally similar to EMM-10, is also of commercial interest. A different type of benefit was found with the IEZ-MWW material. It showed increased uptake of rare earth cations than the conventional 3D form, apparently due only to having expanded structure by 0.2 nm.³²⁴ The incorporation of multi-charged cations has been a big problem with siliceous zeolites. This enhancement is one of the most notable manifestation of a benefit resulting from expanded layered structure. The increased incorporation of Ce made the IEZ-MWW active for CO oxidation at room temperature.

The above examples illustrate possibilities for using layered materials with existing capabilities emphasizing simple procedures and affordable reagents. It does not rule out more difficult and costly methods including the use of more complicated organic materials like surfactants, e.g. for pillaring and delamination. This will be contingent on showing real advantage over the present available materials and optimization of methods for less common procedures like swelling and liquid exfoliation.

Acknowledgements

This work was financed with the funds from the Narodowe Centrum Nauki provided on the basis of decision number DEC-2011/03/B/ST5/01551. P.E. acknowledges the Czech Science Foundation for the project of the Centre of Excellence (P106/12/0189). W.J.R. and P.E. acknowledge the Czech Science Foundation for the project of the Centre of Excellence (P106/12/G015). B.M. also thanks for funding from Marian Smoluchowski Kraków Research Consortium – a Leading National Research Centre KNOW supported by the Ministry of Science and Higher Education.

References

1. G. Alberti and U. Constantino, in *Comprehensive Supramolecular Chemistry*, eds. J. L. Atwood, J. E. D. Davies, D. D. MacNichol and F. Vogtle, Pergamon, Oxford, 1996, vol. 6, pp. 1-23.
2. S. M. Auerbach, K. A. Carrado and P. K. Dutta, *Handbook of Layered Materials*, Marcel Dekker, New York, 2004.
3. W. Schwieger, A. G. Machoke, T. Weissenberger, A. Inayat, T. Selvam, M. Klumpp and A. Inayat, *Chem. Soc. Rev.*, 2015, **accepted**.
4. M. S. Whittingham and A. J. Jacobson, *Intercalation Chemistry*, Academic Press, New York, 1982.
5. W. Müller-Warmuth and R. Schöllhorn, *Progress in Intercalation Research*, Kluwer, Dordrecht, 1994.
6. D. O'Hare, in *Inorganic Materials*, eds. D. W. Bruce and D. O'Hare, Wiley, New York, 2nd edn., 1997, pp. 172-254.
7. A. F. Masters and T. Maschmeyer, *Microporous Mesoporous Mater.*, 2011, **142**, 423-438.
8. D. W. Breck, *Zeolite Molecular Sieves: Structure, Chemistry, and Use*, Wiley, New York, 1973.
9. K. Na and G. A. Somorjai, *Catal. Lett.*, 2014.
10. J. Perez-Ramirez, *Nat. Chem.*, 2012, **4**, 250-251.
11. M. Hartmann, *Angew. Chem. Int. Ed.*, 2004, **43**, 5880-5882.
12. V. Nicolosi, M. Chhowalla, M. G. Kanatzidis, M. S. Strano and J. N. Coleman, *Science*, 2013, **340**, 1-18.
13. A. Clearfield, H. P. Perry and K. J. Gagnon, in *Comprehensive Inorganic Chemistry II (Second Edition): From Elements to Applications*, 2013, vol. 5, pp. 169-211.
14. T. Selvam, A. Inayat and W. Schwieger, *Dalton Trans.*, 2014, **43**, 10365-10387.
15. W. J. Roth, *Stud. Surf. Sci. Catal.*, 2007, **168**, 221-239.
16. W. J. Roth, P. Nachtigall, R. E. Morris and J. Čejka, *Chem. Rev.*, 2014, **114**, 4807-4837.
17. R. Ma and T. Sasaki, *Acc. Chem. Res.*, 2015, **48**, 136-143.
18. J. Liang, R. Ma and T. Sasaki, *Dalton Trans.*, 2014, **43**, 10355-10364.
19. S. A. Solin, *J. Mol. Catal.*, 1984, **27**, 293-303.
20. L. Li, R. Z. Ma, Y. Ebina, K. Fukuda, K. Takada and T. Sasaki, *J. Am. Chem. Soc.*, 2007, **129**, 8000-8007.
21. W. J. Roth and J. Čejka, *Catal. Sci. Technol.*, 2011, **1**, 43-53.
22. F. S. O. Ramos, M. K. de Pietre and H. O. Pastore, *RSC Adv.*, 2013, **3**, 2084-2111.
23. B. Marler and H. Gies, *Eur. J. Mineral.*, 2012, **24**, 405-428.
24. W. J. Roth, B. Gil and B. Marszalek, *Catal. Today*, 2014, **227**, 9-14.
25. U. Brenn, H. Ernst, D. Freude, R. Herrmann, R. Jähnig, H. G. Karge, J. Kärger, T. König, B. Mädler, U. T. Pingel, D. Prochnow and W. Schwieger, *Microporous Mesoporous Mater.*, 2000, **40**, 43-52.
26. B. Marler, N. Stroter and H. Gies, *Microporous Mesoporous Mater.*, 2005, **83**, 201-211.
27. R. K. Iler, *Journal of Colloid Science*, 1964, **19**, 648-657.
28. W. J. Roth and D. L. Dorset, *Microporous Mesoporous Mater.*, 2011, **142**, 32-36.
29. W. J. Roth and C. T. Kresge, *Microporous Mesoporous Mater.*, 2011, **144**, 158-161.
30. P. Wu, J. F. Ruan, L. L. Wang, L. L. Wu, Y. Wang, Y. M. Liu, W. B. Fan, M. Y. He, O. Terasaki and T. Tatsumi, *J. Am. Chem. Soc.*, 2008, **130**, 8178-8187.
31. K. Varoon, X. Y. Zhang, B. Elyassi, D. D. Brewer, M. Gettel, S. Kumar, J. A. Lee, S. Maheshwari, A. Mittal, C. Y. Sung, M. Cococcioni, L. F. Francis, A. V. McCormick, K. A. Mkhoyan and M. Tsapatsis, *Science*, 2011, **334**, 72-75.
32. R. Ishii and Y. Shinohara, *J. Mater. Chem.*, 2005, **15**, 551-553.
33. M. Opanasenko, W. O. Parker, M. Shamzhy, E. Montanari, M. Bellettato, M. Mazur, R. Millini and J. Čejka, *J. Am. Chem. Soc.*, 2014, **136**, 2511-2519.

34. A. Corma, U. Díaz, T. García, G. Sastre and A. Velty, *J. Am. Chem. Soc.*, 2010, **132**, 15011-15021.
35. X. Y. Zhang, D. X. Liu, D. D. Xu, S. Asahina, K. A. Cychosz, K. V. Agrawal, Y. Al Wahedi, A. Bhan, S. Al Hashimi, O. Terasaki, M. Thommes and M. Tsapatsis, *Science*, 2012, **336**, 1684-1687.
36. A. Corma, U. Diaz, M. E. Domine and V. Fornés, *Angew. Chem. Int. Ed.*, 2000, **39**, 1499-1501.
37. K. Na, M. Choi, W. Park, Y. Sakamoto, O. Terasaki and R. Ryoo, *J. Am. Chem. Soc.*, 2010, **132**, 4169-4177.
38. C. T. Kresge and W. J. Roth. U.S. Patent, 5,266,541, 1993.
39. K. Kosuge and A. Tsunashima, *J. Chem. Soc., Chem. Commun.*, 1995, 2427-2428.
40. P. Chlubna, W. J. Roth, H. F. Greer, W. Z. Zhou, O. Shvets, A. Zukal, J. Cejka and R. E. Morris, *Chem. Mater.*, 2013, **25**, 542-547.
41. W. J. Roth, C. T. Kresge, J. C. Vartuli, M. E. Leonowicz, A. S. Fung and S. B. McCullen, *Stud. Surf. Sci. Catal.*, 1995, **94**, 301-308.
42. A. Corma, V. Fornes and U. Diaz, *Chem. Commun.*, 2001, 2642-2643.
43. S. Osada, A. Iribe and K. Kuroda, *Chem. Lett.*, 2013, **42**, 80-82.
44. A. Corma, V. Fornes, S. B. Pergher, T. L. M. Maesen and J. G. Buglass, *Nature*, 1998, **396**, 353-356.
45. Z. Zhao, W. Zhang, P. Ren, X. Han, U. Mueller, B. Yilmaz, M. Feyen, H. Gies, F.-S. Xiao, D. De Vos, T. Tatsumi and X. Bao, *Chem. Mater.*, 2013, **25**, 840-847.
46. G. Borbely, H. K. Beyer, H. G. Karge, W. Schwieger, A. Brandt and K. H. Bergk, *Clays Clay Miner.*, 1991, **39**, 490-497.
47. T. R. Macedo and C. Airoidi, *Microporous Mesoporous Mater.*, 2010, **128**, 158-164.
48. W. J. Roth, O. V. Shvets, M. Shamzhy, P. Chlubna, M. Kubu, P. Nachtigall and J. Čejka, *J. Am. Chem. Soc.*, 2011, **133**, 6130-6133.
49. W. J. Roth, D. L. Dorset, G. J. Kennedy, T. Yorke and T. E. Helton. Pat. Appl., WO2010021795 (A1), 2010.
50. J.-g. Jiang, L. Jia, B. Yang, H. Xu and P. Wu, *Chem. Mater.*, 2013, **25**, 4710-4718.
51. H. Gies, U. Mueller, B. Yilmaz, T. Tatsumi, B. Xie, F.-S. Xiao, X. Bao, W. Zhang and D. De Vos, *Chem. Mater.*, 2011, **23**, 2545-2554.
52. W. J. Roth, P. Nachtigall, R. E. Morris, P. S. Wheatley, V. R. Seymour, S. E. Ashbrook, P. Chlubná, L. Grajciar, M. Položij, A. Zukal, O. Shvets and J. Čejka, *Nat. Chem.*, 2013, **5**, 628-633.
53. W. B. Fan, P. Wu, S. Namba and T. Tatsumi, *Angew. Chem. Int. Ed.*, 2004, **43**, 236-240.
54. Y. Asakura, Y. Matsuo, N. Takahashi and K. Kuroda, *Bull. Chem. Soc. Jpn.*, 2011, **84**, 968-975.
55. A. Burton, R. J. Accardi, R. F. Lobo, M. Falcioni and M. W. Deem, *Chem. Mater.*, 2000, **12**, 2936-2942.
56. L. D. Rollmann, J. L. Schlenker, S. L. Lawton, C. L. Kennedy and G. J. Kennedy, *Microporous Mesoporous Mater.*, 2002, **53**, 179-193.
57. L. L. Wang, Y. M. Liu, W. Xie, H. H. Wu, Y. W. Jiang, M. Y. He and P. Wu, *Stud. Surf. Sci. Catal.*, 2007, **170**, 635-640.
58. T. Moteki, W. Chaikittisilp, Y. Sakamoto, A. Shimojima and T. Okubo, *Chem. Mater.*, 2011, **23**, 3564-3570.
59. K. Na, W. Park, Y. Seo and R. Ryoo, *Chem. Mater.*, 2011, **23**, 1273-1279.
60. M. Choi, K. Na, J. Kim, Y. Sakamoto, O. Terasaki and R. Ryoo, *Nature*, 2009, **461**, 246-249.
61. A. S. Fung, S. L. Lawton and W. J. Roth. U.S. Patent, 5,362,697, 1994.
62. W. J. Roth, *Stud. Surf. Sci. Catal.*, 2005, **158A and B**, 19-26.
63. W. J. Roth, D. L. Dorset and G. J. Kennedy, *Microporous Mesoporous Mater.*, 2011, **142**, 168-177.
64. R. Millini, L. C. Carluccio, A. Carati, G. Bellussi, C. Perego, G. Cruciani and S. Zanardi, *Microporous Mesoporous Mater.*, 2004, **74**, 59-71.

65. L. Schreyeck, P. Caullet, J. C. Mougénel, J. L. Guth and B. Marler, *Microporous Materials*, 1996, **6**, 259-271.
66. D. L. Dorset and G. J. Kennedy, *J. Phys. Chem. B*, 2004, **108**, 15216-15222.
67. T. Ikeda, Y. Akiyama, Y. Oumi, A. Kawai and F. Mizukami, *Angew. Chem. Int. Ed.*, 2004, **43**, 4892-4896.
68. Y. Asakura, R. Takayama, T. Shibue and K. Kuroda, *Chem. - Eur. J.*, 2014, **20**, 1893-1900.
69. T. V. Whittam. U.S. Patent, 4,397,825, 1983.
70. S. Zanardi, A. Alberti, G. Cruciani, A. Corma, V. Fornés and M. Brunelli, *Angew. Chem. Int. Ed.*, 2004, **43**, 4933-4937.
71. A. J. Blake, K. R. Franklin and B. M. Lowe, *J. Chem. Soc., Dalton Trans.*, 1988, 2513-2517.
72. B. Marler, M. A. Cambor and H. Gies, *Microporous Mesoporous Mater.*, 2006, **90**, 87-101.
73. Y. X. Wang, H. Gies, B. Marler and U. Muller, *Chem. Mater.*, 2005, **17**, 43-49.
74. W. Schwieger, D. Heidemann and K. H. Bergk, *Revue De Chimie Minerale*, 1985, **22**, 639-650.
75. S. Vortmann, J. Rius, S. Siegmann and H. Gies, *J. Phys. Chem. B*, 1997, **101**, 1292-1297.
76. F. Wolf and W. Schwieger, *Z. Anorg. Allg. Chem.*, 1979, **457**, 224-228.
77. P. S. Wheatley and R. E. Morris, *J. Mater. Chem.*, 2006, **16**, 1035-1037.
78. A. Rojas and M. A. Cambor, *Chem. Mater.*, 2014, **26**, 1161-1169.
79. M. E. Leonowicz, J. A. Lawton, S. L. Lawton and M. K. Rubin, *Science*, 1994, **264**, 1910-1913.
80. R. Millini, G. Perego, W. O. Parker Jr, G. Bellussi and L. Carluccio, *Microporous Materials*, 1995, **4**, 221-230.
81. M. K. Rubin and P. Chu. U.S. Patent, 4,954,325, 1990.
82. T. Moteki, W. Chaikittisilp, A. Shimojima and T. Okubo, *J. Am. Chem. Soc.*, 2008, **130**, 15780-15781.
83. U. Oberhagemann, P. Bayat, B. Marler, H. Gies and J. Rius, *Angew. Chem. Int. Ed.*, 1996, **35**, 2869-2872.
84. R. P. D. Graham, *Proc. Trans. R. Soc. Can., 3rd series*, 1918, **12**, 185-190.
85. J. Michael Bennett and R. M. Kirchner, *Zeolites*, 1991, **11**, 502-506.
86. R. J. Argauer and G. R. Landolt. U.S. Patent, 3,702,886, 1972.
87. T. Araki, *Z. Kristallogr.*, 1980, **152**, 207-213.
88. H. J. Brooke, *Edinb. Phil. J.*, 1822, **6**, 112-115.
89. R. M. Kirchner and J. M. Bennett, *Zeolites*, 1994, **14**, 523-528.
90. P. A. Barrett, M. J. Díaz-Cabañas and M. A. Cambor, *Chem. Mater.*, 1999, **11**, 2919-2927.
91. M. K. Rubin. U.S. Patent, 4,981,663, 1991.
92. E. Verheyen, L. Joos, K. Van Havenbergh, E. Breynaert, N. Kasian, E. Gobechiya, K. Houthoofd, C. Martineau, M. Hinterstein, F. Taulelle, V. Van Speybroeck, M. Waroquier, S. Bals, G. Van Tendeloo, C. E. A. Kirschhock and J. A. Martens, *Nat. Mater.*, 2012, **11**, 1059-1064.
93. J. L. Paillaud, B. Harbuzaru, J. Patarin and N. Bats, *Science*, 2004, **304**, 990-992.
94. J. M. Bennett, C. D. Chang, S. L. Lawton, M. E. Leonowicz, D. N. Lissy and M. K. Rubin. U.S. Patent, 5,236,575, 1993.
95. S. L. Lawton, A. S. Fung, G. J. Kennedy, L. B. Alemany, C. D. Chang, G. H. Hatzikos, D. N. Lissy, M. K. Rubin, H. K. C. Timken, S. Steuernagel and D. E. Woessner, *J. Phys. Chem.*, 1996, **100**, 3788-3798.
96. T. Thomson, *Journal of Natural Philosophy, Chemistry and the Arts*, 1811, **29**, 285-292.
97. M. Osada and T. Sasaki, *Polym. J.*, 2015, **47**, 89-98.
98. F. Geng, R. Ma and T. Sasaki, *Acc. Chem. Res.*, 2010, **43**, 1177-1185.
99. N. Takahashi and K. Kuroda, *J. Mater. Chem.*, 2011, **21**, 14336-14353.
100. M. Ogawa and D. Iwata, *Crystal Growth & Design*, 2010, **10**, 2068-2072.

101. P. Eliášová, M. Opanasenko, P. S. Wheatley, M. Shamzhy, M. Mazur, P. Nachtigall, W. J. Roth, R. E. Morris and J. Čejka, *Chem. Soc. Rev.*, 2015, DOI: **10.1039/C5CS00045A**.
102. D. E. Akporiaye and G. D. Price, *Zeolites*, 1989, **9**, 23-32.
103. D. Xu, Y. Ma, Z. Jing, L. Han, B. Singh, J. Feng, X. Shen, F. Cao, P. Oleynikov, H. Sun, O. Terasaki and S. Che, *Nat Commun*, 2014, **5**, 4262.
104. D. Xu, Z. Jing, F. Cao, H. Sun and S. Che, *Chem. Mater.*, 2014, **26**, 4612-4619.
105. J. Jung, C. Jo, K. Cho and R. Ryoo, *J. Mater. Chem.*, 2012, **22**, 4637-4640.
106. B. K. Singh, D. Xu, L. Han, J. Ding, Y. Wang and S. Che, *Chem. Mater.*, 2014, **26**, 7183-7188.
107. W. Park, D. Yu, K. Na, K. E. Jelfs, B. Slater, Y. Sakamoto and R. Ryoo, *Chem. Mater.*, 2011, **23**, 5131-5137.
108. J. Weitkamp and L. Puppe, *Catalysis and Zeolites: Fundamentals and Applications*, Springer, Berlin, 1999.
109. L. Emdadi, Y. Q. Wu, G. H. Zhu, C. C. Chang, W. Fan, T. Pham, R. F. Lobo and D. X. Liu, *Chem. Mater.*, 2014, **26**, 1345-1355.
110. L. Emdadi and D. X. Liu, *J. Mater. Chem. A*, 2014, **2**, 13388-13397.
111. B. Y. Liu, Q. Q. Duan, C. Li, Z. H. Zhu, H. X. Xi and Y. Qian, *New Journal of Chemistry*, 2014, **38**, 4380-4387.
112. J. C. Kim, K. Cho and R. Ryoo, *Appl. Catal., A*, 2014, **470**, 420-426.
113. W. Kim, J. C. Kim, J. Kim, Y. Seo and R. Ryoo, *ACS Catal.*, 2013, **3**, 192-195.
114. K. V. Emtsev, A. Bostwick, K. Horn, J. Jobst, G. L. Kellogg, L. Ley, J. L. McChesney, T. Ohta, S. A. Reshanov, J. Rohrl, E. Rotenberg, A. K. Schmid, D. Waldmann, H. B. Weber and T. Seyller, *Nat. Mater.*, 2009, **8**, 203-207.
115. M. Osada and T. Sasaki, *J. Mater. Chem.*, 2009, **19**, 2503-2511.
116. M. Naguib, V. N. Mochalin, M. W. Barsoum and Y. Gogotsi, *Advanced Materials*, 2014, **26**, 992-1005.
117. M. Q. Zhao, M. Sedran, Z. Ling, M. R. Lukatskaya, O. Mashtalir, M. Ghidui, B. Dyatkin, D. J. Tallman, T. Djenizian, M. W. Barsoum and Y. Gogotsi, *Angew. Chem. Int. Ed.*, 2015, **54**, 4810-4814.
118. R. E. Morris and J. Čejka, *Nat. Chem.*, 2015, **7**, 381-388.
119. M. Mazur, P. S. Wheatley, M. Navarro, W. J. Roth, M. Položij, A. Mayoral, P. Eliášová, P. Nachtigall, J. Čejka and R. E. Morris, *Nat. Chem.*, 2015, **accepted**.
120. J. X. Jiang, J. H. Yu and A. Corma, *Angew. Chem. Int. Ed.*, 2010, **49**, 3120-3145.
121. J. X. Jiang, J. L. Jorda, M. J. Diaz-Cabanas, J. H. Yu and A. Corma, *Angew. Chem. Int. Ed.*, 2010, **49**, 4986-4988.
122. L. Grajciar, O. Bludsky, W. J. Roth and P. Nachtigall, *Catal. Today*, 2013, **204**, 15-21.
123. P. Chlubná-Eliášová, Y. Tian, A. B. Pinar, M. Kubů, J. Čejka and R. E. Morris, *Angew. Chem. Int. Ed.*, 2014, **53**, 7048-7052.
124. M. Shamzhy, M. Opanasenko, Y. Y. Tian, K. Konysheya, O. Shyets, R. E. Morris and J. Čejka, *Chem. Mater.*, 2014, **26**, 5789-5798.
125. P. S. Wheatley, P. Chlubna-Eliasova, H. Greer, W. Z. Zhou, V. R. Seymour, D. M. Dawson, S. E. Ashbrook, A. B. Pinar, L. B. McCusker, M. Opanasenko, J. Čejka and R. E. Morris, *Angew. Chem. Int. Ed.*, 2014, **53**, 13210-13214.
126. M. Mazur, P. Chlubna-Eliasova, W. J. Roth and J. Čejka, *Catal. Today*, 2014, **227**, 37-44.
127. J. Ruan, P. Wu, B. Slater, Z. Zhao, L. Wu and O. Terasaki, *Chem. Mater.*, 2009, **21**, 2904-2911.
128. H. K. Jeong, S. Nair, T. Vogt, L. Charles Dickinson and M. Tsapatsis, *Nat. Mater.*, 2003, **2**, 53-58.
129. S. Choi, J. Coronas, E. Jordan, W. Oh, S. Nair, F. Onorato, D. F. Shantz and M. Tsapatsis, *Angew. Chem. Int. Ed.*, 2008, **47**, 552-555.

130. S. Choi, J. Coronas, J. A. Sheffel, E. Jordan, W. Oh, S. Nair, D. F. Shantz and M. Tsapatsis, *Microporous Mesoporous Mater.*, 2008, **115**, 75-84.
131. W. G. Kim, S. Choi and S. Nair, *Langmuir*, 2011, **27**, 7892-7901.
132. W. G. Kim, J. S. Lee, D. G. Bucknall, W. J. Koros and S. Nair, *J. Membr. Sci.*, 2013, **441**, 129-136.
133. O. M. Yaghi, M. O'Keefe, N. W. Ockwig, H. K. Chae, M. Eddaoudi and J. Kim, *Nature*, 2003, **423**, 705-714.
134. F. Gandara, B. Gornes-Lor, E. Gutierrez-Puebla, M. Iglesias, M. A. Monge, D. M. Proserpio and N. Snejko, *Chem. Mater.*, 2008, **20**, 72-76.
135. D. Zhao, D. J. Timmons, D. Yuan and H.-C. Zhou, *Acc. Chem. Res.*, 2011, **44**, 123-133.
136. T. An, Y. Wang, J. Tang, Y. Wang, L. Zhang and G. Zheng, *J. Colloid Interface Sci.*, 2015, **445**, 320-325.
137. J. Choi, J. Park, M. Park, D. Moon and M. S. Lah, *Eur. J. Inorg. Chem.*, 2008, , 5465-5470.
138. S. Motoyama, R. Makiura, O. Sakata and H. Kitagawa, *J. Am. Chem. Soc.*, 2011, **133**, 5640-5643.
139. M. Sadakiyo, T. Yamada and H. Kitagawa, *J. Am. Chem. Soc.*, 2011, **133**, 11050-11053.
140. M. C. Bernini, E. V. Brusau, G. E. Narda, G. Echeverria, A. Fantoni, G. Punte and A. P. Ayala, *Polyhedron*, 2012, **31**, 729-737.
141. F. Costantino, A. Ienco, S. Midollini, A. Orlandini, A. Rossin and L. Sorace, *Eur. J. Inorg. Chem.*, 2010, , 3179-3184.
142. F. Luo, Y.-x. Che and J.-m. Zheng, *Microporous Mesoporous Mater.*, 2009, **117**, 486-489.
143. L.-N. Jia, Y. Zhao, L. Hou, L. Cui, H.-H. Wang and Y.-Y. Wang, *J. Solid State Chem.*, 2014, **210**, 251-255.
144. P. Vishnoi and R. Murugavel, *Z. Anorg. Allg. Chem.*, 2014, **640**, 1075-1080.
145. R. Haldar and T. K. Maji, *J. Chem. Sci. (Berlin, Ger.)*, 2011, **123**, 883-890.
146. J. Sahu, A. Aijaz, Q. Xu and P. K. Bharadwaj, *Inorg. Chim. Acta*, 2015, **430**, 193-198.
147. X.-Y. Cao, Z.-J. Li, J. Zhang, Y.-Y. Qin, J.-K. Cheng and Y.-G. Yao, *Crystengcomm*, 2008, **10**, 1345-1349.
148. X. Zhao, J. Dou, D. Sun, P. Cui, D. Sun and Q. Wu, *Dalton Trans.*, 2012, **41**, 1928-1930.
149. A. Kondo, H. Noguchi, S. Ohnishi, H. Kajiro, A. Tohdoh, Y. Hattori, W.-C. Xu, H. Tanaka, H. Kanoh and K. Kaneko, *Nano Lett.*, 2006, **6**, 2581-2584.
150. E.-C. Yang, X.-J. Shi, Z.-Y. Liu and X.-J. Zhao, *Inorg. Chem. Commun.*, 2010, **13**, 733-736.
151. D.-m. Chen, X.-p. Zhang, W. Shi and P. Cheng, *Crystal Growth & Design*, 2014, **14**, 6261-6268.
152. D. Matoga, B. Gil, W. Nitek, A. D. Todd and C. W. Bielawski, *Crystengcomm*, 2014, **16**, 4959-4962.
153. Y. Cheng, H. Kajiro, H. Noguchi, A. Kondo, T. Ohba, Y. Hattori, K. Kaneko and H. Kanoh, *Langmuir*, 2011, **27**, 6905-6909.
154. J. Gardolinski and G. Lagaly, *Clay Minerals*, 2005, **40**, 547-556.
155. G. Lagaly and I. Dékány, *Developments in Clay Science*, 2013, **5**, 243-345.
156. G. Lagaly, M. Ogawa and I. Dékány, *Developments in Clay Science*, 2013, **5**, 435-505.
157. R. Ma and T. Sasaki, *Advanced Materials*, 2010, **22**, 5082-5104.
158. L. Wang and T. Sasaki, *Chem. Rev.*, 2014, **114**, 9455-9486.
159. G. Lagaly, K. Beneke, P. Dietz and A. Weiss, *Angew. Chem. Int. Ed.*, 1974, **13**, 819-821.
160. G. Lagaly, *Adv. Colloid Interface Sci.*, 1979, **11**, 105-148.
161. R. A. Schoonheydt, T. Pinnavaia, G. Lagaly and N. Gangas, *Pure Appl. Chem.*, 1999, **71**, 2367-2371.
162. R. M. Barrer and D. M. Macleod, *Trans. Faraday Soc.*, 1955, **51**, 1290-&.
163. N. Lahav, U. Shani and J. Shabtai, *Clays Clay Miner.*, 1978, **26**, 107-115.
164. D. E. W. Vaughan, *Catal. Today*, 1988, **2**, 187-198.
165. M. A. Vicente, A. Gil and F. Bergaya, in *Developments in Clay Science*, 2013, vol. 5, pp. 523-557.
166. I. D. Johnson, T. A. Werpy and T. J. Pinnavaia, *J. Am. Chem. Soc.*, 1988, **110**, 8545-8547.

167. A. De Stefanis and A. A. G. Tomlinson, *Catal. Today*, 2006, **114**, 126-141.
168. J. S. Beck, J. C. Vartuli, W. J. Roth, M. E. Leonowicz, C. T. Kresge, K. D. Schmitt, C. T. W. Chu, D. H. Olson, E. W. Sheppard, S. B. McCullen, J. B. Higgins and J. L. Schlenker, *J. Am. Chem. Soc.*, 1992, **114**, 10834-10843.
169. C. T. Kresge, M. E. Leonowicz, W. J. Roth, J. C. Vartuli and J. S. Beck, *Nature*, 1992, **359**, 710-712.
170. M. E. Landis, B. A. Aufdembrink, P. Chu, I. D. Johnson, G. W. Kirker and M. K. Rubin, *J. Am. Chem. Soc.*, 1991, **113**, 3189-3190.
171. A. Galarneau, A. Barodawalla and T. J. Pinnavaia, *Nature*, 1995, **374**, 529-531.
172. K. W. Park, J. H. Jung, S. Y. Jeong and O. Y. Kwon, *Journal of Nanoscience and Nanotechnology*, 2009, **9**, 3160-3165.
173. K. W. Park, J. H. Jung, J. D. Kim, S. K. Kim and O. Y. Kwon, *Microporous Mesoporous Mater.*, 2009, **118**, 100-105.
174. F. Zhang and S. S. Wong, *Chem. Mater.*, 2009, **21**, 4541-4554.
175. A. Clearfield and B. D. Roberts, *Inorg. Chem.*, 1988, **27**, 3237-3240.
176. S. F. Cheng and T. C. Tang, *Inorg. Chem.*, 1989, **28**, 1283-1289.
177. L. Wang, Y. Ebina, K. Takada, R. Kurashima and T. Sasaki, *Advanced Materials*, 2004, **16**, 1412-1416.
178. F. Kooli, T. Sasaki, V. Rives and M. Watanabe, *J. Mater. Chem.*, 2000, **10**, 497-501.
179. S. Omwoma, W. Chen, R. Tsunashima and Y. F. Song, *Coord. Chem. Rev.*, 2013, **258-259**, 58-71.
180. W. J. Roth and J. C. Vartuli, *Stud. Surf. Sci. Catal.*, 2002, **141**, 273-279.
181. W. J. Roth, *Pol. J. Chem.*, 2006, **80**, 703-708.
182. W. J. Roth, J. C. Vartuli and C. T. Kresge, *Stud. Surf. Sci. Catal.*, 2000, **129**, 501-508.
183. A. Corma, U. Diaz, M. E. Domine and V. Fornes, *J. Am. Chem. Soc.*, 2000, **122**, 2804-2809.
184. A. G. Machoke, I. Y. Knoke, S. Lopez-Orozco, M. Schmiele, T. Selvam, V. R. R. Marthala, E. Spiecker, T. Unruh, M. Hartmann and W. Schwieger, *Microporous Mesoporous Mater.*, 2014, **190**, 324-333.
185. J. O. Barth, A. Jentys, J. Kornatowski and J. A. Lercher, *Chem. Mater.*, 2004, **16**, 724-730.
186. J. Kornatowski, J. O. Barth, K. Erdmann and M. Rozwadowski, *Microporous Mesoporous Mater.*, 2006, **90**, 251-258.
187. F. Jin, S. Huang, S. Cheng, Y. Wu, C.-C. Chang and Y.-W. Huang, *Catal. Sci. Technol.*, 2015, **5**, 3007-3016.
188. R. Ishii, T. Ikeda, T. Itoh, T. Ebina, T. Yokoyama, T. Hanaoka and F. Mizukami, *J. Mater. Chem.*, 2006, **16**, 4035-4043.
189. U. Díaz, A. Cantín and A. Corma, *Chem. Mater.*, 2007, **19**, 3686-3693.
190. C. G. Li, L. Xu, P. Wu, H. H. Wu and M. Y. He, *Chem. Commun.*, 2014, **50**, 15764-15767.
191. L. Xu, C. G. Li, K. Zhang and P. Wu, *ACS Catal.*, 2014, **4**, 2959-2968.
192. T. Maluangnont, Y. Yamauchi, T. Sasaki, W. J. Roth, J. Cejka and M. Kubu, *Chem. Commun.*, 2014, **50**, 7378-7381.
193. M. Tsapatsis, *AIChE J.*, 2014, **60**, 2374-2381.
194. P. F. Luckham and S. Rossi, *Adv. Colloid Interface Sci.*, 1999, **82**, 43-92.
195. G. Alberti, C. Dionigi, E. Giontella, S. MurciaMascaros and R. Vivani, *J. Colloid Interface Sci.*, 1997, **188**, 27-31.
196. Q. Wang and D. O'Hare, *Chem. Commun.*, 2013, **49**, 6301-6303.
197. F. Geng, R. Ma, Y. Ebina, Y. Yamauchi, N. Miyamoto and T. Sasaki, *J. Am. Chem. Soc.*, 2014, **136**, 5491-5500.
198. J. Doring, K. Beneke and G. Lagaly, *Colloid. Polym. Sci.*, 1992, **270**, 609-616.
199. N. Takabashi, H. Hata and K. Kuroda, *Chem. Mater.*, 2011, **23**, 266-273.
200. A. Corma, V. Fornes, J. Martinez-Triguero and S. B. Pergher, *J. Catal.*, 1999, **186**, 57-63.

201. P. Frontera, F. Testa, R. Aiello, S. Candamano and J. B. Nagy, *Microporous Mesoporous Mater.*, 2007, **106**, 107-114.
202. S. Maheshwari, E. Jordan, S. Kumar, F. S. Bates, R. L. Penn, D. F. Shantz and M. Tsapatsis, *J. Am. Chem. Soc.*, 2008, **130**, 1507-1516.
203. Y. Bi, J.-F. Lambert, Y. Millot, S. Casale, J. Blanchard, S. Zeng, H. Nie and D. Li, *J. Mater. Chem.*, 2011, **21**, 18403-18411.
204. B. Gil, W. Makowski, B. Marszalek, W. J. Roth, M. Kubu, J. Čejka and Z. Olejniczak, *Dalton Trans.*, 2014, **43**, 10501-10511.
205. I. Ogino, M. M. Nigra, S. J. Hwang, J. M. Ha, T. Rea, S. I. Zones and A. Katz, *J. Am. Chem. Soc.*, 2011, **133**, 3288-3291.
206. I. Ogino, E. A. Eilertsen, S. J. Hwang, T. Rea, D. Xie, X. Y. Ouyang, S. I. Zones and A. Katz, *Chem. Mater.*, 2013, **25**, 1502-1509.
207. X. Y. Ouyang, S. J. Hwang, R. C. Runnebaum, D. Xie, Y. J. Wanglee, T. Rea, S. I. Zones and A. Katz, *J. Am. Chem. Soc.*, 2014, **136**, 1449-1461.
208. J. L. Schlenker and B. K. Peterson, *J. Appl. Crystallogr.*, 1996, **29**, 178-185.
209. G. G. Juttu and R. F. Lobo, *Microporous Mesoporous Mater.*, 2000, **40**, 9-23.
210. D. L. Dorset, W. J. Roth and C. J. Gilmore, *Acta Crystallographica Section A*, 2005, **61**, 516-527.
211. M. Položij, H. V. Thang, M. Rubeš, P. Eliášová, J. Čejka and P. Nachtigall, *Dalton Trans.*, 2014, **43**, 10443-10450.
212. V. A. Drits and C. Tchoubar, *X-Ray Diffraction by Disordered Lamellar Structures*, Springer-Verlag, Berlin, 1989.
213. D. M. Moore and R. C. Reynolds, *X-ray Diffraction and the Identification and Analysis of Clay Minerals*, Oxford University Press, Oxford, 1997.
214. Z. Liu, N. Fujita, K. Miyasaka, L. Han, S. M. Stevens, M. Suga, S. Asahina, B. Slater, C. Xiao, Y. Sakamoto, M. W. Anderson, R. Ryoo and O. Terasaki, *Microscopy*, 2013, **62**, 109-146.
215. U. Díaz and A. Corma, *Dalton Trans.*, 2014, **43**, 10292-10316.
216. A. Gil, S. A. Korili and M. A. Vicente, *Cat. Rev. - Sci. Eng.*, 2008, **50**, 153-221.
217. J. Rouquerol, P. Llewellyn and K. S. W. Sing, in *Adsorption by Powders and Porous Solids: Principles, Methodology and Applications*, eds. J. Rouquerol, F. Rouquerol, K. S. W. Sing, P. Llewellyn and G. Maurin, Elsevier, Amsterdam, 2nd edn., 2014.
218. in *ASTM D3663 - 03(2015)*, ASTM International, West Conshohocken, PA, 2015.
219. W. Makowski, K. Mlekodaj, B. Gil, W. J. Roth, B. Marszałek, M. Kubu, P. Hudec, A. Smiešková and M. Horňáček, *Dalton Trans.*, 2014, **43**, 10574-10583.
220. J. Rouquerol, P. Llewellyn and F. Rouquerol, *Stud. Surf. Sci. Catal.*, 2006, **160**, 49-56.
221. G. Horvath and K. Kawazoe, *J. Chem. Eng. Jpn.*, 1983, **16**, 470-475.
222. E. P. Barrett, L. G. Joyner and P. P. Halenda, *J. Am. Chem. Soc.*, 1951, **73**, 373-380.
223. A. Saito and H. C. Foley, *AIChE J.*, 1991, **37**, 429-436.
224. L. S. Cheng and R. T. Yang, *Chem. Eng. Sci.*, 1994, **49**, 2599-2609.
225. M. Kruk, M. Jaroniec and A. Sayari, *Langmuir*, 1997, **13**, 6267-6273.
226. M. Jaroniec and L. A. Solovyov, *Langmuir*, 2006, **22**, 6757-6760.
227. in *ASTM D4641-12* ed. A. International, West Conshohocken, PA, 2012.
228. J. Landers, G. Y. Gor and A. V. Neimark, *Colloids Surf., A*, 2013, **437**, 3-32.
229. J. P. Olivier and M. L. Occelli, *J. Phys. Chem. B*, 2001, **105**, 623-629.
230. J. P. Olivier and M. L. Occelli, *J. Phys. Chem. B*, 2001, **105**, 5358-5358.
231. M. Thommes, *Chemie Ingenieur Technik*, 2010, **82**, 1059-1073.
232. F. Bergaya, *J. Porous Mater.*, 1995, **2**, 91-96.
233. X. Xie, Z. Li, B. Li, X. Wu and X. An, *RSC Adv.*, 2015, **5**, 46316-46324.

234. H. Y. Zhu, G. Q. Lu, N. Maes and E. F. Vansant, *J. Chem. Soc., Faraday Trans.*, 1997, **93**, 1417-1423.
235. H. Y. Zhu and E. F. Vansant, *J. Porous Mater.*, 1995, **2**, 107-113.
236. N. Maes, I. Heylen, P. Cool and E. F. Vansant, *Applied Clay Science*, 1997, **12**, 43-60.
237. J.-H. Yang, H. Piao, A. Vinu, A. A. Elzatahry, S.-M. Paek and J.-H. Choy, *RSC Adv.*, 2015, **5**, 8210-8215.
238. J. Ahenach, P. Cool and E. F. Vansant, *Physical Chemistry Chemical Physics*, 2000, **2**, 5750-5755.
239. M. Pichowicz and R. Mokaya, *Chem. Commun.*, 2001, 2100-2101.
240. A. Galarneau, A. Barodawalla and T. J. Pinnavaia, *Chem. Commun.*, 1997, 1661-1662.
241. U. Diaz, *ISRN Chemical Engineering*, 2012, **2012**, 1-35.
242. A. Zukal and M. Kubu, *Dalton Trans.*, 2014, **43**, 10558-10565.
243. E. L. Wu, G. R. Landolt and A. W. Chester, *Stud. Surf. Sci. Catal.*, 1986, **28**, 547-554.
244. W. Makowski, L. Chmielarz and P. Kuśtrowski, *Microporous Mesoporous Mater.*, 2009, **120**, 257-262.
245. P. H. Emmett, *Oxidation, Hydration, Dehydration and Cracking Catalysts*, Reinhold Publishing, New York, 1960.
246. G. Centi and S. Perathoner, *Microporous Mesoporous Mater.*, 2008, **107**, 3-15.
247. A. de Roy, C. Forano, K. El Malki and J.-P. Besse, in *Synthesis of Microporous Materials: Expanded Clays and Other Microporous Solids*, eds. M. L. Occelli and H. E. Robson, Springer, New York, 1992, pp. 108-169.
248. G. W. Brindley and R. E. Sempels, *Clay Minerals*, 1977, **12**, 229-237.
249. A. Gil, L. M. Gandia and M. A. Vicente, *Cat. Rev. - Sci. Eng.*, 2000, **42**, 145-212.
250. M. L. Occelli and R. M. Tindwa, *Clays Clay Miner.*, 1983, **31**, 22-28.
251. H. Ming-Yuan, L. Zhonghui and M. Enze, *Catal. Today*, 1988, **2**, 321-338.
252. Z. Ding, J. T. Klopogge, R. L. Frost, G. Q. Lu and H. Y. Zhu, *J. Porous Mater.*, 2001, **8**, 273-293.
253. S. A. Bagshaw and R. P. Cooney, *Chem. Mater.*, 1995, **7**, 1384-1389.
254. J. T. Klopogge, S. Komarneni, K. Yanagisawa, R. L. Frost and R. Fry, *J. Mater. Sci. Lett.*, 1998, **17**, 1853-1855.
255. S. Perathoner and G. Centi, *Top. Catal.*, 2005, **33**, 207-224.
256. J. G. Mei, S. M. Yu and J. Cheng, *Catal. Commun.*, 2004, **5**, 437-440.
257. S. A. Bagshaw and R. P. Cooney, *Chem. Mater.*, 1993, **5**, 1101-1109.
258. A. A. G. Tomlinson, *J. Porous Mater.*, 1998, **5**, 259-274.
259. R. Molina, S. Moreno, A. Vieiracoelho, J. A. Martens, P. A. Jacobs and G. Poncelet, *J. Catal.*, 1994, **148**, 304-314.
260. S. Moreno, R. S. Kou and G. Poncelet, *J. Catal.*, 1996, **162**, 198-208.
261. M. Raimondo, A. De Stefanis, G. Perez and A. A. G. Tomlinson, *Appl. Catal., A*, 1998, **171**, 85-97.
262. A. I. Khan and D. O'Hare, *J. Mater. Chem.*, 2002, **12**, 3191-3198.
263. S. Abello, F. Medina, D. Tichit, J. Perez-Ramirez, J. C. Groen, J. E. Sueiras, P. Salagre and Y. Cesteros, *Chem. - Eur. J.*, 2005, **11**, 728-739.
264. P. S. Braterman, Xu, Z.P., Yarberr, F., in *Handbook of Layered Materials*, ed. K. A. C. Scott M. Auerbach, Prabir K. Dutta, Marcel Dekker, Inc., New York, Basel, 2004, pp. 373-474.
265. F. Prinetto, G. Ghiotti, R. Durand and D. Tichit, *J. Phys. Chem. B*, 2000, **104**, 11117-11126.
266. F. Leroux and J. P. Besse, *Chem. Mater.*, 2001, **13**, 3507-3515.
267. D. S. Robins and P. K. Dutta, *Langmuir*, 1996, **12**, 402-408.
268. J. H. Choy, S. Y. Kwak, J. S. Park and Y. J. Jeong, *J. Mater. Chem.*, 2001, **11**, 1671-1674.
269. A. I. Khan, L. X. Lei, A. J. Norquist and D. O'Hare, *Chem. Commun.*, 2001, 2342-2343.
270. B. F. Sels, D. E. De Vos and P. A. Jacobs, *Cat. Rev. - Sci. Eng.*, 2001, **43**, 443-488.
271. A. Clearfield and J. A. Stynes, *Journal of Inorganic & Nuclear Chemistry*, 1964, **26**, 117-129.

272. B. Z. Wan, R. G. Anthony, G. Z. Peng and A. Clearfield, *J. Catal.*, 1986, **101**, 19-27.
273. N. He, Y. H. Yue and Z. Gao, *Microporous Mesoporous Mater.*, 2002, **52**, 1-9.
274. K. Liu, X. Wang, S. Ding, Y. Li, W. Hua, Y. Yue and Z. Gao, *J. Mol. Catal. A: Chem.*, 2013, **380**, 84-89.
275. S. Cheng, *Catal. Today*, 1999, **49**, 303-312.
276. S. T. Wong and S. F. Cheng, *Chem. Mater.*, 1993, **5**, 770-777.
277. A. Takagaki, T. Yoshida, D. L. Lu, J. N. Kondo, M. Hara, K. Domen and S. Hayashi, *J. Phys. Chem. B*, 2004, **108**, 11549-11555.
278. H. J. Werner, K. Beneke and G. Lagaly, *Z. Anorg. Allg. Chem.*, 1980, **470**, 118-130.
279. Y. Ide, N. Ochi and M. Ogawa, *Angew. Chem. Int. Ed.*, 2011, **50**, 654-656.
280. Y. Ide, N. Kagawa, M. Sadakane and T. Sano, *Chem. Commun.*, 2013, **49**, 9027-9029.
281. C. A. Emeis, *J. Catal.*, 1993, **141**, 347-354.
282. M. V. Shamzhy, M. V. Opanasenko, F. S. d. O. Ramos, L. Brabec, M. Horacek, M. Navarro-Rojas, R. E. Morris, H. d. O. Pastore and J. Cejka, *Catal. Sci. Technol.*, 2015, **5**, 2973-2984.
283. P. Ayrault, J. Datka, S. Laforge, D. Martin and M. Guisnet, *J. Phys. Chem. B*, 2004, **108**, 13755-13763.
284. K. Gora-Marek, K. Tarach and M. Choi, *J. Phys. Chem. C*, 2014, **118**, 12266-12274.
285. N. S. Nesterenko, F. Thibault-Starzyk, V. Montouilliot, V. V. Yushchenko, C. Fernandez, J. P. Gilson, F. Fajula and I. I. Ivanova, *Kinet. Catal.*, 2006, **47**, 40-48.
286. K. Mlekodaj, K. Tarach, J. Datka, K. Gora-Marek and W. Makowski, *Microporous Mesoporous Mater.*, 2014, **183**, 54-61.
287. S. Laforge, P. Ayrault, D. Manin and M. Guisnet, *Appl. Catal., A*, 2005, **279**, 79-88.
288. P. Chlubna, W. J. Roth, A. Zukal, M. Kubu and J. Pavlatova, *Catal. Today*, 2012, **179**, 35-42.
289. Y. J. He, G. S. Nivarthi, F. Eder, K. Seshan and J. A. Lercher, *Microporous Mesoporous Mater.*, 1998, **25**, 207-224.
290. D. Liu, X. Zhang, A. Bhan and M. Tsapatsis, *Microporous Mesoporous Mater.*, 2014, **200**, 287-290.
291. Z. Zhang, W. Zhu, S. Zai, M. Jia, W. Zhang and Z. Wang, *J. Porous Mater.*, 2013, **20**, 531-538.
292. W. J. Roth, J. Čejka, R. Millini, E. Montanari, B. Gil and M. Kubu, *Chem. Mater.*, 2015, **27**, 4620-4629.
293. W. J. Roth, P. Chlubná, M. Kubů and D. Vitvarová, *Catal. Today*, 2013, **204**, 8-14.
294. V. V. Narkhede and H. Gies, *Chem. Mater.*, 2009, **21**, 4339-4346.
295. M. M. Antunes, S. Lima, A. Fernandes, M. Pillinger, M. F. Ribeiro and A. A. Valente, *Appl. Catal., A*, 2012, **417**, 243-252.
296. J. Wang, S. Jaenicke, G. K. Chuah, W. Hua, Y. Yue and Z. Gao, *Catal. Commun.*, 2011, **12**, 1131-1135.
297. J. Wang, X. Tu, W. Hua, Y. Yue and Z. Gao, *Microporous Mesoporous Mater.*, 2011, **142**, 82-90.
298. P. Botella, A. Corma, R. H. Carr and C. J. Mitchell, *Appl. Catal., A*, 2011, **398**, 143-149.
299. M. V. Rodrigues, C. Vignatti, T. Garetto, S. H. Pulcinelli, C. V. Santilli and L. Martins, *Appl. Catal., A*, 2015, **495**, 84-91.
300. O. Kikhtyanin, P. Chlubna, T. Jindrova and D. Kubicka, *Dalton Trans.*, 2014, **43**, 10628-10641.
301. K. Gora-Marek and J. Datka, *Stud. Surf. Sci. Catal.*, 2005, **158**, 837-844.
302. B. Onida, L. Borello, B. Bonelli, F. Geobaldo and E. Garrone, *J. Catal.*, 2003, **214**, 191-199.
303. S. Inagaki, H. Imai, S. Tsujiuchi, H. Yakushiji, T. Yokoi and T. Tatsumi, *Microporous Mesoporous Mater.*, 2011, **142**, 354-362.
304. T. Yokoi, S. Mizuno, H. Imai and T. Tatsumi, *Dalton Trans.*, 2014, **43**, 10584-10592.
305. S. Inagaki, T. Yokoi, Y. Kubota and T. Tatsumi, *Chem. Commun.*, 2007, 5188-5190.
306. S. Inagaki and T. Tatsumi, *Chem. Commun.*, 2009, 2583-2585.

307. Y. Asakura, Y. Sakamoto and K. Kuroda, *Chem. Mater.*, 2014, **26**, 3796-3803.
308. H. Gies, U. Mueller, B. Yilmaz, M. Feyen, T. Tatsumi, H. Imai, H. Zhang, B. Xie, F.-S. Xiao, X. Bao, W. Zhang, T. De Baerdemaeker and D. De Vos, *Chem. Mater.*, 2012, **24**, 1536-1545.
309. T. De Baerdemaeker, H. Gies, B. Yilmaz, U. Mueller, M. Feyen, F.-S. Xiao, W. Zhang, T. Yokoi, X. Bao and D. E. De Vos, *J. Mater. Chem. A*, 2014, **2**, 9709-9717.
310. T. Yanagisawa, T. Shimizu, K. Kuroda and C. Kato, *Bull. Chem. Soc. Jpn.*, 1990, **63**, 988-992.
311. J. C. Vartuli, C. T. Kresge, M. E. Leonowicz, A. S. Chu, S. B. McCullen, I. D. Johnsen and E. W. Sheppard, *Chem. Mater.*, 1994, **6**, 2070-2077.
312. S. Inagaki, Y. Fukushima and K. Kuroda, *J. Chem. Soc., Chem. Commun.*, 1993, 680-682.
313. T. Kimura and K. Kuroda, *Adv. Funct. Mater.*, 2009, **19**, 511-527.
314. T. Kimura, T. Kamata, M. Fuziwara, Y. Takano, M. Kaneda, Y. Sakamoto, O. Terasaki, Y. Sugahara and K. Kuroda, *Angew. Chem. Int. Ed.*, 2000, **39**, 3855-3859.
315. K. A. Carrado, *Applied Clay Science*, 2000, **17**, 1-23.
316. K. A. Carrado and L. Q. Xu, *Microporous Mesoporous Mater.*, 1999, **27**, 87-94.
317. K. A. Carrado, C. L. Marshall, J. R. Brenner and K. Song, *Microporous Mesoporous Mater.*, 1998, **20**, 17-26.
318. M. M. J. Treacy, D. E. W. Vaughan, K. G. Strohmaier and J. M. Newsam, *Proc. R. Soc. London, Ser. A*, 1996, **452**, 813-840.
319. W. J. Roth and D. L. Dorset, *Structural Chemistry*, 2010, **21**, 385-390.
320. A. Inayat, I. Knoke, E. Spiecker and W. Schwieger, *Angew. Chem. Int. Ed.*, 2012, **51**, 1962-1965.
321. A. Inayat, C. Schneider and W. Schwieger, *Chem. Commun.*, 2015, **51**, 279-281.
322. M. Khaleel, A. J. Wagner, K. A. Mkhoyan and M. Tsapatsis, *Angew. Chem. Int. Ed.*, 2014, **53**, 9456-9461.
323. S. I. Zones, *Microporous Mesoporous Mater.*, 2011, **144**, 1-8.
324. W. J. Roth, W. Makowski, B. Marszalek, P. Michorczyk, W. Skuza and B. Gil, *J. Mater. Chem. A*, 2014, **2**, 15722-15725.